

UCSF

UC San Francisco Electronic Theses and Dissertations

Title

Studies of antagonists and selective agonists of the thyroid hormone receptors

Permalink

<https://escholarship.org/uc/item/00k6f1s6>

Author

Yoshihara, Hikari A. I.

Publication Date

2003

Peer reviewed|Thesis/dissertation

Studies of Antagonists and Selective Agonists
of the Thyroid Hormone Receptors

by
Hikari A. I. Yoshihara

DISSERTATION

Submitted in partial satisfaction of the requirements for the degree of

DOCTOR OF PHILOSOPHY

in
Biochemistry and Molecular Biology

in the

GRADUATE DIVISION

of the

UNIVERSITY OF CALIFORNIA, SAN FRANCISCO



© 2003
by
Hikari A. I. Yoshihara

Acknowledgements

Chapter 2 is adapted from the manuscript of: Yoshihara, H.A.I., Chiellini, G., Mitchison, T.J. & Scanlan, T.S. (1998). An efficient substitution reaction for the preparation of thyroid hormone analogues. *Bioorganic & Medicinal Chemistry* **6**, 1179-1183. I prepared and characterized compounds **10 - 14**.

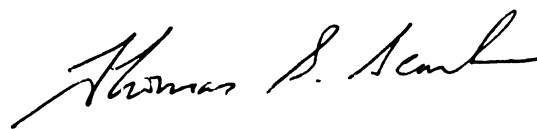
Chapter 3 is adapted from the manuscript of: Yoshihara, H.A.I., Apriletti, J.W., Baxter, J.D. & Scanlan, T.S. (2001). A designed antagonist of the thyroid hormone receptor. *Bioorganic & Medicinal Chemistry Letters* **11**, 2821-2825. The transactivation assays and synthesis and characterization of the compounds were done by me.

I would like to thank Tom Scanlan for putting up with me all these years and the past and current members of the Scanlan Lab for moral support and camaraderie. Jim Apriletti has been a steadfast collaborator whose work has been indispensable for our research on TR. I must also thank Bea Darimont for guidance in TR biochemistry and the molecular biology of nuclear receptors. Additionally, I thank the members of the UCSF nuclear receptor community and the UCSF research community in general for providing a collegial and stimulating environment in which to pursue graduate studies.

Abstract

“Studies of Antagonists and Selective Agonists of the Thyroid Hormone Receptors”

by Hikari A. I. Yoshihara



The modulation of the thyroid hormone receptors (TRs) by selective activators and inactivators has potential utility in medicine and in the study of the biological roles of the receptors. The design and synthesis of analogues of GC-1, an easily prepared high-affinity TR β -selective thyromimetic, are the focus of this thesis.

The design principles used in the estrogen receptor antagonist ICI-164,384 were applied to GC-1 to produce a TR antagonist. Methods were devised for the preparation of GC-1 analogues bearing substituents at the carbon atom bridging the two aromatic rings. This position for derivatization is unavailable in thyroid hormone, where an oxygen atom joins the two aromatic rings. A series of bridge-substituted GC-1 analogues were synthesized and characterized. Substitution at the bridging carbon results in a substantial loss of affinity for TR; however, the GC-1 analogue bearing the same alkylamide side chain as ICI-164,384 retains some affinity for TR and functions as a competitive antagonist of T₃ in cell-based assays of transcription activation.

The structural features of GC-1 that confer its greater TR affinity and selectivity compared to DIMIT were also analysed. GC-1 was designed as an analogue of the thyromimetic DIMIT, which has a lower affinity for TR and is not selective. GC-1 has a methylene group linking its two aromatic rings and an oxyacetic acid polar side chain,

while DIMIT has an ether oxygen linking its aromatic rings and an L-alanine polar side chain. To identify the important factors, analogues were prepared which bear only one of their two different structural features. The analogue of GC-1 with a biaryl ether has comparable selectivity to GC-1, while the analogue of DIMIT with a methylene group linking its aromatic rings is only slightly selective. These results demonstrate that the oxyacetic acid side chain of GC-1 is critical in conferring TR β -selectivity.

Table of Contents

Chapter 1: Introduction: Thyroid hormone synthesis, endocrinology and molecular biology	1
1.1. History of the discovery of thyroid hormones	2
1.2. Biosynthesis of thyroid hormones	2
1.3. Regulation of thyroid hormone production.....	3
1.4. Thyroid hormone transport and uptake.....	4
1.5. Developmental effects of thyroid hormone	5
1.6. Physiological effects of thyroid hormone	6
1.6.1. Skeletal Muscle	6
1.6.2. Liver	6
1.6.3. Adipose tissue	7
1.6.4. Bone	7
1.6.5. Heart.....	8
1.7. Molecular biology of thyroid hormone action	8
1.7.1. TR genes and splice variants	9
1.7.2. TR expression	10
1.7.3. Thyroid hormone response elements	11
1.7.4. Dimerization interface.....	11
1.7.5. Structural studies.....	11
1.7.6. Regulation of transcription	13
1.8. Genetic Approaches to Studying TR Function	16
1.9. Thyroid hormone receptor pharmacophore.....	19
1.10. Thyroid Hormone Receptor Modulators.....	20
1.10.1. Selective agonists	22
1.10.1.1. SK&F L-94901, CGS-23425 & CGS-26214	22
1.10.1.2. GC-1.....	23
1.10.2. Antagonists	25
1.10.2.1. GC-14.....	25
1.10.2.2. DIBRT.....	26
1.10.2.3. NH-3	27
1.11. Conclusion.....	28
1.12. References	29
Chapter 2: An Efficient Substitution Reaction for the Preparation of Thyroid Hormone Analogues	47

2.1. Introduction	48
2.2. Results and Discussion	49
2.3. Acknowledgments	53
2.4. Experimental	53
Chapter 3: Design and Synthesis of a Thyroid Hormone Antagonist	60
3.1. Introduction	61
3.2. Results	62
3.2.1. Synthesis and characterization of bridge-substituted GC-1 analogues	62
3.2.2. HY-4 and TR association with co-regulators	69
3.3. Discussion	71
3.4. Acknowledgements	73
3.5. Experimental	73
3.5.1. Transfection Assay	73
3.5.2. Synthesis	74
3.6. References	85
Chapter 4: Structural Determinants of Selective Thyromimetics	90
4.1. Introduction	91
4.2. Results	96
4.2.1. Synthesis of GC-1 Ether	96
4.2.2. Synthesis of methylene-bridged L-DIMIT	98
4.2.3. Synthesis of propionic acid side chain analogue of GC-1	100
4.2.4. TR Binding	101
4.2.5. TR Transactivation	106
4.3. Discussion	107
4.4. Experimental	111
4.4.1. TR binding assays	111
4.4.2. General Methods	111
4.5. Acknowledgements	130
4.6. References	130
Conclusions	136

List of Figures

Figure 1.1.	Structures of thyroid hormones	2
Figure 1.2.	Domain structure of TRs	10
Figure 1.3.	Structure of the ligand binding domain of hTR β 1 bound to TR.....	12
Figure 1.4.	TR pharmacophore.....	20
Figure 1.5.	Structures of selective thyromimetics and TR antagonists and partial agonists	21
Figure 1.6.	Structures of thyromimetics used to design TR antagonists and selective thyromimetics	26
Scheme 2.1.	Routes for derivatizing the carbon bridge of GC-1.....	50
Figure 3.1.	Chemical structures of thyroid hormone (T ₃), thyromimetic GC-1, amiodarone and ICI-164,384	62
Scheme 3.1.	Synthesis of bridge-substituted analogues of GC-1	63
Figure 3.2.	Modeling of alkylamide side chain antagonists of ER and TR	66
Scheme 3.2.	Synthesis of bridge-substituted analogues of GC-1 (continued)	64
Scheme 3.3.	Synthesis of bridge-substituted analogues of GC-1 with ICI-164,384-like extensions	67
Figure 3.3.	Antagonism by HY-4 (21) of TR-mediated transactivation.....	68
Figure 3.4.	Effect of HY-4 on TR – GRIP1 association.....	70
Figure 4.1.	Structures of thyroid hormones and thyromimetics.....	92
Figure 4.2.	Structures of target compounds to study effects of methylene bridge and oxyacetic acid side chain on TR selectivity.....	95
Scheme 4.1.	Preparation of the ether bridged analogue of GC-1	97

Scheme 4.2.	Preparation of the methylene bridged analogue of DIMIT	99
Scheme 4.3.	Preparation of the propionic acid side chain analogue of GC-1	101
Figure 4.3.	The ether oxygen to methylene and alanine to oxyacetic acid side chain substitutions have distinct independent effects on TR affinity and selectivity	103
Figure 4.4.	The loss of the α -amino group and the side chain ether for methylene substitution both contribute towards TR β -selectivity	104
Figure 4.5.	The oxyacetic acid polar side chain is the key determinant of TR β -selectivity	106
Figure 4.6.	GC-1 and ether-bridged GC-1 behave identically in TR transactivation assays	107
Figure 4.7.	Structures of previously reported GC-1 analogues with substituents at the 5'-position and at the bridging carbon	110

List of Tables

Table 2.1.	Alkyl cerium(III) chloride additions to the benzophenone 4	51
Table 2.2.	Carbon bridge extensions via solvolysis of 3	52
Table 3.1.	Binding affinities of GC-1 bridge-substituted analogues for TR	65
Table 4.1.	Binding affinities of thyromimetics for TR	102
Table 4.2.	Binding energies of thyromimetics for TR	105

Chapter 1: Introduction

1. Thyroid hormone synthesis, endocrinology and molecular biology

1.1. History of the discovery of thyroid hormones

The thyroid hormones, Thyroxine (3,3',5,5'-tetraiodo-L-thyronine, T_4 , 1, Figure 1) and 3,3',5-triiodo-L-thyronine (T_3 , 2, Figure 1) are endocrine signaling molecules secreted by the thyroid gland. Thyroxine was first isolated in crystalline form by Kendall in 1915 [1]. The structure of thyroxine was later assigned by Harington [2; 3] and confirmed by total synthesis [4]. The existence of a postulated form of thyroid hormone with a greater potency than thyroxine was confirmed in the early 1950s with the identification of T_3 [5; 6]. T_3 is recognized as the active form of the hormone but is the minor form secreted by the thyroid gland [7]. T_3 is also produced in peripheral tissues by the action of 5'-deiodinase enzymes [8].

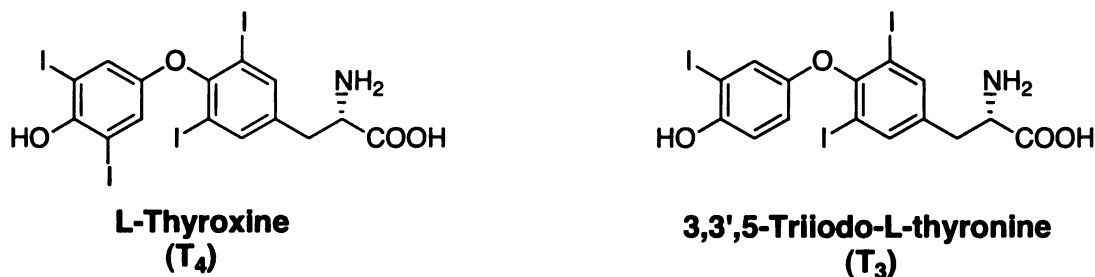


Figure 1.1. The structures of thyroid hormones

1.2. Biosynthesis of thyroid hormones

Thyroxine and T_3 are synthesized in the follicular lumen of the thyroid gland from the proteolysis of the post-translationally modified thyroglobulin (Tg). Iodine, obtained in the diet as iodide, concentrates in the thyroid gland by the action of a sodium-iodide symporter [9]. Membrane-bound thyroperoxidase [10], expressed on the lumen facing

apical surface of thyrocytes, oxidizes iodide with hydrogen peroxide to generate an iodinating species, possibly hypoiodous acid (HOI) [11]. Tg monomer contains 67 tyrosine residues, but there are only four major hormonogenic sites in the protein [12]. Tg serves as a store for iodine, and in the rat 80-90% the iodine in the thyroid is in the form of iodotyrosines in Tg. The thyronine biaryl ether is synthesized by the oxidative coupling of reactive iodinated tyrosine residues in Tg, possibly via a free-radical mechanism to generate iodinated thyronine residues bound in the peptide backbone of Tg. Free thyroid hormones are produced in the thyrocytes. Iodothyronine-containing Tg colloid in the follicular lumen is taken up by endocytosis and the colloid-containing vesicles fuse with lysosomes to generate phagolysosomes. Tg is digested and free amino acids are released. Free iodotyrosines are targeted by deiodinases and little mono- or diiodotyrosine is secreted from the thyroid gland [13].

1.3. Regulation of thyroid hormone production

Thyroid gland activity is regulated by thyrotropin, also known as thyroid stimulating hormone (TSH). The thyroid gland shows hyperplasia and hypertrophy in response to elevated levels of TSH, as well as increased thyroid hormone synthesis and secretion. TSH is recognized by a G-protein coupled thyrotropin receptor [14] (TSHR) which is $G\alpha_s$ and $G\alpha_q$ coupled [15]. TSHR signals via cAMP and can activate both the protein kinase A and phospholipase C pathways [16]. TSH is a heterodimeric glycoprotein secreted by the anterior lobe of the pituitary gland [17]. The α -subunit of TSH is also common to chorionic gonadotrophin, luteinizing hormone and follicle-stimulating hormone, while each hormone consists also of a unique β -subunit. TSH production is

regulated negatively by thyroid hormone, creating a feedback loop to limit thyroid gland stimulation. TSH production is also regulated positively by thyrotropin-releasing hormone (TRH). TRH is a tripeptide consisting of pyroGlu-His-Pro-amide and is secreted by the hypothalamus [18]. The endocrine regulation of the thyroid gland with thyroid hormone, TSH and TRH is known as the hypothalamic-pituitary-thyroid (HPT) axis.

1.4. Thyroid hormone transport and uptake

Thyroid hormones have low solubility in aqueous solution and greater than 99% of thyroid hormones in circulation are bound to transport proteins [19], most prominently thyroxine-binding globulin (TBG) and thyroxine-binding pre-albumin (transthyretin, TTR). TBG has high affinities for T_4 and T_3 (K_d values of $1 \times 10^{10} \text{ M}^{-1}$ and $4.6 \times 10^8 \text{ M}^{-1}$, respectively) [20]. TTR has 1-3 orders of magnitude lower affinity than TBG for T_3 and T_4 , but is more abundant. Serum albumin has even lower affinities for thyroid hormones but is present in high concentrations and may carry ~15% of thyroid hormones in circulation.

Thyroid hormones are amino acids and cannot passively traverse lipid membranes. Active import and export proteins capable of transporting thyroid hormone have been described [21; 22]. By controlling the intracellular concentration of thyroid hormone, these transporters may provide another means of regulating a tissue's responsiveness.

Deiodinase enzymes provide another important means of modulating thyroid hormone action [8]. Type I 5'-deiodinase (5'DI) converts T_4 to T_3 and is expressed most prominently in the thyroid, liver, kidney and pituitary. Its action is believed to contribute to T_3 in circulation, as well as the local production of T_3 from T_4 . Type II 5'-deiodinase (5'DII) catalyses the same reaction as 5'DI but has a different pattern of expression (mainly in the brain and in brown adipose tissue) and is comparatively short-lived. 5'DII is thought to function to rapidly and transiently increase a tissue's responsiveness to thyroid hormone. Type III 5-deiodinase (5DIII) removes iodine from the 5-position of T_4 and T_3 , inactivating thyroid hormone and providing another mechanism for controlling the local concentration of thyroid hormone.

Thyroid hormone is degraded by other means besides deiodination [23]. The biaryl ether bond is susceptible to cleavage and the 4'-hydroxyl group can be conjugated with sulfonyl, methyl or glucuronyl groups. Additionally the alanine side chain can undergo deamination and decarboxylation. Some thyroid hormone metabolites, such as triac (3,5,3'-triiodothyroacetic acid) retain high thyromimetic activity, but are present only at low concentrations compared to T_4 and T_3 and have a much shorter plasma half-life.

1.5. Developmental effects of thyroid hormone

Thyroid hormone is required for normal development. Fetal hypothyroidism leads to a collection of developmental defects called endemic cretinism [24]. Symptoms include mental retardation, stunted growth, hyperthyroidism and may include deaf-mutism and difficulty standing or an unusual gait. Studies show a variety of defects associated with

fetal hypothyroidism in the development of the central nervous system in rats. Defects have been observed in the visual and auditory cortex, the cerebral cortex, hippocampus and cerebellum [25].

1.6. Physiological effects of thyroid hormone

Thyroid hormone has a profound effect on metabolism, affecting many tissues and organs. It regulates the basal metabolic rate and the balance of anabolism and catabolism. While an excess of hormone increases both processes, the balance generally favors catabolism. The following summarizes some of the effects of a deficiency or an excess of thyroid hormone on a number of tissues and organs.

1.6.1. Skeletal Muscle

An excess of thyroid hormone impacts skeletal muscle by causing atrophy and increased susceptibility to fatigue. Additionally, an increase in oxygen consumption is observed [26] along with increased capillarity [27], glucose uptake and expression of Na^+/K^+ ATPase [28].

1.6.2. Liver

Thyroid hormone has profound effects upon lipid metabolism in the liver. Rates of lipid synthesis and degradation are increased with the balance in favor of degradation. Hypercholesterolemia has long been associated with hypothyroidism [29] and medicinal chemists have long sought a liver-selective thyromimetic to treat this condition. Thyroid hormone stimulates fatty acid and triglyceride synthesis in the liver [30] and increases the

serum concentration of free fatty acids in the plasma [31]. While reducing serum cholesterol levels, thyroid hormone increases cholesterol synthesis in the liver by increasing the activity of hydroxymethylglutaryl-coenzyme A (HMG Co A) reductase, [32], the rate-limiting enzyme in the biosynthesis of sterols. This increased rate of synthesis is offset by increased cholesterol degradation. Cytochrome P-450 7a, or cholesterol 7 α -hydroxylase, controls the rate of conversion of cholesterol to bile acids and its expression is positively regulated by thyroid hormone [33]. Of the reduction in serum cholesterol levels observed in hyperthyroid patients, the fraction in low-density lipoprotein (LDL) is especially impacted [34] possibly resulting from the increased expression of LDL-receptor [35]. Thyroid hormone also influences carbohydrate metabolism in the liver, particularly in stimulating gluconeogenesis [36; 37].

1.6.3. Adipose tissue

As in the liver, thyroid hormone increases fatty acid synthesis in adipose tissue [30]. It also increases free fatty acid release [31] and enhances catecholamine-stimulated fatty acid release [38]. Brown adipose tissue (BAT) plays an important role in non-shivering thermogenesis [39], and it shows increased thermogenesis and expression of uncoupling protein 1 (UCP1) in response to thyroid hormone. UCP1 increases oxidative phosphorylation and energy expenditure by dissipating the electrochemical proton gradient across the mitochondrial inner membrane, releasing the energy as heat.

1.6.4. Bone

Thyroid hormones are required for normal bone development and growth [40]. Hypothyroidism during childhood causes delayed bone aging, along with defective epiphyses. Thyroid hormone regulates bone turnover; reduced bone remodeling is observed with hypothyroidism [41], but bone mineral density does not decrease because of the balance of reduced synthesis and degradation. Hyperthyroidism, on the other hand, increases both osteoclast and osteoblast activity [42], but increases osteoclast activity to a greater extent such that bone mass is reduced [43; 44].

1.6.5. Heart

Thyroid hormone also has important effects on the heart. Hypothyroidism results in bradycardia and lowered cardiac output, [45; 46] while tachycardia and increased cardiac output are observed with hyperthyroidism [47]. Hyperthyroid patients are also at risk for developing arrhythmia, a potentially life threatening condition [48]. Several proteins regulated by thyroid hormone are implicated in its effects on the heart. The myosin heavy chains [49; 50] and the sarcoplasmic reticulum calcium ATPase (SERCa2) [51] which influence contractility, and HCN 2 [52; 53] which is involved in pacemaker function, are examples of such proteins.

1.7. Molecular biology of thyroid hormone action

The study of the molecular biology of thyroid hormone began with the cloning of the nuclear thyroid hormone receptors in the mid 1980s. Biochemical studies by several laboratories in the 1970s described specific high-affinity binding sites for T₃, which were associated with chromatin and were protease sensitive [54-56]. Support for these nuclear

T₃ binding sites being mediators of thyroid hormone action came from the correlation of the concentration of receptor in a given tissue to that tissue's responsiveness to T₃ [57]. Additionally, the nuclear receptors bound thyroid hormone analogues with affinities that corresponded to the analogue's potency as a thyromimetic [58; 59]. Multiple forms of the receptor were described by photoaffinity labeling [60] and isoelectric focusing [61], so it was not unexpected when two closely related but distinct isoforms of the thyroid hormone receptor were cloned [62; 63].

1.7.1. TR genes and splice variants

In humans, TR α resides on chromosome 17 [64], while TR β is found on chromosome 3 [63]. TRs belong to the nuclear receptor superfamily of transcription regulators [65; 66] and have a modular domain structure characteristic of this receptor family. They have a short (50-100 residue) unconserved N-terminal domain; a small DNA binding domain, which has a high degree of sequence conservation with other nuclear receptors; and a moderately conserved C-terminal ligand binding domain. TR transcripts are alternatively spliced to generate four isoforms: TR β 1, TR β 2, TR α 1 and TR α 2 (Figure 1.2) [67]. TR α 2 has a different C-terminal end of its ligand binding domain compared to TR α 1 and is unable to bind T₃ or activate transcription; instead it functions as a constitutive repressor. TR β 1 and TR β 2 have different N-terminal domains. For TR, the role of the N-terminal domain is not well defined, but it appears to confer TR β 2 the ability to activate transcription in the absence of ligand in certain contexts [68; 69].

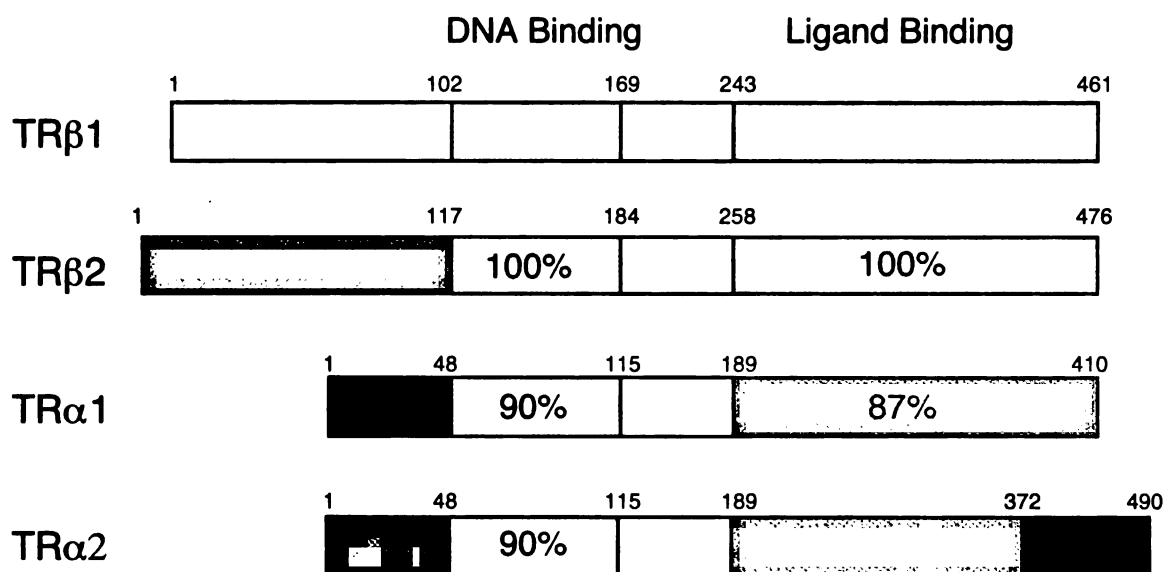


Figure 1.2. Domain structure of the TRs. Isoforms are generated by alternative splicing and promoter usage of the *TRα* and *TRβ* genes. Percentage amino acid residue identity values are given for the conserved domains. The variant C-terminal tail of TRα2 renders it unable to bind ligand or activate transcription.

1.7.2. TR expression

The levels of TR expression and the relative ratios of the four subtypes vary widely between different tissues and different stages of development [70]. In the rat, where TR expression is best characterized, TRα1, TRα2 and TRβ1 transcripts are found in most tissues. TRα1 mRNA is highly expressed in brown fat and skeletal muscle, whereas TRα2 expression is highest in the brain. TRβ1 mRNA expression is especially prominent in the kidney, liver and brain. Published studies of the expression of the receptor proteins are limited, but the available data do not show a perfect correlation with the transcript expression data. For instance, while rat brain has high levels of TR mRNA,

and the liver has comparatively low levels, the liver has much higher levels of TR protein expression than the brain [71].

1.7.3. Thyroid hormone response elements

Studies of the regulatory regions of genes responsive to thyroid hormone have described several motifs that are the key determinants for conferring this regulation. These thyroid hormone response elements (TREs) consist generally of two hexanucleotide motifs with a consensus sequence of AGGTCA arranged either as a direct repeat with a four intervening nucleotides, an inverted palindrome with a six nucleotide spacer or as a palindrome with no spacer [67]. This hexanucleotide half-site is also recognized by a number of other nuclear receptors, and the spacing of the half-sites is a determinant of the specificity for TR binding [72]. TR recognizes TREs through its DNA binding domain and binds them either as a homodimer or as a heterodimer with the retinoid-X receptor (RXR).

1.7.4. Dimerization interface

Structural and functional studies of the DNA binding domain and the ligand binding domain have shown regions on both domains that are important for dimerization. On the TR β 1 DNA binding domain, residues Asp104, Tyr117, Arg120 and Asp177 directly interact with the RXR DBD [73], while a series of heptad repeats on helix 11 of the ligand binding domain form the ligand binding domain's dimerization interface.

1.7.5. Structural studies

The DNA binding domain is of the zinc-finger type, and its structure in a complex with the DBD of RXR on a DR-4 type TRE has been reported [73]. The ligand binding domain of TR α 1 was among the first nuclear receptor LBDs to have an X-ray crystal structure reported [74]. The structure of the TR-LBD has the same fold as all the nuclear receptors characterized to date, consisting of a series of twelve alpha helices folded in a globular domain three helices thick with the ligand completely surrounded by protein, forming the hydrophobic core of a subdomain (Figure 1.3). The conformational changes associated with ligand binding result in the formation of functional surfaces that interact preferentially with different co-regulatory factors depending on the presence or absence of ligand.

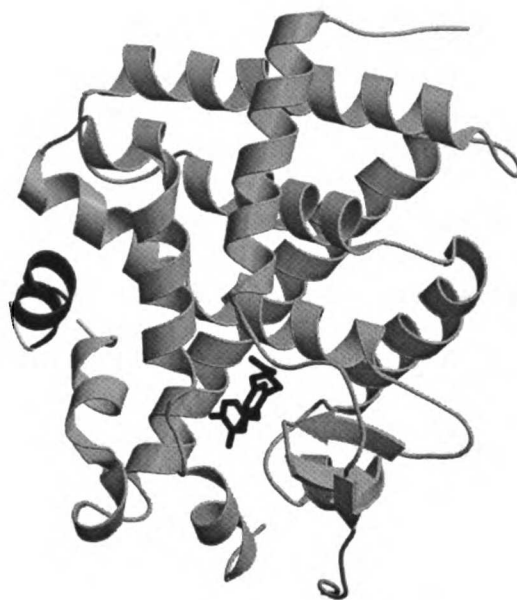


Figure 1.3. Structure of the ligand binding domain of hTR β 1 bound to TR. The left hand side of the figure shows a 16-residue peptide from the NR-box 2 of the co-activator GRIP1, containing an LXXLL motif, binding to the hydrophobic groove composed of helices 3, 4, 5 and 12 [75]

1.7.6. Regulation of transcription

TR can positively and negatively regulate the transcription of target genes. The unliganded receptor is resident in the nucleus and bound to TREs where it can actively repress transcriptional activation. Upon ligand binding, TR can become an activator of transcription. Among the genes regulated in this fashion are myosin heavy chain- α , LDL receptor, malic enzyme and fatty acid synthase [67].

There is also a class of genes regulated in the opposite fashion by TR and T_3 . Negative regulation of transcription by liganded TR is not well understood but is of critical importance for the regulation of thyroid hormone levels by the pituitary where transcription of TSH is downregulated by T_3 , providing a negative feedback loop for thyroid hormone production. A DNA microarray study in mice of hepatic genes regulated by T_3 found changes in the mRNA levels of 55 genes. Forty-one of these genes were negatively regulated directly or indirectly, suggesting that negative regulation of transcription by TR may be more common than positive regulation [76]. Complexes of co-regulatory proteins which associate with TRs in a ligand-dependent manner are believed to be critical factors in mediating TR's repression and activation of transcription. The p160-type co-activators are the best characterized among the co-activators. Members of this family of proteins include the steroid receptor co-activator 1 (SRC-1), TIF2/GRIP1 and pCIP/ACTR/AIB1/TRAM1/RAC3 [77]. These proteins can interact with several different nuclear receptors, including TRs, and enhance their activation of transcription in a ligand-dependent fashion. The minimal interaction domain of the p160 co-activators contains a series of three LXXLL motifs, where X is

any amino acid residue. These motifs are critical for the interaction with nuclear receptors and structural studies have shown that the motifs form an amphipathic helix which binds to a hydrophobic cleft on the liganded ligand binding domain formed by helices 3, 4, 5 and 12 [75; 78; 79]. SRC-1 contains two activation domains [80] and also has histone acetyltransferase activity which maps to its C-terminal end [81]. Histone acetylation is correlated with gene activation [82], presumably by allowing the adoption of a more open chromatin structure that allows access by the transcription machinery. SRC-1 may also activate transcription through its association with the cAMP response element binding protein (CBP) or p300 [77]. The functional significance of the interaction of SRC-1 or other p160 co-activators and TR is illustrated by studies that show their interaction is required for transcriptional activation by TR [83] and that mice deficient in SRC-1 show resistance to thyroid hormone [84].

Another class of co-activator is the thyroid hormone receptor associated protein (TRAP) complex. Identified by co-immunoprecipitation with epitope-tagged TR α [85] the complex has structural and functional homology to the Mediator complex of yeast [86]. The complex has been isolated in association with other transcription regulators, including such nuclear receptors as the vitamin D receptor, indicating a role beyond mediating transcription activation by TR. One member of the complex, TRAP220, interacts with TR and several other nuclear receptors in a ligand-dependent fashion, and like the p160 co-activators, contains an LXXLL motif that is necessary for this interaction [87]. While mice deficient in TRAP220 are inviable, fibroblasts isolated from *Trap220*^{-/-} mouse embryos show significantly reduced levels of transcriptional activation

by T₃ and TR. This reduction can be rescued with the ectopic expression of TRAP220, strongly indicating an important role of TRAP220 and the TRAP complex in transcription activation by TR [88].

The repressive effects of the unliganded TR are believed to be mediated via co-repressor complexes. Characterized co-repressors include the silencing mediator of retinoic acid and thyroid hormone receptors (SMRT) [89] and nuclear receptor co-repressor (NCoR) [90]. These co-repressors interact with the unliganded forms of TR and other nuclear receptors including RAR and RXR, but not their liganded counterparts. Important regions of TR required for interaction with co-repressor have been reported to include the hinge region between the DBD and LBD, parts of the surface defined by helices 10 and 11 of the LBD, and a surface defined by helices 3, 5 and 12. Interestingly, the latter surface overlaps with the hydrophobic cleft that interacts with the LXXLL motifs of p160 co-activators, and the co-repressor's receptor interaction domains contain IXXII motifs that are important for binding [91-93]. NCoR and SMRT are believed to function in a complex with other proteins including the mSin3 complex and histone deacetylases (HDACs) [94; 95]. In contrast to the transcription activation promoted by the chromatin remodeling effects of histone acetylation, histone deacetylation is believed to have the opposite effect, keeping chromatin in a closed form inaccessible to the transcription machinery [82].

The biological significance of repression by unliganded TR, especially in the hypothyroid state, is underscored by transgenic mouse models of generalized resistance to thyroid

hormone (GRTH). These mice have tissue hypothyroidism caused by a mutant form of TR β ($\Delta 337T$) found in a human patient with GRTH [96]. This mutant TR β is unable to bind T₃ and remains constitutively bound to NCoR and SMRT. These mice show severe defects in cerebellar development and learning reminiscent of mice with congenital hypothyroidism, while having extremely high circulating T₃, T₄ and TSH levels. By contrast, mice deficient in one or both forms of TR β are relatively healthy, though they were initially expected to mimic the hypothyroid state. Similar results were observed in a study that compared cerebellar development between either wild-type mice or those deficient in TR $\alpha 1$ kept in a hypothyroid state. The TR $\alpha 1^{-/-}$ mice showed normal cerebellar structure, while the wild-type mice showed cerebellar defects. These results strongly implicate the inability to overcome the repressive effects of unliganded TR in the pathogenesis of hypothyroidism and resistance to thyroid hormone.

The syndrome of GRTH is linked to dominant negative mutations of TR β . GRTH is characterized by high circulating levels of thyroid hormone and TSH, yet some patients exhibit symptoms similar to those seen in congenital hypothyroidism such as goiter, short stature and mental retardation. Mutations in TR β isolated from patients with GRTH map to the ligand binding domain and consist mostly of point mutants that show reduced affinity for T₃ [97], though some mutations interfere with co-repressor [98] release or co-activator recruitment [99].

1.8. Genetic Approaches to Studying TR Function

A number of different mice deficient in either one or several TR isoforms has been generated and reported over the past six years. The mice show a range of phenotypes, from which one can infer varied developmental and regulatory roles for the different subtypes. While these mice are viable, all show some defects of varying severity.

TR β knockout mice show a subset of the abnormalities found in patients with autosomal dominant resistance to thyroid hormone. They have normal cerebellar and hippocampal structures and the only effect seen in the CNS is congenital deafness [100], a condition that appears in some patients with RTH. Dysregulation of the hypothalamic-pituitary-thyroid axis is also observed with elevated TSH and free T₄ levels, similar to patients with RTH. TR β is normally expressed in the pituitary, which negatively regulates TSH levels in response to T₃. Unlike mice with congenital hypothyroidism, TR β knockout mice have normal learning and neurological function and do not show hippocampal or cerebellar defects [101]. The TR β 2 subtype has been selectively knocked out and these mice show more specific defects than mice devoid of all TR β . The central resistance to thyroid hormone is present in TR β 2^{-/-} [102] though it is less severe, indicating either both TR β subtypes are involved in regulating TSH levels, or some functional overlap with TR β 1. While TR β 2 deficient mice show normal hearing function, they have a defect in the development of the retina. M-cones do not form, instead a greater number of S-cones form, and the mice have a defect in detecting medium wavelength light.

Mice deficient in one or more forms of TR α have phenotypes distinct from the TR β knockouts. Mice with a disrupted TR α locus and unable to make TR α 1 and TR α 2

become hypothyroid progressively two weeks after birth, fail to grow, and die within five weeks of birth [103]. Reduced TSH levels and a smaller thyroid gland showing degradation of follicular cells accompany the hypothyroidism, and the failure to gain weight and lethality can be rescued with T_3 injections between the second and third weeks of life. $TR\alpha^{-/-}$ mice show additional defects in the maturation of the small intestine and delayed bone development, which are also ameliorated by T_3 treatment.

In contrast, mice deficient only in $TR\alpha 1$ are viable and have fewer defects but have reduced heart rate and body temperature [104]. Although these mice have slightly reduced TSH levels, free T_3 levels are normal, and males have reduced free T_4 . T_3 treatment raises heart rate and body temperature, though only the latter returns to normal levels. These results suggest that $TR\alpha 1$ plays an important role in mediating T_3 's stimulatory effects on the heart.

The contrasting phenotypes of $TR\alpha^{-/-}$ and $TR\alpha 1^{-/-}$ mice suggest a vital role for the hormone unresponsive $TR\alpha 2$; however, $TR\alpha 2^{-/-}$ mice are viable [105] and exhibit a complex phenotype of aspects of hyper- and hypothyroidism that may be partially due to the overexpression of $TR\alpha 1$ that occurs with the disruption of transcription at the $TR\alpha 2$ -specific exon 10. This discrepancy between the phenotypes of $TR\alpha^{-/-}$ and $TR\alpha 1^{-/-}$ mice has instead been ascribed to the production of short forms of $TR\alpha 1$ and $TR\alpha 2$ in $TR\alpha^{-/-}$ mice which interfere with TR and retinoic acid receptor- α activity [106]. Support for this notion comes from the report that a knockout mouse strain that expresses neither $TR\alpha 1$, $TR\alpha 2$, nor the shorter forms has a phenotype that more resembles that of $TR\alpha^{-/-}$ mice

[107]. Mice deficient in all forms of TR have phenotypes that are a combination of the phenotypes of the single knockouts, though some effects are more severe than in the single knockouts, suggesting separate and overlapping functions for TR α and TR β . *TR α ^{-/-} β ^{-/-}* mice fail to grow and die within five weeks of birth, much like *TR α ^{-/-}* mice. They also have the same defects in bone development and small intestine with more severe defects in the ileum [108]. However, their thyroid function resembles that of *TR β ^{-/-}* mice with the appearance of large goiters and T₄, T₃ and TSH even further elevated from the very high levels observed in *TR β ^{-/-}* mice. *TR α 1^{-/-} β ^{-/-}* mice also show the goiter, retarded bone maturation and extremely elevated TSH and thyroid hormone levels of *TR α ^{-/-} β ^{-/-}* mice [109]. In contrast to the *TR α ^{-/-} β ^{-/-}* mice, *TR α 1^{-/-} β ^{-/-}* mice are viable, albeit with approximately 30% mortality within nine months of age.

1.9. Thyroid hormone receptor pharmacophore

The structural features necessary for an active thyromimetic were defined by medicinal chemistry studies in the 1950s through the 1970s [110; 111]. The SAR studies reveal the minimal requirements for a high-affinity TR ligand: (1) two aromatic rings joined with a one atom linker; (2) the 4'-hydroxyl and carboxylic acid-containing side chain at the 1-position are essential for tight TR binding and thyromimetic activity; (3) halogen or hydrocarbon substitution at the 3, 5, 3'-positions is required (Figure 1.4). This crude picture of the thyromimetic pharmacophore is further supported by the crystal structure, which shows the 4'- and 1-positions of the thyronine structure are involved, respectively, in hydrogen bonding and electrostatic contacts with residues in the binding pocket. The 3,5- and 3'-iodo substituents of T₃ reside in small hydrophobic pockets, and the ligand

occupies almost 90% of the volume of the binding pocket [74]. Substituents significantly larger than iodine atoms hinder ligand binding and activity, presumably due to size limitations in the binding pocket of the receptor. However, the nature of the 3'-substituent is the least critical, and T₃ analogues with small and large 3'-substituents can retain high-affinity binding. The bridging moiety can be an oxygen or sulphur atom or methylene carbon, though these linkers are not completely equivalent. The methylene-bridged T₃ analogue has 2.5-fold higher nuclear binding activity but only half the activity of T₃ in rats, while the thioether analogue has equivalent binding, but only 14% of the activity [111]. These studies provide important structural constraints for developing high-affinity T₃ analogues.

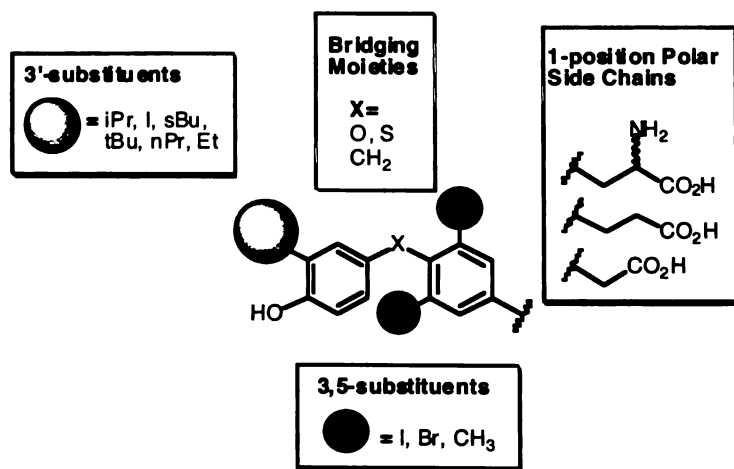


Figure 1.4. The thyroid hormone receptor pharmacophore

1.10. Thyroid Hormone Receptor Modulators

The ligand binding pocket of TR is an attractive target for compounds that modulate TR activity. Ligands capable of selectively activating or inactivating TR, in a tissue or isoform-selective fashion are already proving to be useful probes for *in vivo* studies of TR

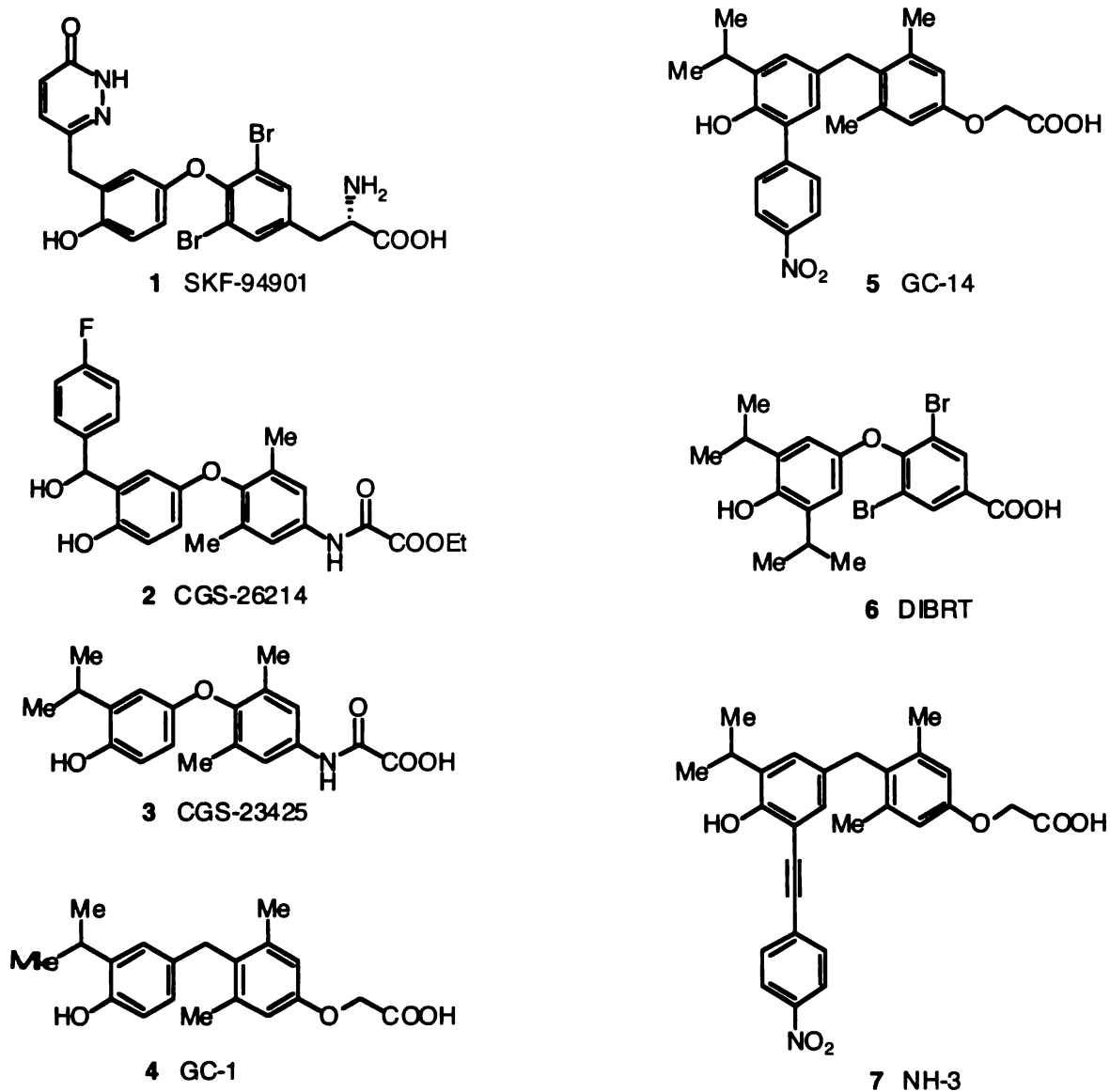


Figure 1.5. Structures of selective thromimimetics and TR antagonists and partial agonists

function. The continued development of such compounds with increased selectivity and potency opens the possibility of using TR modulating ligands as drugs either to promote

the beneficial effects of TR activation or to prevent the deleterious effects of excessive or inappropriate TR activity. The following is an overview of recent developments in selective thyromimetics and TR antagonists.

1.10.1. Selective agonists

1.10.1.1. SK&F L-94901, CGS-23425 & CGS-26214

The selective thyromimetics SK&F L-94901 (1, Figure 1.5), CGS-23425 (3) and CGS-26214 (2) have recently been reviewed [112]. In rats, SK&F L-94901 shows thyromimetic activity selectively lowering plasma cholesterol levels without stimulating the heart. It acts in the pituitary and lowers TSH levels along with T_3 and T_4 . SK&F L-94901 does not bind preferentially to $TR\alpha$ or $TR\beta$ and its selective action is attributed to selective uptake by the liver versus the heart. CGS-26214 is a potent cholesterol lowering agent in animal models and shows cardiac effects only at doses far higher (>25x) than those required to lower lipid levels. It is believed to work in a TR isoform selective fashion as it binds to nuclei from cultured liver cells with 100-fold higher affinity than to nuclei derived from cardiac myocytes, but data on its *in vitro* binding to purified TRs are not available. CGS-23425 has similar behavior to CGS-26214 in its cardiac-sparing cholesterol lowering thyromimetic effects. It increases transcription of ApoA1, one of the major apolipoproteins of HDL, and transactivation assays of the ApoA1 promoter show that CGS-23425 behaves as a $TR\beta$ selective agonist.

1.10.1.2. GC-1

GC-1 (4, Figure 1.5) was designed in our laboratory as an easily synthesized and derivatizable isosteric analogue of T_3 . Its design was based on the structure of 3,5-dimethyl-3'-isopropyl-L-thyronine (DIMIT, 8, Figure 1.6), a biologically active halogen free T_3 analogue. GC-1 retains the 3,5-dimethyl-3'-isopropyl substitution pattern of DIMIT, but for synthetic expediency a methylene unit was chosen to link the two aromatic rings instead of the ether oxygen characteristic of thyronines, and the L-alanine polar side chain was replaced with an oxyacetic acid side chain. GC-1 is a full agonist of both $TR\alpha 1$ and $TR\beta 1$ and binds to $TR\beta 1$ with an affinity comparable to T_3 [113; 114]. It binds to $TR\alpha 1$ with approximately 10-fold lower affinity, and even with this modest level of selectivity GC-1 has proven to be a useful probe for the action of $TR\beta$.

Compared to T_3 , GC-1 has distinct effects *in vivo*. In tadpoles, T_3 is a regulator of metamorphosis and $TR\alpha$ is expressed in tissues that develop, such as limb buds, while $TR\beta$ is expressed in tissues such as the tail and gills, which are resorbed. GC-1 treated tadpoles show tail and gill resorption with little or no limb development, a result consistent with the selective activation of $TR\beta$ over $TR\alpha$ [115].

Hypothyroid mice have bradycardia that is reversed by T_3 treatment, but GC-1 does not raise heart rate in hypothyroid mice to normal levels [52]. $TR\alpha 1$ is associated with the cardiac-stimulating effects of T_3 as $TR\alpha 1^{-/-}$ mice have reduced heart rate that is only partially restored by T_3 treatment. The same dose of GC-1 is as effective as T_3 , however, in lowering elevated cholesterol levels in hypothyroid mice and is even more effective

than T_3 in lowering elevated triglyceride levels. In cholesterol-fed rats, GC-1 reduced cholesterol and TSH levels as effectively as T_3 , though with around six-fold lower potency, without raising heart rate.

In brown adipose tissue (BAT) of hypothyroid mice, GC-1 is as effective as T_3 in restoring expression of uncoupling protein 1 (UCP1), which is a key factor in adaptive thermogenesis by generating heat by dissipating the electrochemical proton gradient across the inner membrane of mitochondria. However, while infusion of norepinephrine normally causes thermogenesis in BAT, GC-1 treated hypothyroid mice had only a slight response to norepinephrine treatment, suggesting that T_3 not only regulates UCP1 levels in BAT, but that it also potentiates BAT's responsiveness to catecholamine stimulation, possibly via a $TR\alpha 1$ -mediated pathway [116].

GC-1 also has an effect different from T_3 on cerebellar development in hypothyroid mice [117]. Cerebellar development is defective in the hypothyroid state, with Purkinje cells showing stunted development of their branched dendritic structures and granule cells showing reduced migration from the external germinal layer to the internal granular layer. GC-1 partially restores proper Purkinje cell morphology and dendrite density but does not affect the defective granule cell migration in hypothyroid mice and rats, suggesting a role for $TR\alpha 1$ in this process.

GC-1's $TR\beta$ selectivity has been studied using genetic and structural approaches. The $TR\beta$ -LBD•GC-1 co-crystal structure shows a rearrangement of the hydrogen-bonding

network of arginine residues near the oxyacetic acid side chain of GC-1. Asn331, the one amino acid residue in the ligand binding pocket that varies between TR β and TR α (where it is Ser277 in TR α) shows an altered interaction with the hydrogen-bonding network compared to the T₃ and 3,5,3'-triiodothyroacetic acid (triac) bound crystal structures [118]. Mutant TR β with N331S behaves like TR α toward GC-1 and conversely TR α -S277N behaves like TR β , demonstrating a key role for this varying amino acid residue in α/β selectivity. The proximity of this residue to the oxyacetic acid polar side chain of GC-1 implies that this feature of the ligand may play a role in determining selectivity.

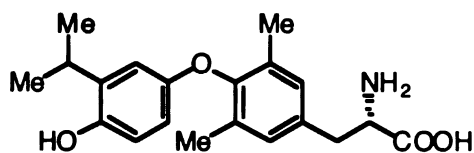
1.10.2. Antagonists

A number of TR partial agonist and antagonist ligands have recently been reported. Based upon a strategy that has successfully generated antagonist ligands for several other nuclear receptors [119], these ligands were designed to perturb the structure of the ligand-bound receptor with the addition of various appendages to the structure of a high-affinity thyromimetic. These ligands all show markedly reduced affinity for TR, to the extent that *in vivo* studies are difficult, but one antagonist ligand in particular, NH-3, has been shown to interfere with T₃-induced metamorphosis in tadpoles, the first *in vivo* demonstration of thyroid hormone antagonism at TR.

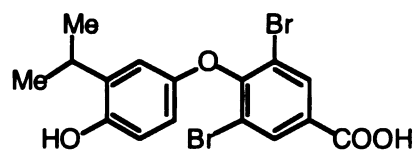
1.10.2.1. GC-14

GC-14 (5, Figure 1.5) is a GC-1 analogue bearing a 4-nitrophenyl extension group at the 5'-position. Based on the TR-LBD crystal structures, an extension at this position should point in the direction of Helix 12 and the hydrophobic cleft formed with Helices 3 and 5

that is crucial for the interaction with co-activators. Having K_d values of 220 ± 60 nM and 35 ± 12 nM for TR α 1 and TR β 1, respectively, GC-14 shows a maximal activation of 35% compared to T₃ for TR α 1 and 18% for TR β 1 [120]. This partial agonism/antagonism was confirmed in a competition with 1 nM T₃, where 10 μ M GC-14 gave as low a level of activation as 10 μ M of GC-14 alone. The 4-nitro group on the 5' extension is critical for this activity, and analogues bearing a phenyl or 3-nitrophenyl group at the 5' position function as full agonists.



8 DIMIT



9 MIBRT

Figure 1.6. Structures of DIMIT and MIBRT, thyromimetics used to design TR antagonists and selective thyromimetics

1.10.2.2. DIBRT

DIBRT (6, Figure 1.5) is a TR antagonist based on MIBRT (9, Figure 1.6), a thyromimetic with a carboxylic acid group at the 1-position. The addition of the 5'-isopropyl group to generate DIBRT results in a 1500-fold reduction in affinity for TR, nonetheless, at high doses DIBRT is able to reduce T₃-induced transactivation at a DR-4 type TRE [121]. Interestingly, at the TSH β promoter, where T₃ treatment represses TR-mediated transactivation, DIBRT alone only slightly represses transactivation and is able

to reverse the repression caused by 0.5 nM T_3 . In a GST-pulldown assay, DIBRT interferes with the T_3 -induced association between TR and the co-activator GRIP1.

1.10.2.3. NH-3

NH-3 (7, Figure 1.5). is a GC-1 analogue with a 4-nitrophenylethynyl extension at the 5'-position. It resembles GC-14, but with the addition of an acetylene spacer to the extension. NH-3 binds to TR with K_d values of 93 ± 29 nM and 20 ± 7 nM for TR α 1 and TR β 1, respectively, and induces maximal transactivation to 10% and 3%, respectively, of the values observed with T_3 [122]. NH-3 is able to antagonize T_3 -induced transactivation and appears to function as an antagonist by interfering with the interaction between TR and p160 type co-activators. In mammalian two-hybrid assays and GST-pulldowns, NH-3 does not promote the association of TR with GRIP1 and is able to block the association observed with T_3 treatment. NH-3 appears, however, to behave like an agonist ligand in promoting the dissociation of co-repressors from TR in a two-hybrid assay with NCoR. As with GC-14 the nitro group is required for antagonist activity and full agonism and partial antagonism is observed with other substituents at the 4-position of the extension. NH-3 interacts with *Xenopus* TRs in much the same fashion as with hTRs and with the same functional consequences [123]. NH-3 is able to block or reduce some of the effects of T_3 -induced metamorphosis in tadpoles, including gill and tail resorption, and inhibits the T_3 -induced upregulation of collagenase-3. Additionally, NH-3 is able to block spontaneous metamorphosis in a dose-dependent manner. Importantly, this blockade is reversed upon the removal of NH-3, indicating its non-toxicity and competitive antagonism of TR [123].

1.11. Conclusion

The chemical biology of the thyroid hormone receptor remains largely unexplored, compared to other nuclear receptors, making it a particularly attractive target. The following two chapters cover the synthesis and characterization of a series of analogues of GC-1 that bear substituents at the bridging carbon. One of these compounds has the properties of a thyroid hormone antagonist. The last chapter describes a study to determine the structural features of GC-1 that are responsible for its TR β -selectivity.

1.12. References

- [1] Kendall, E.C. (1915). The isolation in crystalline form of the compound containing iodine, which occurs in the thyroid. Its chemical nature and physiologic activity. *Transactions of the Association of American Physicians* **30**, 420-449.
- [2] Harington, C.R. (1926). Chemistry of thyroxine. I. Isolation of thyroxine from the thyroid gland. *Biochemical Journal* **20**, 293-299.
- [3] Harington, C.R. (1926). Chemistry of thyroxine. II. Constitution and synthesis of desiodo-thyroxine. *Biochemical Journal* **20**, 300-313.
- [4] Harington, C.R. & Barger, G. (1927). Chemistry of thyroxine. III. Constitution and synthesis of thyroxine. *Biochemical Journal* **21**, 169-183.
- [5] Gross, J. & Pitt-Rivers, R. (1952). Effect of 3,5,3'-L-triiodothyronine in myxedema. *Lancet* 1044-1045.
- [6] Gross, J. & Pitt-Rivers, R. (1952). The identification of 3,5,3'-triiodothyronine in human plasma. *Lancet* 439-441.
- [7] Chopra, I.J. (1991). Nature, sources, and relative biologic significance of circulating thyroid hormones. 6th Ed. ed. In "Werner and Ingbar's the thyroid: a fundamental and clinical text" (L. E. Braverman and R. D. Utiger, eds.), pp. 126-143. J. B. Lippincott Company, Philadelphia.
- [8] Kohrle, J. (2000). The selenoenzyme family of deiodinase isozymes controls local thyroid hormone availability. *Reviews in Endocrine and Metabolic Disorders* **1**, 49-58.
- [9] Dai, G., Levy, O. & Carrasco, N. (1996). Cloning and characterization of the thyroid iodide transporter. *Nature* **379**, 458-60.

- [10] Taurog, A. (1991). Hormone synthesis: thyroid iodine metabolism. 6th Ed. ed. *In* "Werner and Ingbar's the thyroid: a fundamental and clinical text" (R. D. Utiger, ed.), pp. 51-97. J. B. Lippincott Company, Philadelphia.
- [11] Sun, W. & Dunford, H.B. (1993). Kinetics and mechanism of the peroxidase-catalyzed iodination of tyrosine. *Biochemistry* **32**, 1324-31.
- [12] Dunn, J.T. (1995). Thyroglobulin, hormone synthesis and thyroid disease. *European Journal of Endocrinology* **132**, 603-4.
- [13] Taurog, A., Porter, J.C. & Thio, D.T. (1964). Nature of the ¹³¹I-compounds released into the thyroid veins of rabbits dogs and cats before and after TSH administration. *Endocrinology* **74**, 902-913.
- [14] Parmentier, M., Libert, F., Maenhaut, C., Lefort, A., Gerard, C., Perret, J., Van Sande, J., Dumont, J.E. & Vassart, G. (1989). Molecular cloning of the thyrotropin receptor. *Science* **246**, 1620-2.
- [15] Allgeier, A., Offermanns, S., Van Sande, J., Spicher, K., Schultz, G. & Dumont, J.E. (1994). The human thyrotropin receptor activates G-proteins Gs and Gq/11. *Journal of Biological Chemistry* **269**, 13733-5.
- [16] Davies, T., Marians, R. & Latif, R. (2002). The TSH receptor reveals itself. *Journal of Clinical Investigation* **110**, 161-4.
- [17] Szkudlinski, M.W., Fremont, V., Ronin, C. & Weintraub, B.D. (2002). Thyroid-stimulating hormone and thyroid-stimulating hormone receptor structure-function relationships. *Physiological Reviews* **82**, 473-502.
- [18] Nillni, E.A. & Sevarino, K.A. (1999). The biology of pro-thyrotropin-releasing hormone-derived peptides. *Endocrine Reviews* **20**, 599-648.

- [19] Robbins, J. (1991). Thyroid hormone transport proteins and the physiology of hormone binding. 6th Ed. ed. *In* "Werner and Ingbar's the thyroid: a fundamental and clinical text" (L. E. Braverman and R. D. Utiger, eds.), pp. 111-125. J. B. Lippincott Company, Philadelphia.
- [20] Robbins, J. & Rall, J.E. (1979). The iodine containing hormones. 3rd ed. *In* "Hormones in blood" (C. H. Gray and V. H. T. James, eds.), Vol. 1, pp. 576-688. 3 vols. Academic Press, London.
- [21] Ribeiro, R.C., Cavalieri, R.R., Lomri, N., Rahmaoui, C.M., Baxter, J.D. & Scharschmidt, B.F. (1996). Thyroid hormone export regulates cellular hormone content and response. *Journal of Biological Chemistry* **271**, 17147-51.
- [22] Shi, Y.B., Ritchie, J.W. & Taylor, P.M. (2002). Complex regulation of thyroid hormone action: multiple opportunities for pharmacological intervention. *Pharmacology & Therapeutics* **94**, 235-51.
- [23] Kohrle, J., Hesch, R.D. & Leonard, J.L. (1991). Intracellular pathways of iodothyronine metabolism. 6th Ed. ed. *In* "Werner and Ingbar's the thyroid: a fundamental and clinical text" (L. E. Braverman and R. D. Utiger, eds.), pp. 144-189. J. B. Lippincott Company, Philadelphia.
- [24] Delange, F.M. (1991). Endemic cretinism. 6th Ed. ed. *In* "Werner and Ingbar's the thyroid: a fundamental and clinical text" (L. E. Braverman and R. D. Utiger, eds.), pp. 942-955. J. B. Lippincott Company, Philadelphia.
- [25] Oppenheimer, J.H. & Schwartz, H.L. (1997). Molecular basis of thyroid hormone-dependent brain development. *Endocrine Reviews* **18**, 462-75.

- [26] Everts, M.E., van Hardeveld, C., Ter Keurs, H.E. & Kassenaar, A.A. (1983). Force development and metabolism in perfused skeletal muscle of euthyroid and hyperthyroid rats. *Hormone and Metabolic Research* **15**, 388-93.
- [27] Capo, L.A. & Sillau, A.H. (1983). The effect of hyperthyroidism on capillarity and oxidative capacity in rat soleus and gastrocnemius muscles. *Journal of Physiology* **342**, 1-14.
- [28] Leijendekker, W.J., van Hardeveld, C. & Kassenaar, A.A. (1983). The influence of the thyroid state on energy turnover during tetanic stimulation in the fast-twitch (mixed type) muscle of rats. *Metabolism* **32**, 615-21.
- [29] Mason, R.L., Hunt, H.M. & Hurxthal, L. (1930). Blood cholesterol values in hyperthyroidism and hyperthyroidism. *New England Journal of Medicine* **203**, 1273-1278.
- [30] Freake, H.C., Schwartz, H.L. & Oppenheimer, J.H. (1989). The regulation of lipogenesis by thyroid hormone and its contribution to thermogenesis. *Endocrinology* **125**, 2868-74.
- [31] Harlan, W.R., Lazlo, J., Bogdonoff, M.D. & Estes, E.H., Jr. (1963). Alterations in free fatty acid metabolism in endocrine disorders. I. Effect of thyroid hormone. *Journal of Clinical Endocrinology and Metabolism* **23**, 33-40.
- [32] Ness, G.C., Dugan, R.E., Lakshmanan, M.R., Nepokroeff, C.M. & Porter, J.W. (1973). Stimulation of hepatic beta-hydroxy-beta-methylglutaryl coenzyme A reductase activity in hypophysectomized rats by L-triiodothyronine. *Proceedings of the National Academy of Sciences of the United States of America* **70**, 3839-42.

- [33] Ness, G.C., Pendelton, L.C. & Zhao, Z. (1994). Thyroid hormone rapidly increases cholesterol 7 alpha-hydroxylase mRNA levels in hypophysectomized rats. *Biochimica Biophysica Acta* **1214**, 229-33.
- [34] Duntas, L.H. (2002). Thyroid disease and lipids. *Thyroid* **12**, 287-93.
- [35] Ness, G.C. & Zhao, Z. (1994). Thyroid hormone rapidly induces hepatic LDL receptor mRNA levels in hypophysectomized rats. *Archives of Biochemistry and Biophysics* **315**, 199-202.
- [36] Freedland, R.A. & Krebs, H.A. (1967). The effect of thyroxine treatment on the rate of gluconeogenesis in the perfused rat liver. *Biochemical Journal* **104**, 45P.
- [37] Svedmyr, N. (1966). Studies on the relationships between some metabolic effects of thyroid hormones and catecholamines in animals and man. *Acta Physiologica Scandinavica. Supplementum* **274**, 1-46.
- [38] Debons, A.F. & Schwartz, I.L. (1961). Dependence of the lipolytic action of epinephrine in vitro upon thyroid hormone. *Journal of Lipid Research* **2**, 86-89.
- [39] Himms-Hagen, J. (1985). Brown adipose tissue metabolism and thermogenesis. *Annual Review of Nutrition* **5**, 69-94.
- [40] Reiter, E.O. & Rosenfeld, R.G. (1998). Normal and aberrant growth. In "Williams Textbook of Endocrinology" (J. D. Wilson, D. W. Foster, H. M. Kronenberg and P. R. Larsen, eds.), pp. 1427-1507. Saunders, Philadelphia.
- [41] Eriksen, E.F., Mosekilde, L. & Melsen, F. (1986). Kinetics of trabecular bone resorption and formation in hypothyroidism: evidence for a positive balance per remodeling cycle. *Bone* **7**, 101-8.

- [42] Hasling, C., Eriksen, E.F., Charles, P. & Mosekilde, L. (1987). Exogenous triiodothyronine activates bone remodeling. *Bone* **8**, 65-9.
- [43] Eriksen, E.F., Mosekilde, L. & Melsen, F. (1985). Trabecular bone remodeling and bone balance in hyperthyroidism. *Bone* **6**, 421-8.
- [44] Fallon, M.D., Perry, H.M., 3rd, Bergfeld, M., Droke, D., Teitelbaum, S.L. & Avioli, L.V. (1983). Exogenous hyperthyroidism with osteoporosis. *Archives of Internal Medicine* **143**, 442-4.
- [45] Crowley, W.F., Jr., Ridgway, E.C., Bough, E.W., Francis, G.S., Daniels, G.H., Kourides, I.A., Myers, G.S. & Maloof, F. (1977). Noninvasive evaluation of cardiac function in hypothyroidism. Response to gradual thyroxine replacement. *New England Journal of Medicine* **296**, 1-6.
- [46] Wieshammer, S., Keck, F.S., Waitzinger, J., Henze, E., Loos, U., Hombach, V. & Pfeiffer, E.F. (1989). Acute hypothyroidism slows the rate of left ventricular diastolic relaxation. *Canadian Journal of Physiology and Pharmacology* **67**, 1007-10.
- [47] Klein, I. & Ojamaa, K. (2001). Thyroid hormone and the cardiovascular system. *New England Journal of Medicine* **344**, 501-9.
- [48] Klein, I. & Ojamaa, K. (1998). Thyrotoxicosis and the heart. *Endocrinology and Metabolism Clinics of North America* **27**, 51-62.
- [49] Ojamaa, K. & Klein, I. (1993). In vivo regulation of recombinant cardiac myosin heavy chain gene expression by thyroid hormone. *Endocrinology* **132**, 1002-6.

- [50] Ojamaa, K., Klemperer, J.D., MacGilvray, S.S., Klein, I. & Samarel, A. (1996). Thyroid hormone and hemodynamic regulation of beta-myosin heavy chain promoter in the heart. *Endocrinology* **137**, 802-8.
- [51] Hartong, R., Villarreal, F.J., Giordano, F., Hilal-Dandan, R., McDonough, P.M. & Dillmann, W.H. (1996). Phorbol myristate acetate-induced hypertrophy of neonatal rat cardiac myocytes is associated with decreased sarcoplasmic reticulum Ca²⁺ ATPase (SERCA2) gene expression and calcium reuptake. *Journal of Molecular and Cellular Cardiology* **28**, 2467-77.
- [52] Trost, S.U., Swanson, E., Gloss, B., Wang-Iverson, D.B., Zhang, H.J., Volodarsky, T., Grover, G.J., Baxter, J.D., Chiellini, G., Scanlan, T.S. & Dillmann, W.H. (2000). The thyroid hormone receptor-beta-selective agonist GC-1 differentially affects plasma lipids and cardiac activity. *Endocrinology* **141**, 3057-3064.
- [53] Pachucki, J., Burmeister, L.A. & Larsen, P.R. (1999). Thyroid hormone regulates hyperpolarization-activated cyclic nucleotide-gated channel (HCN2) mRNA in the rat heart. *Circulation Research* **85**, 498-503.
- [54] Oppenheimer, J.H., Koerner, D., Schwartz, H.L. & Surks, M.I. (1972). Specific nuclear triiodothyronine binding sites in rat liver and kidney. *Journal of Clinical Endocrinology and Metabolism* **35**, 330-3.
- [55] Samuels, H.H. & Tsai, J.S. (1973). Thyroid hormone action in cell culture: demonstration of nuclear receptors in intact cells and isolated nuclei. *Proceedings of the National Academy of Sciences of the United States of America* **70**, 3488-92.

- [56] Surks, M.I., Koerner, D., Dillman, W. & Oppenheimer, J.H. (1973). Limited capacity binding sites for L-triiodothyronine in rat liver nuclei. Localization to the chromatin and partial characterization of the L-triiodothyronine-chromatin complex. *Journal of Biological Chemistry* **248**, 7066-72.
- [57] Oppenheimer, J.H., Schwartz, H.L. & Surks, M.I. (1974). Tissue differences in the concentration of triiodothyronine nuclear binding sites in the rat: liver, kidney, pituitary, heart, brain, spleen, and testis. *Endocrinology* **95**, 897-903.
- [58] Oppenheimer, J.H., Schwartz, H.L., Dillman, W. & Surks, M.I. (1973). Effect of thyroid hormone analogues on the displacement of ¹²⁵I-L-triiodothyronine from hepatic and heart nuclei in vivo: possible relationship to hormonal activity. *Biochemical and Biophysical Research Communications* **55**, 544-50.
- [59] Koerner, D., Schwartz, H.L., Surks, M.I. & Oppenheimer, J.H. (1975). Binding of selected iodothyronine analogues to receptor sites of isolated rat hepatic nuclei. High correlation between structural requirements for nuclear binding and biological activity. *Journal of Biological Chemistry* **250**, 6417-23.
- [60] Casanova, J., Horowitz, Z.D., Copp, R.P., McIntyre, W.R., Pascual, A. & Samuels, H.H. (1984). Photoaffinity labeling of thyroid hormone nuclear receptors. Influence of n-butyrate and analysis of the half-lives of the 57,000 and 47,000 molecular weight receptor forms. *Journal of Biological Chemistry* **259**, 12084-91.
- [61] Ichikawa, K. & DeGroot, L.J. (1987). Thyroid hormone receptors in a human hepatoma cell line: multiple receptor forms on isoelectric focusing. *Molecular and Cellular Endocrinology* **51**, 135-43.

- [62] Sap, J., Munoz, A., Damm, K., Goldberg, Y., Ghysdael, J., Leutz, A., Beug, H. & Vennstrom, B. (1986). The c-erb-A protein is a high-affinity receptor for thyroid hormone. *Nature* **324**, 635-40.
- [63] Weinberger, C., Thompson, C.C., Ong, E.S., Lebo, R., Gruol, D.J. & Evans, R.M. (1986). The c-erb-A gene encodes a thyroid hormone receptor. *Nature* **324**, 641-6.
- [64] Benbrook, D. & Pfahl, M. (1987). A Novel Thyroid-Hormone Receptor Encoded by a Cdna Clone from a Human Testis Library. *Science* **238**, 788-791.
- [65] Evans, R.M. (1988). The steroid and thyroid hormone receptor superfamily. *Science* **240**, 889-95.
- [66] Mangelsdorf, D.J., Thummel, C., Beato, M., Herrlich, P., Schutz, G., Umesono, K., Blumberg, B., Kastner, P., Mark, M., Chambon, P. & et al. (1995). The nuclear receptor superfamily: the second decade. *Cell* **83**, 835-9.
- [67] Glass, C.K. & Holloway, J.M. (1990). Regulation of gene expression by the thyroid hormone receptor. *Biochimica et Biophysica Acta* **1032**, 157-76.
- [68] Hollenberg, A.N., Monden, T., Madura, J.P., Lee, K. & Wondisford, F.E. (1996). Function of nuclear co-repressor protein on thyroid hormone response elements is regulated by the receptor A/B domain. *Journal of Biological Chemistry* **271**, 28516-20.
- [69] Hollenberg, A.N., Monden, T. & Wondisford, F.E. (1995). Ligand-independent and -dependent functions of thyroid hormone receptor isoforms depend upon their distinct amino termini. *Journal of Biological Chemistry* **270**, 14274-80.
- [70] Lazar, M.A. (1993). Thyroid hormone receptors: multiple forms, multiple possibilities. *Endocrine Reviews* **14**, 184-93.

- [71] Tagami, T., Nakamura, H., Sasaki, S., Miyoshi, Y. & Imura, H. (1993). Estimation of the protein content of thyroid hormone receptor alpha 1 and beta 1 in rat tissues by western blotting. *Endocrinology* **132**, 275-9.
- [72] Umesono, K., Murakami, K.K., Thompson, C.C. & Evans, R.M. (1991). Direct repeats as selective response elements for the thyroid hormone, retinoic acid, and vitamin D3 receptors. *Cell* **65**, 1255-66.
- [73] Rastinejad, F., Perlmann, T., Evans, R.M. & Sigler, P.B. (1995). Structural determinants of nuclear receptor assembly on DNA direct repeats. *Nature* **375**, 203-11.
- [74] Wagner, R.L., Apriletti, J.W., McGrath, M.E., West, B.L., Baxter, J.D. & Fletterick, R.J. (1995). A structural role for hormone in the thyroid hormone receptor. *Nature* **378**, 690-7.
- [75] Darimont, B.D., Wagner, R.L., Apriletti, J.W., Stallcup, M.R., Kushner, P.J., Baxter, J.D., Fletterick, R.J. & Yamamoto, K.R. (1998). Structure and specificity of nuclear receptor-coactivator interactions. *Genes & Development* **12**, 3343-56.
- [76] Feng, X., Jiang, Y., Meltzer, P. & Yen, P.M. (2000). Thyroid hormone regulation of hepatic genes in vivo detected by complementary DNA microarray. *Molecular Endocrinology* **14**, 947-55.
- [77] Zhang, J.S. & Lazar, M.A. (2000). The mechanism of action of thyroid hormones. *Annual Review of Physiology* **62**, 439-466.
- [78] Nolte, R.T., Wisely, G.B., Westin, S., Cobb, J.E., Lambert, M.H., Kurokawa, R., Rosenfeld, M.G., Willson, T.M., Glass, C.K. & Milburn, M.V. (1998). Ligand

- binding and co-activator assembly of the peroxisome proliferator-activated receptor-gamma. *Nature* **395**, 137-43.
- [79] Shiau, A.K., Barstad, D., Loria, P.M., Cheng, L., Kushner, P.J., Agard, D.A. & Greene, G.L. (1998). The structural basis of estrogen receptor/coactivator recognition and the antagonism of this interaction by tamoxifen. *Cell* **95**, 927-37.
- [80] Onate, S.A., Boonyaratanakornkit, V., Spencer, T.E., Tsai, S.Y., Tsai, M.J., Edwards, D.P. & O'Malley, B.W. (1998). The steroid receptor coactivator-1 contains multiple receptor interacting and activation domains that cooperatively enhance the activation function 1 (AF1) and AF2 domains of steroid receptors. *Journal of Biological Chemistry* **273**, 12101-8.
- [81] Spencer, T.E., Jenster, G., Burcin, M.M., Allis, C.D., Zhou, J., Mizzen, C.A., McKenna, N.J., Onate, S.A., Tsai, S.Y., Tsai, M.J. & O'Malley, B.W. (1997). Steroid receptor coactivator-1 is a histone acetyltransferase. *Nature* **389**, 194-8.
- [82] Kadonaga, J.T. (1998). Eukaryotic transcription: an interlaced network of transcription factors and chromatin-modifying machines. *Cell* **92**, 307-13.
- [83] Feng, W., Ribeiro, R.C., Wagner, R.L., Nguyen, H., Apriletti, J.W., Fletterick, R.J., Baxter, J.D., Kushner, P.J. & West, B.L. (1998). Hormone-dependent coactivator binding to a hydrophobic cleft on nuclear receptors. *Science* **280**, 1747-9.
- [84] Weiss, R.E., Xu, J., Ning, G., Pohlenz, J., O'Malley, B.W. & Refetoff, S. (1999). Mice deficient in the steroid receptor co-activator 1 (SRC-1) are resistant to thyroid hormone. *EMBO Journal* **18**, 1900-4.

- [85] Fondell, J.D., Ge, H. & Roeder, R.G. (1996). Ligand induction of a transcriptionally active thyroid hormone receptor coactivator complex. *Proceedings of the National Academy of Sciences of the United States of America* **93**, 8329-33.
- [86] Malik, S. & Roeder, R.G. (2000). Transcriptional regulation through Mediator-like coactivators in yeast and metazoan cells. *Trends in Biochemical Sciences* **25**, 277-83.
- [87] Yuan, C.X., Ito, M., Fondell, J.D., Fu, Z.Y. & Roeder, R.G. (1998). The TRAP220 component of a thyroid hormone receptor-associated protein (TRAP) coactivator complex interacts directly with nuclear receptors in a ligand-dependent fashion. *Proceedings of the National Academy of Sciences of the United States of America* **95**, 7939-44.
- [88] Ito, M., Yuan, C.X., Okano, H.J., Darnell, R.B. & Roeder, R.G. (2000). Involvement of the TRAP220 component of the TRAP/SMCC coactivator complex in embryonic development and thyroid hormone action. *Molecular Cell* **5**, 683-93.
- [89] Chen, J.D. & Evans, R.M. (1995). A transcriptional co-repressor that interacts with nuclear hormone receptors. *Nature* **377**, 454-7.
- [90] Horlein, A.J., Naar, A.M., Heinzl, T., Torchia, J., Gloss, B., Kurokawa, R., Ryan, A., Kamei, Y., Soderstrom, M., Glass, C.K. & et al. (1995). Ligand-independent repression by the thyroid hormone receptor mediated by a nuclear receptor co-repressor. *Nature* **377**, 397-404.

- [91] Nagy, L., Kao, H.Y., Love, J.D., Li, C., Banayo, E., Gooch, J.T., Krishna, V., Chatterjee, K., Evans, R.M. & Schwabe, J.W. (1999). Mechanism of corepressor binding and release from nuclear hormone receptors. *Genes & Development* **13**, 3209-16.
- [92] Perissi, V., Staszewski, L.M., McInerney, E.M., Kurokawa, R., Krones, A., Rose, D.W., Lambert, M.H., Milburn, M.V., Glass, C.K. & Rosenfeld, M.G. (1999). Molecular determinants of nuclear receptor-corepressor interaction. *Genes & Development* **13**, 3198-208.
- [93] Webb, P., Anderson, C.M., Valentine, C., Nguyen, P., Marimuthu, A., West, B.L., Baxter, J.D. & Kushner, P.J. (2000). The nuclear receptor corepressor (N-CoR) contains three isoleucine motifs (I/LXXII) that serve as receptor interaction domains (IDs). *Molecular Endocrinology* **14**, 1976-85.
- [94] Nagy, L., Kao, H.Y., Chakravarti, D., Lin, R.J., Hassig, C.A., Ayer, D.E., Schreiber, S.L. & Evans, R.M. (1997). Nuclear receptor repression mediated by a complex containing SMRT, mSin3A, and histone deacetylase. *Cell* **89**, 373-80.
- [95] Heinzl, T., Lavinsky, R.M., Mullen, T.M., Soderstrom, M., Laherty, C.D., Torchia, J., Yang, W.M., Brard, G., Ngo, S.D., Davie, J.R., Seto, E., Eisenman, R.N., Rose, D.W., Glass, C.K. & Rosenfeld, M.G. (1997). A complex containing N-CoR, mSin3 and histone deacetylase mediates transcriptional repression. *Nature* **387**, 43-8.
- [96] Hashimoto, K., Curty, F.H., Borges, P.P., Lee, C.E., Abel, E.D., Elmquist, J.K., Cohen, R.N. & Wondisford, F.E. (2001). An unliganded thyroid hormone

- receptor causes severe neurological dysfunction. *Proceedings of the National Academy of Sciences of the United States of America* **98**, 3998-4003.
- [97] Refetoff, S., Weiss, R.E. & Usala, S.J. (1993). The syndromes of resistance to thyroid hormone. *Endocrine Reviews* **14**, 348-99.
- [98] Clifton-Bligh, R.J., de Zegher, F., Wagner, R.L., Collingwood, T.N., Francois, I., Van Helvoirt, M., Fletterick, R.J. & Chatterjee, V.K. (1998). A novel TR beta mutation (R383H) in resistance to thyroid hormone syndrome predominantly impairs corepressor release and negative transcriptional regulation. *Molecular Endocrinology* **12**, 609-21.
- [99] Collingwood, T.N., Wagner, R., Matthews, C.H., Clifton-Bligh, R.J., Gurnell, M., Rajanayagam, O., Agostini, M., Fletterick, R.J., Beck-Peccoz, P., Reinhardt, W., Binder, G., Ranke, M.B., Hermus, A., Hesch, R.D., Lazarus, J., Newrick, P., Parfitt, V., Raggatt, P., de Zegher, F. & Chatterjee, V.K. (1998). A role for helix 3 of the TRbeta ligand-binding domain in coactivator recruitment identified by characterization of a third cluster of mutations in resistance to thyroid hormone. *EMBO Journal* **17**, 4760-70.
- [100] Forrest, D., Erway, L.C., Ng, L., Altschuler, R. & Curran, T. (1996). Thyroid hormone receptor beta is essential for development of auditory function. *Nature Genetics* **13**, 354-7.
- [101] Forrest, D., Hanebuth, E., Smeyne, R.J., Everds, N., Stewart, C.L., Wehner, J.M. & Curran, T. (1996). Recessive resistance to thyroid hormone in mice lacking thyroid hormone receptor beta: evidence for tissue-specific modulation of receptor function. *EMBO Journal* **15**, 3006-15.

- [102] Ng, L., Hurley, J.B., Dierks, B., Srinivas, M., Salto, C., Vennstrom, B., Reh, T.A. & Forrest, D. (2001). A thyroid hormone receptor that is required for the development of green cone photoreceptors. *Nature Genetics* **27**, 94-8.
- [103] Fraichard, A., Chassande, O., Plateroti, M., Roux, J.P., Trouillas, J., Dehay, C., Legrand, C., Gauthier, K., Kedinger, M., Malaval, L., Rousset, B. & Samarut, J. (1997). The T3R alpha gene encoding a thyroid hormone receptor is essential for post-natal development and thyroid hormone production. *EMBO Journal* **16**, 4412-20.
- [104] Wikstrom, L., Johansson, C., Salto, C., Barlow, C., Campos Barros, A., Baas, F., Forrest, D., Thoren, P. & Vennstrom, B. (1998). Abnormal heart rate and body temperature in mice lacking thyroid hormone receptor alpha 1. *EMBO Journal* **17**, 455-61.
- [105] Salto, C., Kindblom, J.M., Johansson, C., Wang, Z., Gullberg, H., Nordstrom, K., Mansen, A., Ohlsson, C., Thoren, P., Forrest, D. & Vennstrom, B. (2001). Ablation of TRalpha2 and a concomitant overexpression of alpha1 yields a mixed hypo- and hyperthyroid phenotype in mice. *Molecular Endocrinology* **15**, 2115-28.
- [106] Chassande, O., Fraichard, A., Gauthier, K., Flamant, F., Legrand, C., Savatier, P., Laudet, V. & Samarut, J. (1997). Identification of transcripts initiated from an internal promoter in the c-erbA alpha locus that encode inhibitors of retinoic acid receptor-alpha and triiodothyronine receptor activities. *Molecular Endocrinology* **11**, 1278-90.

- [107] Macchia, P.E., Takeuchi, Y., Kawai, T., Cua, K., Gauthier, K., Chassande, O., Seo, H., Hayashi, Y., Samarut, J., Murata, Y., Weiss, R.E. & Refetoff, S. (2001). Increased sensitivity to thyroid hormone in mice with complete deficiency of thyroid hormone receptor alpha. *Proceedings of the National Academy of Sciences of the United States of America* **98**, 349-354.
- [108] Gauthier, K., Chassande, O., Plateroti, M., Roux, J.P., Legrand, C., Pain, B., Rousset, B., Weiss, R., Trouillas, J. & Samarut, J. (1999). Different functions for the thyroid hormone receptors TRalpha and TRbeta in the control of thyroid hormone production and post-natal development. *EMBO Journal* **18**, 623-31.
- [109] Gothe, S., Wang, Z., Ng, L., Kindblom, J.M., Barros, A.C., Ohlsson, C., Vennstrom, B. & Forrest, D. (1999). Mice devoid of all known thyroid hormone receptors are viable but exhibit disorders of the pituitary-thyroid axis, growth, and bone maturation. *Genes & Development* **13**, 1329-41.
- [110] Jorgensen, E.C. (1978). Thyroid hormones and analogs. I. synthesis, physical properties and theoretical calculations. In "Hormonal Proteins and Peptides" (C. H. Li, ed.), Vol. 6, pp. 57-105. Academic Press, New York.
- [111] Jorgensen, E.C. (1978). Thyroid hormones and analogs. II. structure-activity relationships. In "Hormonal Proteins and Peptides" (C. H. Li, ed.), Vol. 6, pp. 107-204. Academic Press, New York.
- [112] Scanlan, T.S., Yoshihara, H.A.I., Nguyen, N.H. & Chiellini, G. (2001). Selective thyromimetics: Tissue-selective thyroid hormone analogs. *Current Opinion in Drug Discover & Development* **4**, 614-622.

- [113] Chiellini, G., Nguyen, N.H., Yoshihara, H.A.I. & Scanlan, T.S. (2000). Improved synthesis of the iodine-free thyromimetic GC-1. *Bioorganic & Medicinal Chemistry Letters* **10**, 2607-2611.
- [114] Chiellini, G., Apriletti, J.W., Yoshihara, H.A.I., Baxter, J.D., Ribeiro, R.C.J. & Scanlan, T.S. (1998). A high-affinity subtype-selective agonist ligand for the thyroid hormone receptor. *Chemistry & Biology* **5**, 299-306.
- [115] Baxter, J.D., Dillmann, W.H., West, B.L., Huber, R., Furlow, J.D., Fletterick, R.J., Webb, P., Apriletti, J.W. & Scanlan, T.S. (2001). Selective modulation of thyroid hormone receptor action. *Journal of Steroid Biochemistry and Molecular Biology* **76**, 31-42.
- [116] Ribeiro, M.O., Carvalho, S.D., Schultz, J.J., Chiellini, G., Scanlan, T.S., Bianco, A.C. & Brent, G.A. (2001). Thyroid hormone-sympathetic interaction and adaptive thermogenesis are thyroid hormone receptor isoform-specific. *Journal of Clinical Investigation* **108**, 97-105.
- [117] Morte, B., Manzano, J., Scanlan, T., Vennstrom, B. & Bernal, J. (2002). Deletion of the thyroid hormone receptor alpha 1 prevents the structural alterations of the cerebellum induced by hypothyroidism. *Proceedings of the National Academy of Sciences of the United States of America* **99**, 3985-3989.
- [118] Wagner, R.L., Huber, B.R., Shiau, A.K., Kelly, A., Lima, S.T.C., Scanlan, T.S., Apriletti, J.W., Baxter, J.D., West, B.L. & Fletterick, R.J. (2001). Hormone selectivity in thyroid hormone receptors. *Molecular Endocrinology* **15**, 398-410.
- [119] Weatherman, R.V., Fletterick, R.J. & Scanlan, T.S. (1999). Nuclear-receptor ligands and ligand-binding domains. *Annual Review of Biochemistry* **68**, 559-581.

- [120] Chiellini, G., Nguyen, N.H., Apriletti, J.W., Baxter, J.D. & Scanlan, T.S. (2002). Synthesis and biological activity of novel thyroid hormone analogues: 5'-aryl substituted GC-1 derivatives. *Bioorganic & Medicinal Chemistry* **10**, 333-346.
- [121] Baxter, J.D., Goede, P., Apriletti, J.W., West, B.L., Feng, W.J., Mellstrom, K., Fletterick, R.J., Wagner, R.L., Kushner, P.J., Ribeiro, R.C.J., Webb, P., Scanlan, T.S. & Nilsson, S. (2002). Structure-based design and synthesis of a thyroid hormone receptor (TR) antagonist. *Endocrinology* **143**, 517-524.
- [122] Nguyen, N.H., Apriletti, J.W., Cunha Lima, S.T., Webb, P., Baxter, J.D. & Scanlan, T.S. (2002). Rational design and synthesis of a novel thyroid hormone antagonist that blocks coactivator recruitment. *Journal of Medicinal Chemistry* **45**, 3310-20.
- [123] Lim, W., Nguyen, N.H., Yang, H.Y., Scanlan, T.S. & Furlow, J.D. (2002). A Thyroid Hormone Antagonist That Inhibits Thyroid Hormone Action in Vivo. *Journal of Biological Chemistry* **277**, 35664-35670.

Chapter 2: An Efficient Substitution Reaction for the Preparation of Thyroid Hormone Analogues

Originally published as: Yoshihara, H.A.I., Chiellini, G., Mitchison, T.J. & Scanlan, T.S. (1998). An efficient substitution reaction for the preparation of thyroid hormone analogues. *Bioorganic & Medicinal Chemistry* **6**, 1179-1183. I prepared and characterized compounds **10 - 14**.

2.1. Introduction

3,5,3'-Triiodo-L-thyronine (T_3) is the major active form of thyroid hormone which is an important endocrine signaling molecule in vertebrates [1]. Most of the physiological actions of T_3 result from transcriptional regulation T_3 -responsive genes that is mediated through thyroid hormone receptors (TRs). The TR belongs to the nuclear receptor superfamily of ligand-activated transcription regulators that includes steroid receptors such as the estrogen receptor (ER) and glucocorticoid receptor (GR), as well as receptors that like TR, are activated by non-steroid ligands such as the retinoic acid receptor (RAR) and retinoid X receptor (RXR) [2-4]. There are two different TRs in vertebrates designated $TR\alpha$ and $TR\beta$ that are coexpressed in different ratios in different tissue [5]. The hypothesis that the different TRs are linked to the different tissue-specific effects of T_3 guides our efforts in TR ligand design.

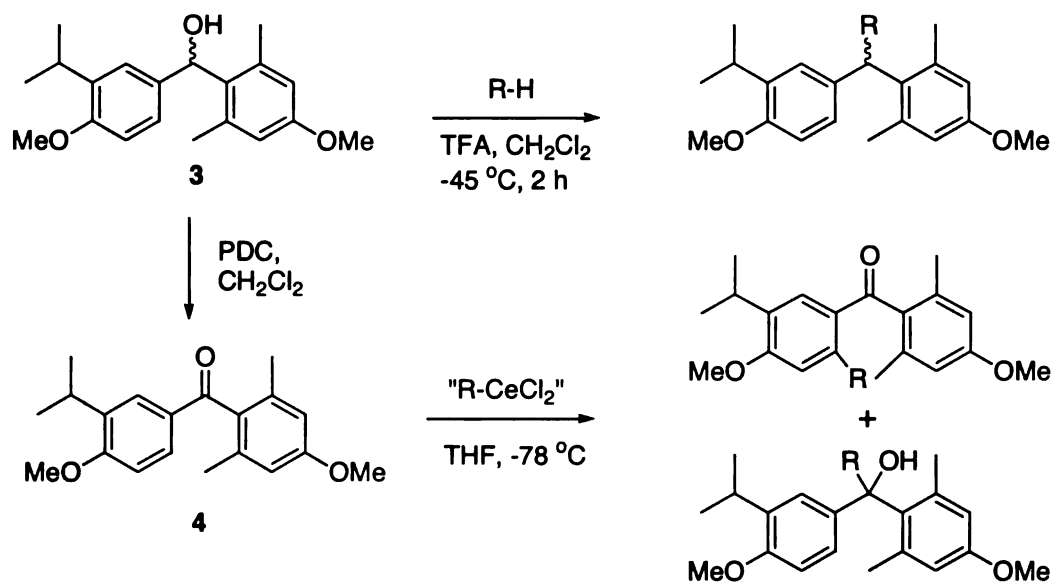
Although antagonist ligands have been developed for a number of nuclear receptors, there is currently no reported high-affinity antagonist for the TR. Examination of known nuclear receptor antagonist ligands reveals that these compounds structurally resemble their agonist counterparts but contain a large (> 8 carbon atom) extension group attached to the middle of the molecule [6]. This has led us to undertake synthetic studies of thyroid hormone analogs in an effort to prepare a high-affinity antagonist that contain an extension group attached to the middle of a TR agonist. We have recently prepared and characterized a high affinity $TR\beta$ -selective agonist ligand, GC-1, that contains several structural differences from T_3 [7]. In particular, the methylene unit bridging the two phenyl rings introduces a new derivatizable position in the middle of the molecule which is unavailable in the natural ligand where an ether oxygen joins the rings.

It was toward this bridging carbon that we first directed our efforts in synthesizing derivatives of GC-1. Initial attempts at adding extensions to the benzophenone **4** failed

using alkyl lithium and Grignard reagents. Organocerium reagents were more successful but yields were generally too low to be useful. Using an S_N1 reaction inspired by one used in the preparation of semi-synthetic rapamycin derivatives [8; 9] we have found a route to the efficient derivatization of the bridging carbon with a panel of nucleophiles. The resulting derivatives can be converted to thyromimetics using the same chemistry that was established for the synthesis of GC-1 [7].

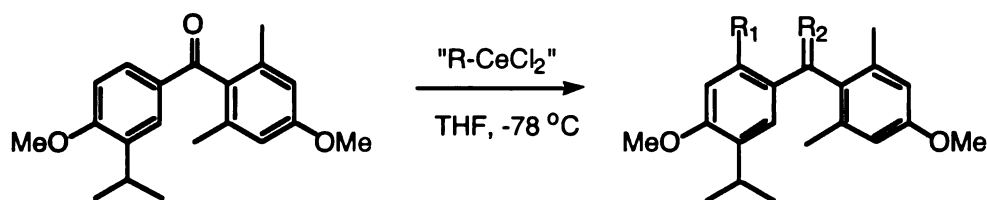
2.2. Results and Discussion

The benzyl alcohol **3** produced by the coupling of the two rings was oxidized with PDC to the benzophenone **4** (Scheme 2.1). It was our plan to add extensions to the carbonyl function of **4** using organolithium nucleophiles. Attempts with *n*-butyllithium, *sec*-butyllithium, phenyllithium and lithium phenylacetylide resulted in poor yields and recovery of starting material. Grignard reagents also fared poorly, with *sec*-butylmagnesium chloride and octylmagnesium bromide both failing to react. Rationalizing the low reactivity of the carbonyl to its sterically congested environment, we then tried the organocerium(III) analogues, which had been previously shown to react with similarly sterically hindered phenyl ketones [10]. Butylcerium(III) reagents were prepared *in situ* via transmetalation from the corresponding butyllithiums and $CeCl_3$. 1.3 equivalents of *n*-butylcerium(III) chloride reacted with **4** to yield an approximate equimolar mix of the 1,4- and 1,2-addition products **5** and **6**, respectively; whereas a ten-fold excess of cerium reagent yielded **5** only (Table 2.1). The apparent 1,4-addition to the phenyl ring seen in **5** was also observed when *sec*-butylcerium(III) chloride was used. It is notable that this side reaction should occur given that organocerium reagents were previously observed to add exclusively in a 1,2 fashion to α,β -unsaturated ketones and furfural [11]. Methylcerium(III) chloride reacted with **4** to produce the 1,2-addition product **9** in 42% yield, which was the only product obtained in sufficient quantities to allow conversion into a thyroid hormone analogue.



Scheme 2.1. Routes for derivatizing the carbon bridge of GC-1

This route clearly was not efficient or versatile enough for our purposes and a new scheme was devised based on the solvolysis of the benzyloxy group of **3**. We reasoned that a carbonium ion would be formed easily from **3** in acidic conditions. This carbonium ion would be stabilized by the two electron-rich aromatic rings leaving it vulnerable to attack by acid-stable nucleophilic species at the desired bridging carbon (Scheme 1). Following the conditions used for rapamycin [8; 9] (TFA, CH_2Cl_2 , $-45\text{ }^\circ\text{C}$), we found ethanol to substitute in high yield with no detectable starting material or side products. Subsequent attempts with allyltrimethylsilane, 1,3-dimethoxybenzene, ethanethiol and thiophenol all proceeded in high yield (Table 2.2). Furan also seemed to work as a nucleophile, but the product decomposed during subsequent handling. Acetamide failed to react, and 1-phenyl-1-(trimethylsilyloxy)ethylene gave a series of decomposition products, probably owing to the strong acidic conditions.

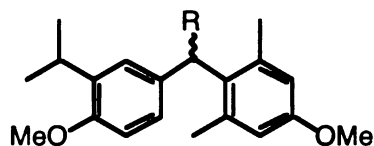
Table 2.1. Alkyl cerium(III) chloride additions to the benzophenone **4**

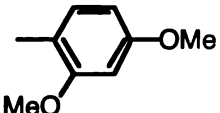
Organocerium Reagent	Ratio (eq.)	Product	R ₁	R ₂	Yield ^a
<i>n</i> -BuCeCl ₂	10	5	<i>n</i> -Bu	O	38%
<i>n</i> -BuCeCl ₂	1.3	5	<i>n</i> -Bu	O	27%
		6	H	OH, <i>n</i> -Bu	22%
<i>sec</i> -BuCeCl ₂	1.3	7	<i>sec</i> -Bu	O	22%
		8	H	OH, <i>sec</i> -Bu	17%
MeCeCl ₂	1.5	9	H	OH, Me	42%

a. isolated yield

While these results are very encouraging and the wide scope of these reactions promise to make easy the creation of many derivatives at this site, some problems remain. Most significantly, the acidic conditions that allow the easy formation of these derivatives are also routes to their decomposition. The substituents with nucleophilic heteroatoms, in this case the ethers and thioethers, require all subsequent steps in the synthesis of their corresponding thyroid hormone analogues to avoid both acidic and hydrogenating conditions or the extensions will be lost to solvolysis or hydrogenolysis. Consequently, the phenolic methyl protecting groups, which are removed by BBr₃, will have to be replaced with silyl protecting groups, which can be removed by milder fluoride treatment.

Table 2.2. Carbon bridge extensions via solvolysis of **3**



R	Compound	Yield ^a
—OEt	10	73%
—SEt	11	89%
—SPh	12	66%
—CH ₂ CH=CH ₂	13	93%
	14	90%

a. isolated yield

The substitution reaction yields racemic product from racemic starting material (**3**) as a result of the extension attached to the bridging carbon. This site of asymmetry will be preserved in the conversion of these intermediates to thyroid hormone analogs. This affords the opportunity to probe stereochemical issues related to receptor binding and activation with these analogues. The thyroid hormone analogues easily accessible by this chemistry should provide valuable probes for studying the nature of the receptor-ligand interaction. Moreover, any high-affinity antagonists that result from this approach may be useful as biological probes of thyroid hormone signaling.

2.3. Acknowledgments

This work was supported by a grant from the National Institutes of Health (DK52798). Mass spectrometry analysis of synthetic compounds was provided by the UCSF Mass Spectrometry Facility supported by the NIH Division of Research Resources (RR01614). T.S.S. is an Alfred P. Sloan Research Fellow. H.A.I.Y. gratefully acknowledges support from the National Cancer Institute (NIH Institution Training Grant T32-CA09270) and from the Markey Program in Biological Science. G.C. gratefully acknowledges support from a postdoctoral fellowship from the University of Pisa, Italy.

2.4. Experimental

General Methods

Proton and carbon-13 nuclear magnetic resonance spectra (^1H NMR, ^{13}C NMR) were obtained on a General Electric QE-300 (300 Mhz) spectrometer, with tetramethylsilane used as the reference. High resolution mass spectrometry was performed by the National Bio-Organic, Biomedical Mass Spectrometry Resource at UCSF.

Flash chromatography on crude products was performed using 230-400 mesh silica gel (Aldrich Chemical Co.). Purity of compounds was determined by TLC using commercial silica gel plates (Alltech, Alugram® Sil G/UV 254) and by ^1H NMR and HRMS.

Glassware was oven or flame-dried prior to use. Methylene chloride (anhydrous), tetrahydrofuran (anhydrous) and reagents were purchased from Aldrich Chemical Co. and used without further purification. Reactions were performed under Argon inert atmosphere.

4,4'-dimethoxy-3'-(1-methylethyl)-2,6-dimethylbenzophenone (4):

To alcohol **3** (10 g, 31.80 mmol) in 150 mL of methylene chloride at 0 °C was added pyridinium dichromate (23.93 g, 63.60 mmol). The reaction mixture was stirred for 4h at 0 °C and then filtered through Celite. The filtrate was evaporated, and the residue was purified by flash column chromatography (silica gel, 95:5 hexane/ethyl acetate) to give **4** (6 g, 19.23 mmol, 60%); ¹H NMR (CDCl₃, 300 MHz) δ 1.13 (d, *J* = 6.9 Hz, 6 H), 2.02 (s, 6 H), 3.22 (heptet, *J* = 6.9 Hz, 1 H), 3.73 (s, 3 H), 3.79 (s, 3 H), 6.53 (s, 2 H), 6.71 (d, *J* = 8.4 Hz, 1 H), 7.41 (d, *J* = 8.4 Hz, 1 H), 7.78 (s, 1 H). ¹³C NMR (CDCl₃, 75 MHz) δ 199.5, 161.5, 159.5, 137.7, 136.2, 133.1, 130.6, 130.4, 127.2, 113.0, 109.7, 55.7, 55.3, 27.0, 22.5, 19.9. HRMS exact mass calcd for C₂₀H₂₄O₃: 312.1725, found: 312.1724.

4,4'-dimethoxy-6'-butyl-3'-(1-methylethyl)-2,6-dimethylbenzophenone (**5**):

To a suspension of cerous chloride anhydrous (CeCl₃) (1.580 g, 6.41 mmol) in 20 mL of dry tetrahydrofuran at -78 °C was added 3.2 mL of butyllithium (2.0 M in pentane). The reaction mixture was stirred for 30 min at -78 °C and then ketone **4** (0.2 g, 0.641 mmol) in 5 mL of tetrahydrofuran was added and the mixture was stirred for 3-4 h. Then, the reaction mixture was treated with sat. NH₄Cl solution, filtered through silica, and extracted with ethyl acetate. The organic portion was dried (MgSO₄), filtered, and evaporated to give the crude product, which was purified by flash column chromatography (silica gel, 98:2 hexane/ethyl acetate) to yield 90 mg (0.24 mmol, 38%) of addition product **5** as an oil. ¹H NMR (CDCl₃, 300 Mhz) δ 7.22 (s, 1 H), 1.62 (quintet, *J* = 7.5, 7.8 Hz, 2H), 6.73 (s, 1 H), 6.58 (s, 2 H), 3.89 (s, 3H), 3.82 (s, 3 H), 3.18 (heptet, *J* = 6.9 Hz, 1 H), 3.05 (t, *J* = 7.8 Hz, 2 H), 2.09 (s, 6 H), 1.44 (sextet, *J* = 7.2, 7.5 Hz, 2 H), 1.03 (d, *J* = 6.9 Hz, 6 H), 0.96 (t, *J* = 7.2 Hz, 3 H). ¹³C NMR (CDCl₃, 125MHz) δ 201.1, 159.8, 159.4, 145.5, 136.4, 134.9, 134.2, 131.6, 129.5, 113.4, 113.0, 55.6, 55.3, 34.8, 33.8, 26.7, 23.3, 22.6, 20.2, 14.2. HRMS exact mass calcd for C₂₄H₃₂O₃: 368.2351, found: 368.2347.

4,4'-dimethoxy-6'-butyl-3'-(1-methylethyl)-2,6-dimethylbenzophenone (5)

& 1-(4-methoxy-2,6-dimethylphenyl)-1-[4-methoxy-3-(1-methylethyl)phenyl] pentanol (6):

To a suspension of CeCl_3 (0.205 g, 0.832 mmol) in 3 mL of dry tetrahydrofuran at $-78\text{ }^\circ\text{C}$ was added 0.420 mL of butyllithium (2.0 M in pentane). After stirring for 30 min at $-78\text{ }^\circ\text{C}$ ketone 4 (0.2 g, 0.641 mmol) in 5 mL of tetrahydrofuran was added and the mixture was stirred for 3-4 h. Then, the reaction mixture was treated with sat. NH_4Cl solution, filtered through silica, and extracted with ethyl acetate. The organic portion was dried (MgSO_4), filtered, and evaporated to give the crude product, which was purified by flash column chromatography (silica gel, 98:2 hexane/ethyl acetate) to give 5 (64 mg, 0.173 mmol, 27%) and 6 (52 mg, 0.141 mmol, 22%). (6): ^1H NMR (CDCl_3 , 300 Mhz) δ 7.24 (d, $J = 2.1$ Hz, 1 H), 7.08 (dd, $J = 2.1, 9$ Hz, 1 H), 6.76 (d, $J = 9$ Hz, 1 H), 6.54 (s, 2 H), 3.81 (s, 3 H), 3.77 (s, 3 H), 3.27 (heptet, $J = 6.9$ Hz, 1 H), 2.31 (m, 2 H), 2.21 (s, 6 H), 1.57 (m, 2 H), 1.35 (m, 2 H), 1.18 (dd, $J = 6.9$ Hz, 6 H), 0.93 (t, $J = 7.2$ Hz, 3 H). ^{13}C NMR (CDCl_3 , 75 MHz) δ 157.1, 155.9, 142.1, 138.8, 136.9, 135.2, 124.2, 123.9, 115.9, 110.3, 81.9, 55.4, 55.1, 40.7, 27.3, 26.7, 25.1, 23.6, 22.9, 14.4.

4,4'-dimethoxy-6'-(1-methylpropyl)-3'-(1-methylethyl)-2,6-dimethylbenzophenone (7) & 1-(4-methoxy-2,6-dimethylphenyl)-1-[4-methoxy-3-(1-methylethyl)phenyl]-2-methylbutanol (8):

To a suspension of CeCl_3 (0.515 g, 2.1 mmol) in 7 mL of dry tetrahydrofuran at $-78\text{ }^\circ\text{C}$ was added 1.6 mL of *sec*-butyllithium (1.3 M in cyclohexane). After stirring for 30 min at $-78\text{ }^\circ\text{C}$ ketone 4 (0.5 g, 1.6 mmol) in 12 mL of tetrahydrofuran was added and the mixture was stirred for 3-4 h. Then, the reaction mixture was treated with sat. NH_4Cl solution, filtered through silica, and extracted with ethyl acetate. The organic portion was dried (MgSO_4), filtered, and evaporated to give the crude product, which was purified by flash column chromatography (silica gel, 98:2 hexane/ethyl acetate) to give 7 (130 mg, 0.35 mmol, 22%)

and **8** (100 mg, 0.27 mmol, 17%). (**7**) ^1H NMR (CDCl_3 , 300 MHz) δ 7.18 (s, 1 H), 6.85 (s, 1 H), 6.57 (s, 2 H), 3.88 (s, 3 H), 3.83 (m, 1 H), 3.82 (s, 3 H), 3.15 (heptet, $J = 6.9$, 1 H), 2.10 (s, 6 H), 1.78 (m, 1 H), 1.57 (m, 1 H), 1.26 (d, $J = 6.6$ Hz, 3 H), 1.04 (d, $J = 6.9$ Hz, 6 H), 0.88 (t, $J = 7.5$ Hz, 3 H). ^{13}C NMR (C_6D_6 , 75 MHz) δ 201.1, 160.5, 160.3, 150.6, 137.1, 136.1, 134.5, 131.6, 131.1, 113.9, 109.2, 55.2, 55.0, 36.3, 31.9, 27.4, 23.0, 22.7, 20.7, 13.1. HRMS exact mass calcd for $\text{C}_{24}\text{H}_{32}\text{O}_3$: 368.2351, found: 368.2345. (**8**) ^1H NMR (CDCl_3 , 300 MHz) δ 7.82 (d, $J = 1.8$ Hz, 1 H), 7.46 (dd, $J = 1.8, 8.1$ Hz, 1 H), 7.21 (d, $J = 8.1$ Hz, 1 H), 6.61 (s, 2 H), 3.83 (s, 3 H), 3.82 (s, 3 H), 3.26 (heptet, $J = 6.9$, 1 H), 3.04 (m, 1 H), 2.11 (s, 6 H), 1.61 (m, 2 H), 1.23 (m, 9 H), 0.86 (t, $J = 7.2$ Hz, 3 H).

α -methyl-[4,4'-dimethoxy-3'-(1-methylethyl)-2,6-dimethyl] benzhydrol (**9**):

To a suspension of CeCl_3 (0.592 g, 2.4 mmol) in 7 mL of dry tetrahydrofuran at -78°C was added 1.71 mL of methyllithium (1.4 M in diethylether). After stirring for 30 min at -78°C ketone **4** (0.5 g, 1.6 mmol) in 10 mL of tetrahydrofuran was added and the mixture was stirred for 3-4 h. Then, the reaction mixture was treated with sat. NH_4Cl solution, filtered through silica, and extracted with ethyl acetate. The organic portion was dried (MgSO_4), filtered, and evaporated to give the crude product, which was purified by flash column chromatography (silica gel, 95:5 hexane/ethyl acetate) to yield the alcohol **9** (221 mg, 0.67 mmol, 42%). ^1H NMR (CDCl_3 , 300 MHz) δ 7.35 (d, $J = 2.1$, 1 H), 7.20 (dd, $J = 2.1, 7.5$ Hz, 1 H), 6.80 (d, $J = 7.5$ Hz, 1 H), 6.64 (s, 2 H), 3.89 (s, 3 H), 3.85 (s, 3 H), 3.35 (heptet, $J = 6.9$ Hz, 1 H), 2.22 (s, 6 H), 2.00 (s, 3 H), 1.20 (dd, $J = 6.9$ Hz, 6 H).

General procedure for substitution of the bridging carbon:

A solution of benzyl alcohol **3** (40 mg, 0.13 mmol) and nucleophile (5.1 mmol) in methylene chloride (8 mL) was cooled to -45°C (dry ice/acetonitrile bath). Trifluoroacetic acid (167 μL , 2.2 mmol) was added and the reaction stirred 2 h at -45°C . The reaction was

quenched by adding sat. NaHCO₃ (5 mL) and water (5 mL). Layers were separated and the aqueous phase extracted twice with Et₂O (7 mL). Combined extracts were washed with brine (10ml), dried over MgSO₄ and evaporated. Purification by flash chromatography (1:20 Et₂O-hexanes) was performed. Note: In reactions involving thiols, the reaction was quenched with 0.5 M NaOH (10 mL), and the extracted aqueous phase treated with bleach to reduce the stench.

Spectral and analytical data of the prepared carbon-bridge derivatives.

ethoxy-4,4'-dimethoxy-2,6-dimethyl-3'-(1-methylethyl)diphenylmethane (10):

¹H NMR (CDCl₃) δ 7.17 (d, *J* = 1.6 Hz, 1 H), 6.90 (dd, *J* = 1.5, 8.4 Hz, 1 H), 6.71 (d, *J* = 8.4 Hz, 1 H), 6.57 (s, 2 H), 5.80 (s, 1 H), 3.79 (s, 3 H), 3.78 (s, 3 H), 3.47 (br q, *J* = 7.0 Hz, 2 H), 3.26 (heptet, *J* = 6.9 Hz, 1 H), 2.24 (s, 6 H), 1.26 (t, *J* = 7.0 Hz, 3 H), 1.17 (d, *J* = 6.7 Hz, 3 H), 1.15 (d, *J* = 6.7 Hz, 3 H); HRMS exact mass calcd for C₂₂H₃₀O₃ 342.2195, found 342.2189.

ethylthio-4,4'-dimethoxy-2,6-dimethyl-3'-(1-methylethyl)diphenylmethane (11):

¹H NMR (CDCl₃) δ 7.30 (d, *J* = 2.0 Hz, 1 H), 7.05 (dd, *J* = 1.6, 8.4 Hz, 1 H), 6.73 (d, *J* = 8.5 Hz, 1 H), 6.56 (s, 2 H), 5.58 (s, 1 H), 3.79 (s, 3 H), 3.77 (s, 3 H), 3.27 (heptet, *J* = 6.9 Hz, 1 H), 2.67-2.48 (M, 2 H), 2.23 (br s, 6 H), 1.28 (t, *J* = 7.4 Hz, 3 H), 1.17 (app t, *J* = 7.0 Hz, 6 H); HRMS exact mass calcd for C₂₂H₃₀O₂S 358.1966, found 358.1953.

4,4'-dimethoxy-2,6-dimethyl-3'-(1-methylethyl)diphenylthio methane (12):

¹H NMR (CDCl₃) δ 7.34 (s, 1 H), 7.32 (s, 1 H), 7.25-7.17 (m, 3 H), 7.08 (dd, *J* = 1.7, 8.4 Hz, 1 H), 6.72 (d, *J* = 8.5 Hz, 1 H), 6.55 (s, 2 H), 5.89 (s, 1 H), 3.79 (s, 3 H), 3.78 (s, 3 H), 3.26 (heptet, *J* = 6.9 Hz, 1 H), 2.13 (br s, 6 H), 1.15 (d, *J* = 6.9 Hz, 3 H), 1.09 (d, *J* = 6.9 Hz, 3H); HRMS exact mass calcd for C₂₆H₂₉O₂S (M - H⁺) 405.1888, found 405.1894.

4,4-[4',4''-dimethoxy-2',6'-dimethyl-3'-(1-methylethyl)diphenyl]butan-1-ene (13):

^1H NMR (CDCl_3) δ 7.05 (d, $J = 1.7$ Hz, 1 H), 6.87 (dd, $J = 1.6, 8.4$ Hz, 1 H), 6.71 (d, $J = 8.5$ Hz, 1 H), 6.54 (s, 2 H), 5.78-5.67 (m, 1 H), 5.09 (dd, $J = 1.0, 17.1$ Hz, 1 H), 4.93 (d, $J = 10.2$ Hz, 1 H), 4.50 (t, $J = 7.9$ Hz, 1 H), 3.78 (s, 3 H), 3.77 (s, 3 H), 3.26 (heptet, $J = 6.9$ Hz, 1 H), 3.09-3.00 (m, 1 H), 2.80-2.70 (m, 1H), 2.15 (br s, 6 H), 1.16 (d, $J = 7.1$ Hz, 3 H), 1.14 (d, $J = 7.1$ Hz, 3H); HRMS exact mass calcd for $\text{C}_{23}\text{H}_{30}\text{O}_2$ 338.2246, found 338.2247.

4,4',2'',4''-tetramethoxy-2,6-dimethyl-3'-(1-methylethyl)triphenylmethane (14):

^1H NMR (CDCl_3) δ 6.85 (s, 1 H), 6.76 (d, $J = 8.4$ Hz, 1 H), 6.68 (s, 1 H), 6.54 (s, 2 H), 6.47 (d, $J = 2.2$ Hz, 1 H), 6.36 (dd, $J = 2.3, 8.5$ Hz, 1 H), 5.93 (s, 1 H), 3.79 (s, 3 H), 3.78 (s, 3 H), 3.77 (s, 3 H), 3.67 (s, 3 H), 3.24 (heptet, $J = 6.9$ Hz, 1 H), 1.99 (s, 6 H), 1.09 (d, $J = 6.9$ Hz, 6 H); HRMS exact mass calcd for $\text{C}_{28}\text{H}_{34}\text{O}_4$ 434.2457, found 434.2458.

2.5. References

- [1] Greenspan, F.S. (1994). The Thyroid Gland. *In* "Basic and Clinical Endocrinology" (F. S. Greenspan and J. D. Baxter, eds.), pp. 160-226. Appleton and Lange, Norwalk.
- [2] Mangelsdorf, D.J., Thummel, C., Beato, M., Herrlich, P., Schutz, G., Umesono, K., Blumberg, B., Kastner, P., Mark, M., Chambon, P. & Evans, R.M. (1996). The nuclear receptor superfamily: the second decade. *Cell* **83**, 835-839.
- [3] Mangelsdorf, D.J. & Evans, R.M. (1996). The RXR heterodimers and orphan receptors. *Cell* **83**, 841-850.
- [4] Katzenellenbogen, J.A. & Katzenellenbogen, B.S. (1996). Nuclear hormone receptors: ligand-activated regulators of transcription and diverse cell responses. *Chemistry & Biology* **3**, 529-536.

- [5] Oppenheimer, J.H., Schwartz, H.L. & Strait, K.A. (1994). Thyroid hormone action 1994: the plot thickens. *European Journal of Endocrinology* **130**, 15-24.
- [6] Ribeiro, R.C.J., Apriletti, J.W., Wagner, R.L., West, B.L., Feng, W., Huber, R., Kushner, P.J., Nilsson, S., Scanlan, T.S., Fletterick, R.J., Shaufele, F. & Baxter, J.D. (1998). Mechanisms of thyroid hormone action: insights from x-ray crystallographic and functional studies. *Recent Progress in Hormone Research* **53**, 351-394.
- [7] Chiellini, G., Apriletti, J.W., Yoshihara, H.A., Baxter, J.D., Ribeiro, R.C.J. & Scanlan, T.S. (1998). A high-affinity subtype-selective agonist ligand for the thyroid hormone receptor. *Chemistry & Biology* **5**, 299-306.
- [8] Luengo, J.I., Konialianbeck, A., Rozamus, L.W. & Holt, D.A. (1994). Manipulation of the Rapamycin Effector Domain - Selective Nucleophilic-Substitution of the C-7 Methoxy Group. *Journal of Organic Chemistry* **59**, 6512-6513.
- [9] Luengo, J.I., Yamashita, D.S., Dunnington, D., Beck, A.K., Rozamus, L.W., Yen, H.K., Bossard, M.J., Levy, M.A., Hand, A., Newmantarr, T., Badger, A., Faucette, L., Johnson, R.K., Dalessio, K., Porter, T., Shu, A.Y.L., Heys, R., Choi, J.W., Kongsaree, P., Clardy, J. & Holt, D.A. (1995). Structure-Activity Studies of Rapamycin Analogs - Evidence That the C-7 Methoxy Group Is Part of the Effector Domain and Positioned at the Fkbp12-Frap Interface. *Chemistry & Biology* **2**, 471-481.
- [10] Imamoto, T., Sugiura, Y. & Takiyama, N. (1984). Organocerium Reagents - Nucleophilic-Addition to Easily Enolizable Ketones. *Tetrahedron Letters* **25**, 4233-4236.
- [11] Imamoto, T., Kusumoto, T., Tawarayama, Y., Sugiura, Y., Mita, T., Hatanaka, Y. & Yokoyama, M. (1984). Carbon Carbon Bond-Forming Reactions Using Cerium Metal or Organocerium(III) Reagents. *Journal of Organic Chemistry* **49**, 3904-3912.

Chapter 3: Design and Synthesis of a Thyroid Hormone Antagonist

Adapted from the manuscript of: Yoshihara, H.A.I., Apriletti, J.W., Baxter, J.D. & Scanlan, T.S. (2001). A designed antagonist of the thyroid hormone receptor. *Bioorganic & Medicinal Chemistry Letters* **11**, 2821-2825. The transactivation and GST-pulldown assays, synthesis and characterization of the compounds were done by me.

3.1. Introduction

Thyroid hormone, 3,3',5-triiodo-L-thyronine (T_3 , Figure 3.1), plays important roles in development and homeostasis [1]. Synthesized in the thyroid gland from a precursor protein, the hormone is recognized in target tissues by thyroid hormone receptors (TRs) [2]. TRs are members of the nuclear receptor superfamily of transcription regulators [3], which mediate the effects of thyroid hormone by positively and negatively regulating the transcription of target genes [2].

Current approaches to treating hyperthyroidism include surgical or radiological ablation of the thyroid gland, or the administration of drugs such as propylthiouracil and methimazole that inhibit the biosynthesis of T_3 [1]. The antiarrhythmia drug amiodarone has antithyroid effects [4; 5], and its major metabolite desethylamiodarone (Figure 3.1) antagonizes TR under certain *in vitro* conditions [6-8]. Desethylamiodarone, a non-competitive antagonist of $TR\beta$ has been shown to interfere with the interaction of $TR\beta$ with p160 co-activator GRIP1 [9].

Previously we reported the potent halogen-free thyromimetic GC-1 (Figure 3.1) with a modest selectivity for $TR\beta$ over $TR\alpha$ [10]. In this study we report the design and synthesis of GC-1 analogues bearing substituents on the carbon atom that bridges the two aromatic rings [11]. One of these analogues was found to antagonize T_3 in transactivation assays using cultured cells. To our knowledge, this study is the first report of a designed competitive thyroid hormone antagonist.

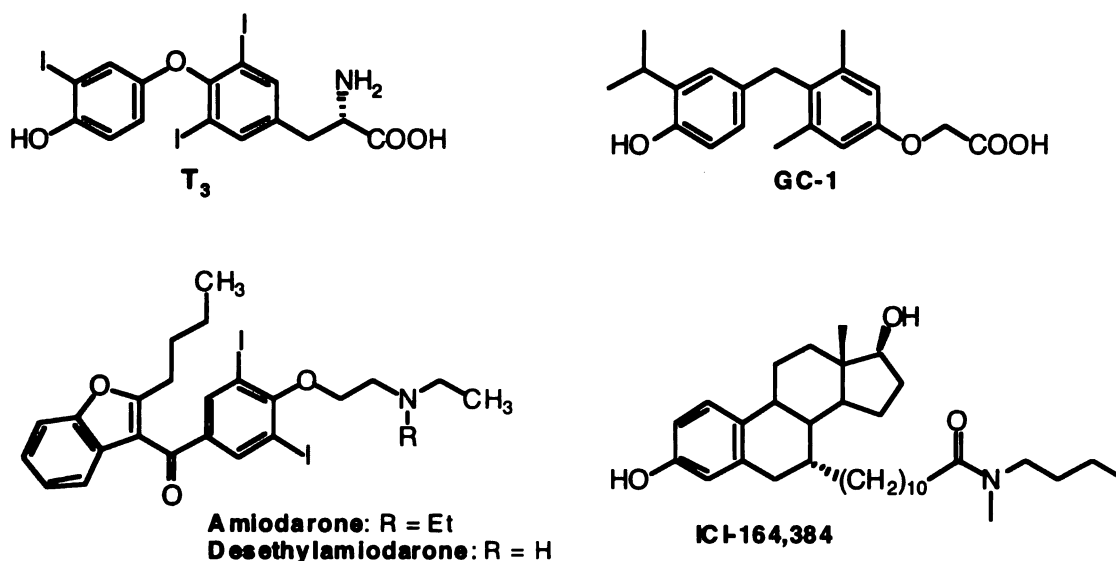


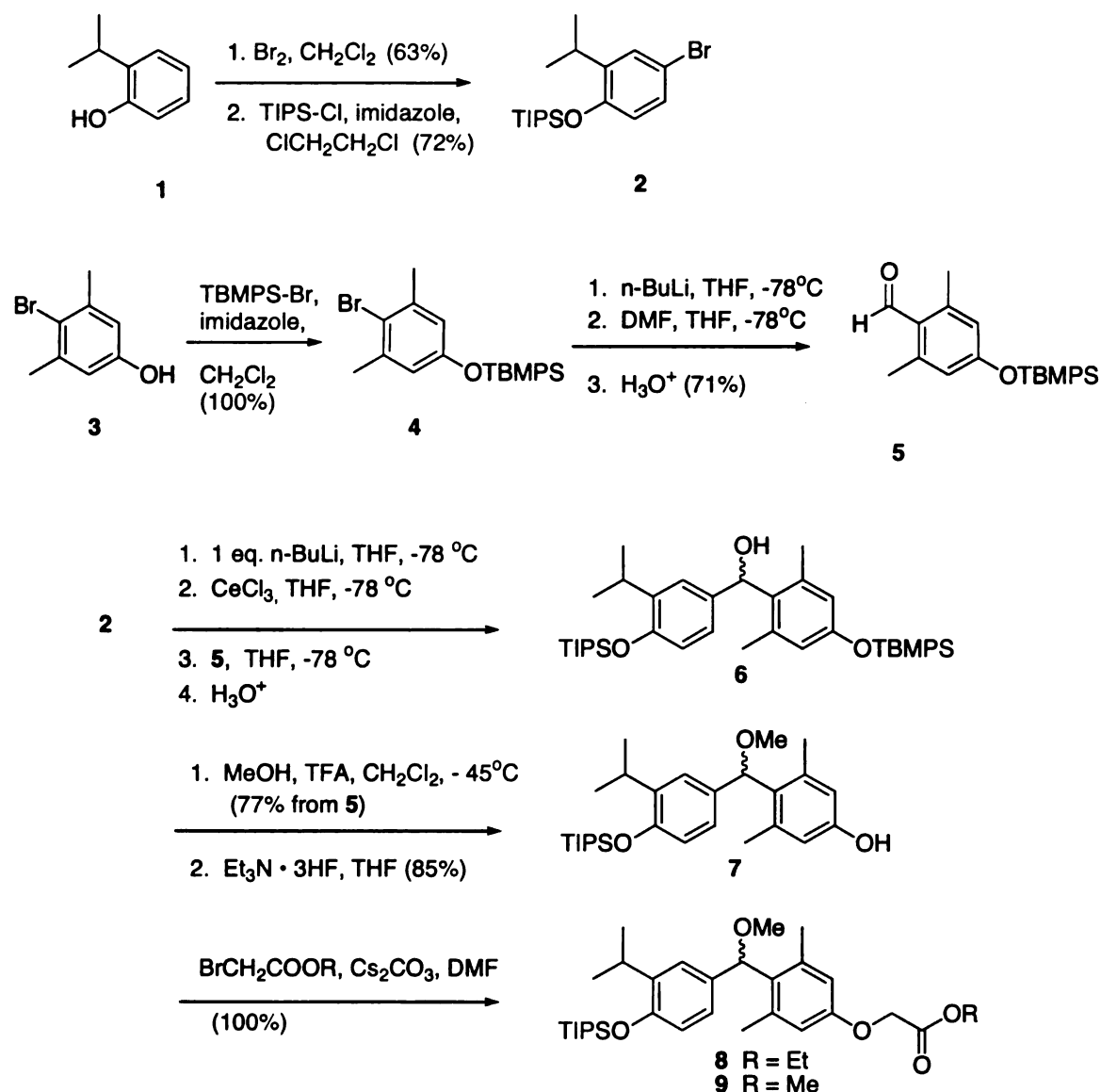
Figure 3.1. Chemical structures of thyroid hormone (T₃), thyromimetic GC-1, the antithyroid & antiarrhythmia drug amiodarone, and estrogen antagonist ICI-164,384.

3.2. Results

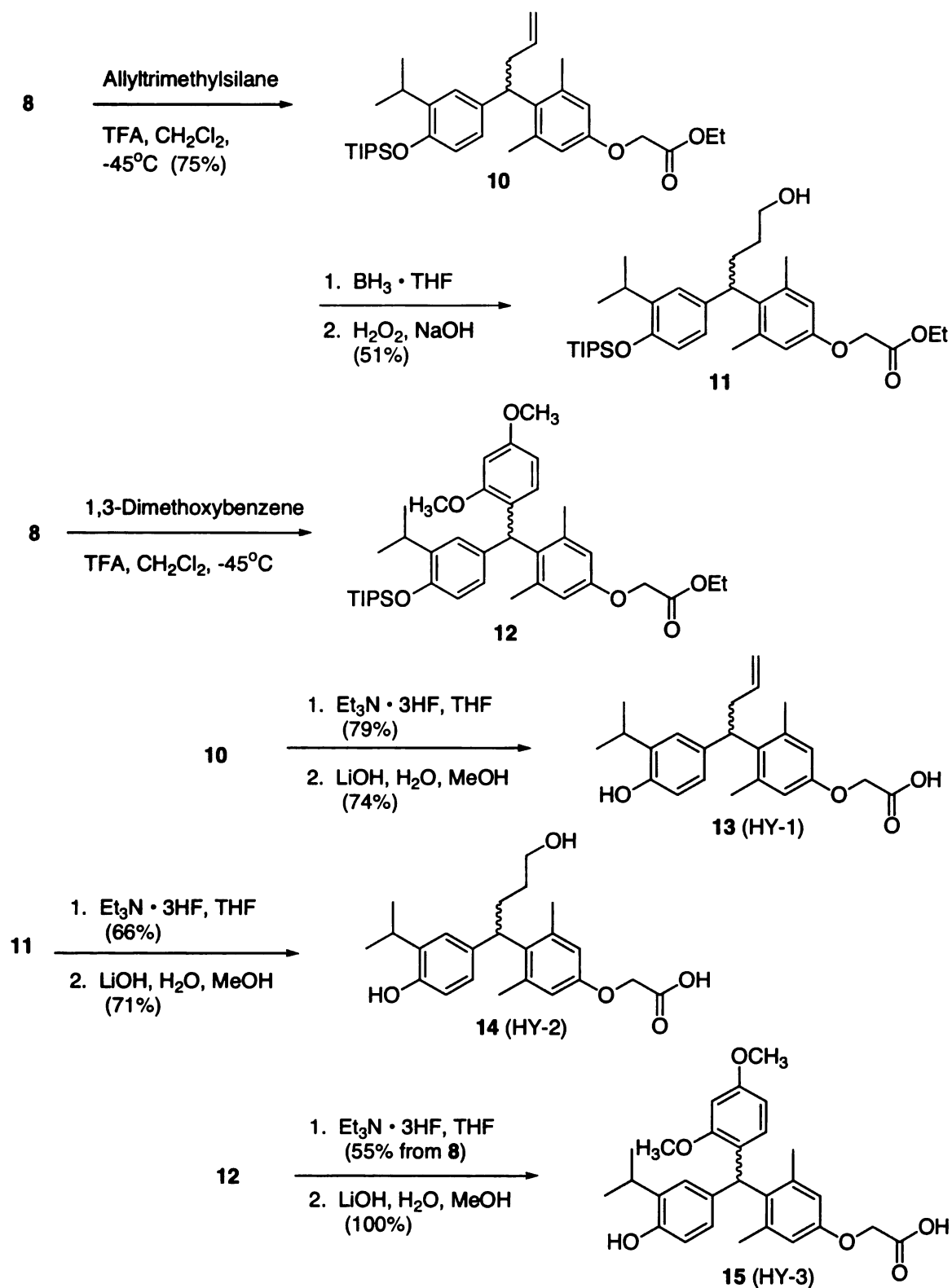
3.2.1. Synthesis and characterization of bridge-substituted GC-1 analogues

In this and previous [12] reports we differentially protected the phenolic hydroxyls to improve a low-yielding step in the original synthesis of GC-1. Starting with 2-isopropylphenol (**1**, Scheme 3.1a), bromination and treatment with triisopropylsilyl chloride yielded bromoarylsilylether **2**. 4-Bromo-3,5-dimethylphenol (**3**) was protected as the *tert*-butylmethoxyphenylsilyl (TBMPS) acetal, which can be selectively cleaved in the presence of silyl ethers [13; 14]. Formylation of **4** to benzaldehyde **5** was followed by the coupling of the two aryl rings via the aryl cerium (III) reagent prepared *in situ* from the aryllithium derived from arylbromide **2**. Using the arylcerium reagent [15; 16] instead of its aryllithium precursor gave much higher yields with this sterically hindered electrophile. Crude carbinol **6** was reacted with methanol under acid conditions,

substituting the hydroxyl with a methoxyl group. The resulting product was more chromatographically mobile and easier to purify than **6**. Selective removal of the TBMPS protecting group with triethylamine trihydrofluoride produced phenol **7**, which was alkylated with either ethyl- or methylbromoacetate, yielding oxyacetic esters **8** and **9**, respectively.



Scheme 3.1. Synthesis of bridge-substituted analogues of GC-1



Scheme 3.2. Synthesis of bridge-substituted analogues of GC-1 (continued)

Attempts at preparing GC-1 analogues with alkoxy substituents at the bridging carbon were unsuccessful, presumably due to the lability of the ether. The products of allylation (**10**, Scheme 3.1b) or arylation (**12**) reactions of ethyl ester **8** via acid solvolysis were sufficiently stable to be deprotected, yielding GC-1 analogues **13** and **15**. Hydroboration and oxidation of butene **10** followed by the removal of TIPS and methyl ester protecting groups produced GC-1 analogue HY-1 (**14**).

TR binding data of analogues HY-1 – 3 (**13-15**) are summarized in Table 3.1. Analogue HY-1, having the highest affinity was tested for its ability to activate TR-mediated transactivation; it exhibited low-potency agonistic activity with EC₅₀ values of approximately 1 μ M for TR β and 10 μ M for TR α (data not shown).

Table 3.1. Binding affinities of GC-1 bridge-substituted analogues for TR

Compound	K _d (hTR α ₁) \pm S.E. (nM)	K _d (hTR β ₁) \pm S.E. (nM)
T ₃	0.17 \pm 0.02	0.14 \pm 0.01
HY-1 (13)	430 \pm 60	90 \pm 10
HY-2 (14)	1400 \pm 800	3600 \pm 140
HY-3 (15)	1400 \pm 700	4200 \pm 200
HY-4 (21)	112 \pm 18	148 \pm 13
HY-5 (20)	240 \pm 50	720 \pm 100

Inspection of the X-ray crystal structures of the ligand binding domains of estrogen receptor α [17] and rat TR α ₁ [18] suggested that the estrogen antagonist ICI-164,384 [19;

20] (Figure 3.1) projects its long alkylamide appendage in a direction similar to the direction a substituent on the bridging carbon of GC-1 would project (Figure 3.2). This led us to synthesize a GC-1 analogue with the same alkylamide extension. As shown in Scheme 3.2, methyl ether **9** was allylated, hydroborated and oxidized to butanal **18**. 8-Bromooctanoic acid was coupled with N-methylbutylamine using HBTU, then reacted neat with molten triphenylphosphine at 125 °C. The crude triphenylphosphonium bromide was deprotonated with lithium bis(trimethylsilyl)amide to generate the ylid and coupled with butanal **18**. The resulting olefin (**19**) was deprotected with and without first subjecting it to catalytic hydrogenation, yielding GC-1 analogues HY-5 (**20**) and HY-4 (**21**).

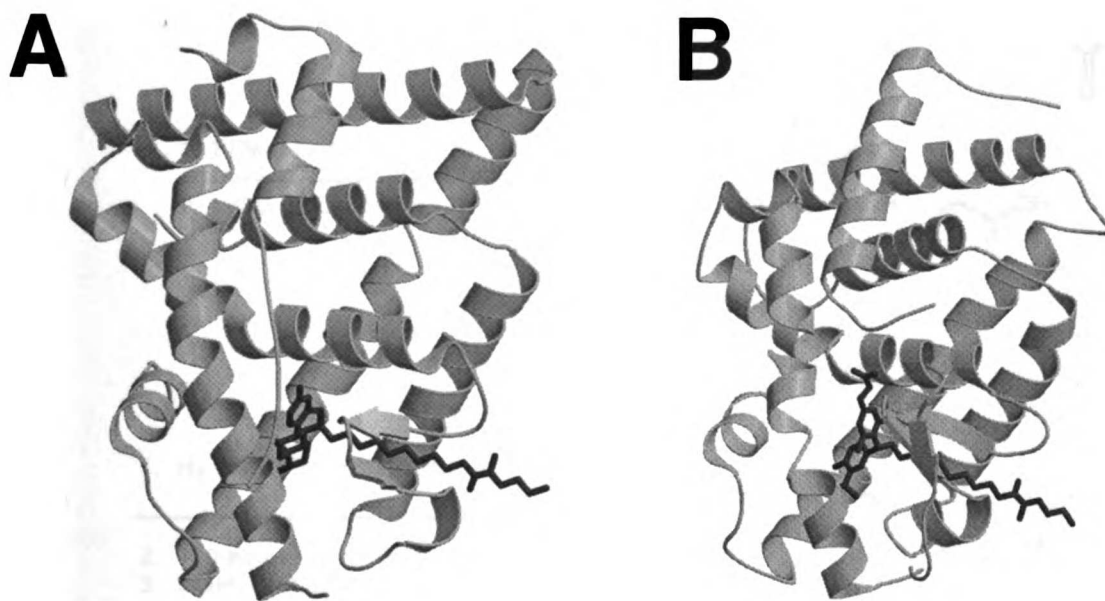
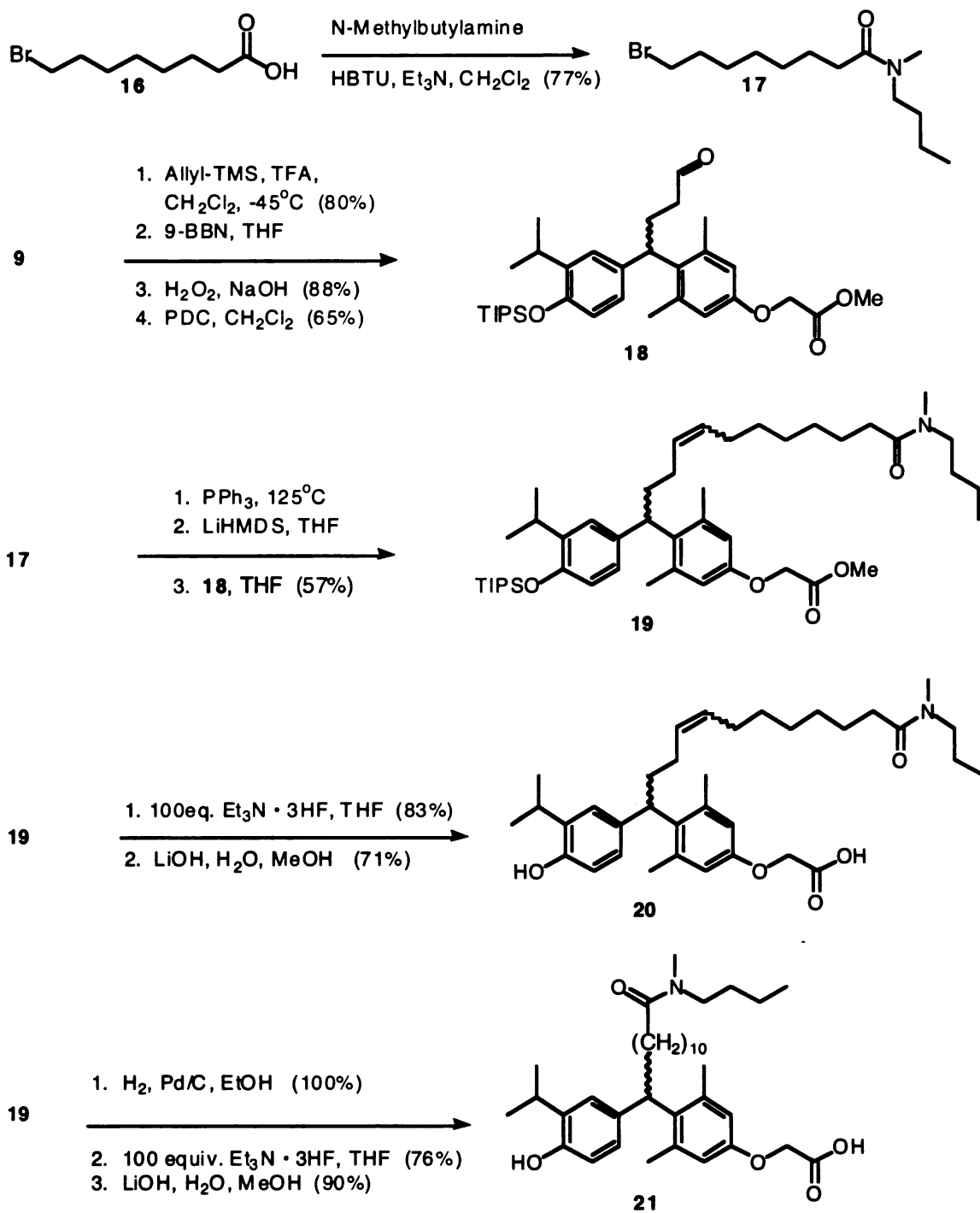


Figure 3.2. Modeling of alkylamide side chain antagonists. (A) Superposition of ICI-164,384 modeled in place of estradiol and hER α (B) Superposition of HY-4 (R-enantiomer) modeled in place of DIMIT and rTR α_1



Scheme 3.3. Synthesis of bridge-substituted analogues of GC-1 with ICI-164,384-like extensions

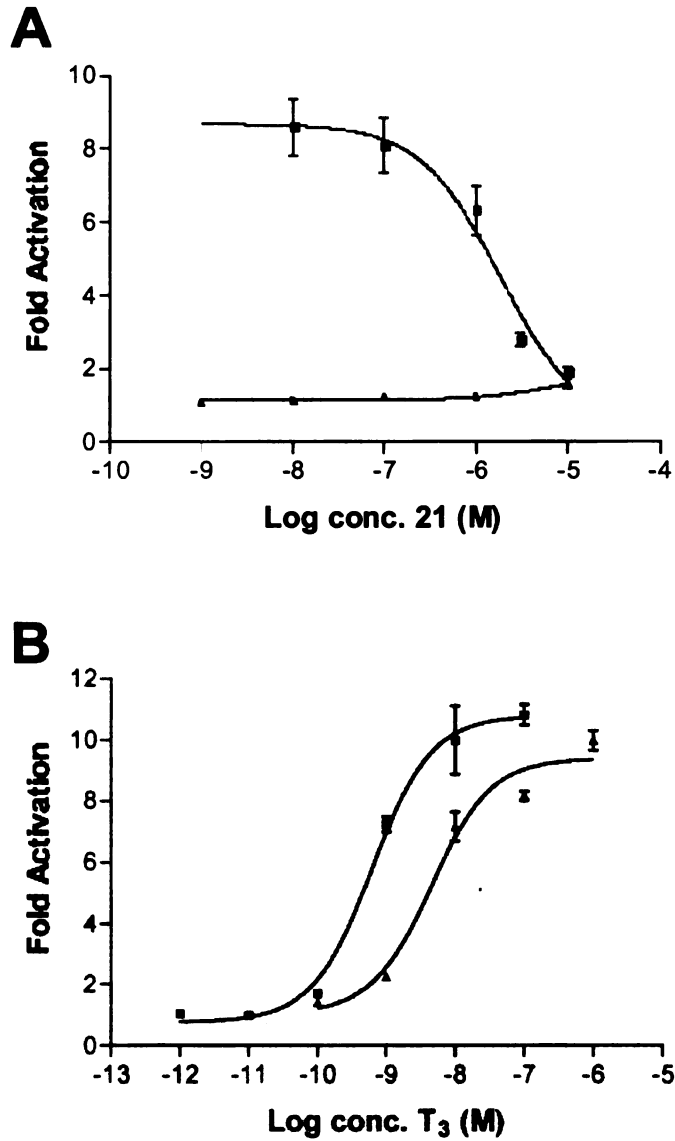


Figure 3.3. Antagonism by HY-4 (21) of TR-mediated transactivation of luciferase under the control of a DR4-type thyroid hormone response element in transiently transfected JEG-3 cells. a) Dose-response of HY-4 alone (triangles) or in competition with 300 pM T₃ (squares). b) Dose-response of T₃ in presence (triangles) and absence (squares) of 10 μM HY-4.

The tighter binding analogue HY-4 (Table 3.1) was tested for its ability to activate TR-mediated transcription. The assay consisted of JEG-3 cells transiently transfected via electroporation with a TR-expression plasmid and a DR-4-driven luciferase reporter construct. Having only the slightest ability to activate transcription, its ability to block agonist-induced transactivation was examined. The competition curve against 300 pM T₃ (Figure 3.2a) indicates antagonism with increasing concentrations of HY-4 resulting in reduced transactivation. To assess whether the decrease in transactivation was due to competition with T₃ for TR rather than the inhibition of another factor required for transactivation or reporter activity, dose-response curves of T₃ in the presence and absence of 10 μM HY-4 were obtained (Figure 3.2b). The similarity of the curves, differing only in potency (EC₅₀: 0.64±0.14 → 4.7±1.3 nM), is indicative of competition between T₃ and HY-4. Similar results were observed with TRα₁ (data not shown) with the EC₅₀ of T₃ shifting from 0.17±0.05 nM to 2.2±1.1 nM in the presence of 10 μM HY-4. Antagonism was observed when the method of transfection was either electroporation or calcium phosphate but not when using lipofection, presumably due to the sequestration of HY-4 by residual lipofection reagent.

3.2.2. HY-4 and TR association with co-regulators

The agonist ligand promoted association between TR and co-activators, such as the p160 co-activator GRIP1, is believed to be important in the mechanism of transcription activation by TR. Conversely, the association between unliganded TR and co-repressors such as NCoR and SMRT is important in TR mediated repression. An antagonist ligand

is likely to affect these interactions, as has been observed with other nuclear receptor antagonists. Different classes of nuclear receptor antagonists have been described which affect these receptor-co-regulator interactions in distinct ways. For instance, the RAR antagonist BMS 614 has been shown to prevent co-activator recruitment, while promoting co-repressor dissociation [21; 22]. In contrast, the RAR antagonist BMS 493 has been shown not to promote co-repressor dissociation [21; 22]. Both categories may exist for TR antagonists. A co-repressor dissociating antagonist basically neutralizes TR and could function somewhat like a genetic null, while a non co-repressor dissociating antagonist could function more like a dominant negative allele, mimicking the constitutive unliganded state.

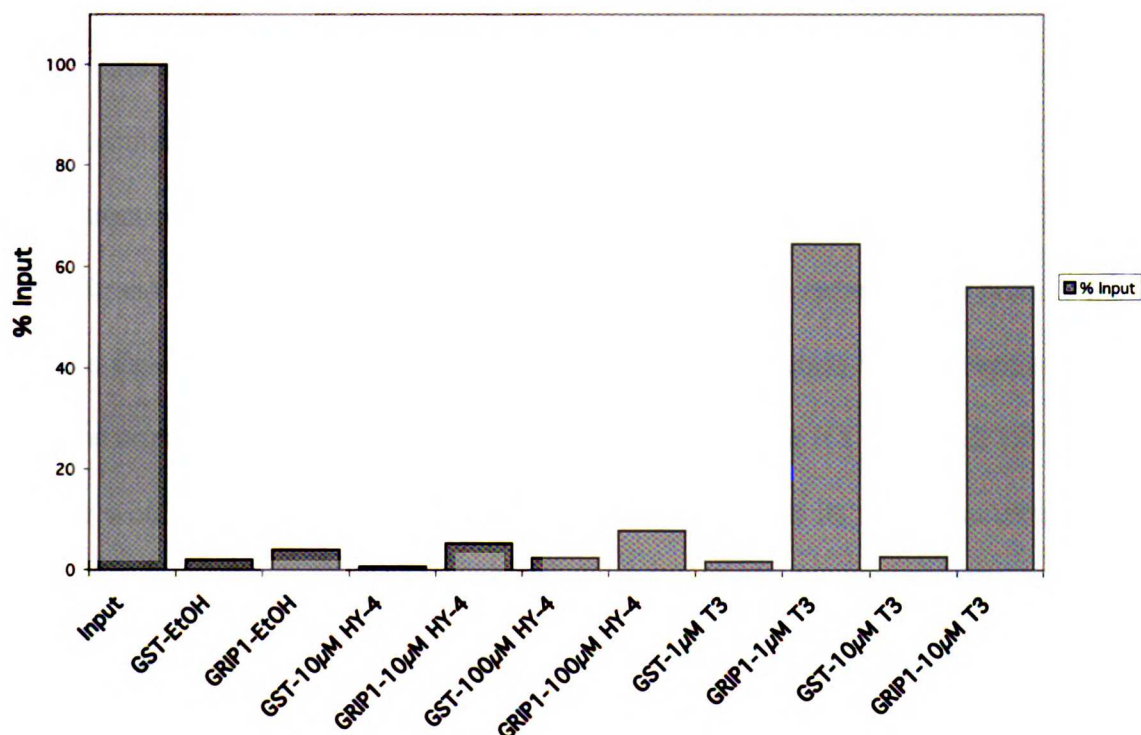


Figure 3.4. Effect of HY-4 on TR – GRIP1 association

The effect of HY-4 on TR's association with co-regulators was examined. Using a GST-pulldown type assay with GST-GRIP1 and ³⁵S-TR β , HY-4 only weakly promotes the association of TR and GRIP1 (Figure 3.4). These data, however, are not complete as competition experiments were not performed. The effect of HY-4 on co-repressor dissociation was examined with GST-pulldown and mammalian two-hybrid assays, however these data were not of sufficient quality to answer the question.

3.3. Discussion

With its structural similarity to thyroid hormone and competitive binding to the receptor, HY-4 likely binds in the same ligand binding pocket as agonist ligands. The recently published X-ray crystal structure of ER β •ICI-164,384 [23] shows the steroid core in the ligand binding pocket with the alkylamide sidechain protruding from the pocket in a manner similar to that observed for the hydrophobic extensions of other estrogen receptor modulators complexed with ER, [17; 24] resulting in structural perturbations to a surface of the ligand binding domain that interacts with co-regulatory factors. This binding mode requires the steroid core of ICI-164,384 to change its orientation by approximately 180° from the orientation found in the ER α •estradiol structure. For HY-4 to bind TR in such a fashion would require a similar change in the orientation of its thyronine core, which, with its bent profile incurred by the sp³-hybridized carbon linking the two aromatic rings, may have a higher energetic cost than the comparatively planar steroid estradiol. A significant penalty with regard to binding affinity is incurred with substitution at the bridging carbon (Table 3.1). However, comparing HY-1 to HY-4, increasing the

sidechain length from 3 to 16 carbons has no additional cost in binding affinity and changes the analogue from an agonist to an antagonist.

All analogues were synthesized as racemic mixtures with the substitution reactions of **8** and **9** proceeding under solvolytic conditions through a presumed carbocation intermediate. Attempts to prepare enantiopure versions of HY-4, via resolution of diastereomeric derivatives of HY-4 or intermediates to HY-4, were unsuccessful. It seems likely that one enantiomer is the antagonistic species, as in the case of the estrogen antagonist ICI-164,384, where antagonism correlates with the 7α -epimer [19].

Unlike GC-1, analogues HY-2, -3, -4 and -5 do not show a preference in binding to the β subtype of TR, although they share many structural features, including an oxyacetic acid side chain, which may be responsible for conferring GC-1's β -selectivity [25]. Indeed, they have varying degrees of preference for TR α (Table 3.1). Thus in the context of non-isosteric thyroid hormone analogues, additional factors may influence the preferential binding to one TR-subtype.

These results support the notion that the design principles of other nuclear receptor antagonists [26] can also be successfully applied to the thyroid hormone receptor. Thyroid hormone analogue HY-4 represents a prototype for a new class of antithyroid compounds that will serve as useful pharmacological probes of thyroid hormone action.

3.4. Acknowledgements

This work was supported by the National Institutes of Health (DK52798, T.S.S.). H.A.I.Y. is grateful for financial support from the National Cancer Institute, Institutional Training Grant T32 CA09270, with supplemental support from the UCSF Dept. of Biochemistry's Herbert W. Boyer Fund. We thank Martin Privalsky and Keith Yamamoto for the gifts of plasmids, used in the transfection assay.

3.5. Experimental

3.5.1. Transfection Assay

JEG-3 cells were grown to ~80% confluency in MEM Eagle's with Earle's BSS with 5% FBS, penicillin and streptomycin. Approximately 1.5×10^6 cells were transfected by electroporation (BioRad Gene Pulser, 0.22 kV, 960 μ F, 0.4 cm cuvettes) in 500 μ L electroporation buffer with 5 μ g of a DR4-pGL3 reporter construct, 1 μ g of pRL-TK (Promega) and 1 μ g of hTR in a pSG5 vector, per transfection. Cells were plated in 12-well plates in growth medium. After 6 hours, medium was changed to a version containing charcoal-stripped FBS and drugs or vehicle (EtOH) were added in triplicate. After 24 hours, cells were harvested and assayed for luciferase activity using the Promega Dual Luciferase kit and Analytical Luminescence Laboratory Monolight® 3010 luminometer.

Binding assay

The TR-binding assay was performed as previously described [10].

3.5.2. Synthesis

4-Bromo-2-isopropylphenol (**1a**):

To a stirred, chilled (0 °C) solution of 2-isopropyl phenol (**1**) (30.0 g, 220 mmol) in anhydrous methylene chloride (250 mL), elemental bromine (10 mL, 19 mmol) was added. After stirring for 1 h at 0 °C, the reaction was quenched with NH₄OH (50 mL), water (250 mL) and saturated NaHCO₃ (200 mL). The aqueous phase was extracted with diethyl ether and combined organic fractions were washed with brine and dried (MgSO₄), followed by filtration; solvent was removed by rotary evaporation to yield a golden oil (42 g). ¹H NMR analysis indicated only ~75% reaction, thus the crude product was subjected to the same reaction conditions with only 2.8 mL (54 mmol) of bromine added, which yielded a golden oil (50.6 g). Purification by column chromatography (4" x 7", 5% → 20% EtOAc/Hexanes) yielded bromophenol **1a** as a colourless oil (30 g, 63%). ¹H NMR (600 MHz, CDCl₃) δ 7.28 (d, *J* = 2.6 Hz, 1 H), 7.15 (dd, *J* = 8.4, 2.2 Hz, 1 H), 6.63, (d, *J* = 8.4 Hz, 1 H), 4.79 (s, 1 H), 3.17 (heptet, *J* = 6.9 Hz, 1 H), 1.24 (d, *J* = 7.0 Hz, 6 H); ¹³C NMR (100 MHz, CDCl₃) δ 151.67, 136.92, 129.41, 129.28, 116.95, 113.19, 27.03, 22.29. HRMS exact mass calcd for C₉H₁₁BrO: 213.9993, found: 213.9943.

3-isopropyl-4-triisopropylsilyloxybromobenzene (**2**):

To a stirred solution of triisopropylsilyl chloride (12 mL, 56 mmol) in anhydrous 1,2-dichloroethane (70 mL) was added phenol **1a** (9.6 g, 46 mmol) and imidazole (7.8 g, 114 mmol). Reaction was refluxed from 30 min, then allowed to stir overnight at room temperature. Reaction was refluxed 1 hour further, then 150 mL of 0.6 M HCl was

added, layers separated and the aqueous phase extracted with diethyl ether. Combined organic fractions were washed with saturated NaHCO₃, dried (MgSO₄), filtered through a Celite plug and solvent was removed by rotary evaporation to yield an oil (18.3 g). Purification by fractional distillation (bp 137 °C, 0.3 mm) yielded bromobenzene **2** as a white solid (12.3 g, 72%). ¹H NMR (600 MHz, CDCl₃) δ 7.27 (d, *J* = 2.6 Hz, 1 H), 7.11 (dd, *J* = 8.4, 2.6 Hz, 1 H), 6.64 (d, *J* = 8.8 Hz, 1 H), 3.33 (heptet, *J* = 6.8 Hz, 1 H), 1.30 (heptet, *J* = 7.5 Hz, 3 H), 1.19 (d, *J* = 6.6 Hz, 6 H), 1.10 (d, *J* = 7.7 Hz, 18 H); ¹³C NMR (100 MHz, CDCl₃) δ 152.29, 140.98, 129.27, 128.93, 119.36, 113.14, 26.85, 22.61, 18.04, 13.05. HRMS exact mass calcd for C₁₈H₃₁BrOSi: 370.1328, found: 370.1336.

4-*tert*-Butylmethoxyphenylsilyloxy-2,6-dimethylbromobenzene (4):

To a stirred solution of 4-Bromo-3,5-dimethylphenol (**3**, 13.5 g, 66.9 mmol) and imidazole (11.4 g, 167 mmol) in anhydrous methylene chloride (125 mL) was added *tert*-Butylmethoxyphenylsilyl bromide (19.2 g, 70.3 mmol). Reaction was stirred 2.5 h, then 200 mL 0.1 M HCl was added and the layers separated. The aqueous layer was extracted with diethyl ether, and the combined organic fractions were washed with brine and dried (MgSO₄). Removal of drying agent by filtration and solvent by rotary evaporation yielded bromobenzene **4** as a golden oil (26.6 g, 100%) which was used without further purification. ¹H NMR (600 MHz, CDCl₃) δ 7.66 (d, *J* = 7.3 Hz, 2 H), 7.44 (t, *J* = 8.8 Hz, 1 H), 7.39 (t, *J* = 7.5 Hz, 2 H), 6.73 (s, 2 H), 3.61 (s, 3 H), 2.33 (s, 6 H), 0.99 (s, 9 H); ¹³C NMR (100 MHz, CDCl₃) δ 153.53, 139.07, 126.15, 130.95, 130.21, 127.80, 119.32, 119.18, 51.88, 26.02, 23.85, 19.03. HRMS exact mass calcd for C₁₉H₂₅BrO₂Si: 392.0807, found: 392.0866.

Benzaldehyde 5:

To a solution bromobenzene **4** (26.2 g, 66.6 mmol) in anhydrous tetrahydrofuran cooled to -78°C was added a solution of butyllithium in hexanes (2.5 M, 76.6 mmol) over several min. Anhydrous dimethylformamide (7.7 mL, 99.9 mmol) was then added over 5 min. After stirring 50 minutes at -78°C , 250 mL 0.2 M HCl was added and the mixture extracted with diethyl ether. The organic fractions were washed with brine and dried (MgSO_4). Filtration followed by rotary evaporation yielded a green syrup. Column chromatography (4" x 7", 10% \rightarrow 20% ether/hexanes) yielded compound **5** as a white solid (16.3 g, 71%). ^1H NMR (600 MHz, CDCl_3) δ 10.47 (s, 1 H), 7.66 (d, $J = 7.3$ Hz, 2 H), 7.45 (t, $J = 7.0$ Hz, 1 H), 7.40 (t, $J = 7.3$ Hz, 2 H), 6.69 (s, 2 H), 3.64 (s, 3 H), 2.55 (s, 6 H), 1.01 (s, 9 H); ^{13}C NMR (100 MHz, CDCl_3) δ 191.63, 191.58, 158.70, 144.26, 135.00, 130.42, 130.36, 127.85, 126.70, 120.49, 51.89, 25.90, 20.76, 19.04. HRMS exact mass calcd for $\text{C}_{20}\text{H}_{26}\text{O}_3\text{Si}$: 342.1651, found: 342.1656.

Benzyl alcohol 6:

To a stirred solution of bromobenzene **2** (11.0 g, 29.6 mmol) in anhydrous tetrahydrofuran (125 mL) at -78°C was added solution of butyllithium in hexanes (2.5 M, 32.3 mmol). This mixture was transferred via cannula to a stirred suspension of cerous chloride (7.96 g, 32.3 mmol) in anhydrous tetrahydrofuran (150 mL) at -78°C . After stirring 30 min. at -78°C , benzaldehyde **5** (9.21 g, 26.9 mmol) in anhydrous tetrahydrofuran (25 mL) was added via cannula. After a further 90 min. at -78°C , dilute HCl (170 mL, 0.3 M) was added and the mixture extracted with diethyl ether. Combined

organic fractions were washed with a mixture of brine and saturated NaHCO_3 , then dried (MgSO_4) and filtered through a Celite plug. Removal of solvent by rotary evaporation yielded a yellow syrup (20.7 g) which was used directly in the next reaction.

Methyl ether **6a**:

To a stirred solution of crude alcohol **6** (20.6 g) and anhydrous methanol (10.9 mL, 269 mmol) in anhydrous methylene chloride (400 mL) at -45°C (dry ice/acetonitrile slush) was added trifluoroacetic acid (10.4 mL, 135 mmol). After stirring 50 min. at -45°C , reaction was quenched with 230 mL of a mixture of brine, saturated NaHCO_3 and water (9:9:4). Layers were separated and the aqueous phase extracted with diethyl ether. Combined organic fractions were dried (MgSO_4), filtered through Celite and solvent removed by rotary evaporation to yield an orange oil (20.5 g). Column chromatography (silica gel, 4" x 7", 0% \rightarrow 15% ether/hexanes) yielded methyl ether **6a** as a yellow syrup (14.8 g, 77% from **5**). ^1H NMR (600 MHz, CDCl_3) δ 7.70 (d, $J = 6.6$ Hz, 2 H), 7.43 (t, $J = 7.0$ Hz, 1 H), 7.39 (t, $J = 7.1$ Hz, 2 H), 7.04 (s, 1 H), 6.78 (d, $J = 8.1$ Hz, 1 H), 6.67 (s, 2 H), 6.64 (d, $J = 8.4$ Hz, 1 H), 5.69 (s, 1 H), 3.62 (s, 3 H), 3.31 (app. s, 4 H), 2.17 (s, 6 H), 1.28 (heptet, $J = 7.5$ Hz, 3 H), 1.13 (d, $J = 7.0$ Hz, 3 H), 1.11 (d, $J = 3.7$ Hz, 3 H), 1.09 (d, $J = 7.3$ Hz, 18 H), 1.00 (s, 9 H); ^{13}C NMR (100 MHz, CDCl_3) δ 153.73, 151.76, 139.37, 137.82, 135.28, 133.78, 131.33, 130.12, 130.08, 127.72, 124.05, 123.94, 119.87, 117.33, 80.00, 56.20, 51.86, 26.69, 26.05, 22.81, 22.72, 20.74, 19.03, 18.10, 13.07. HRMS exact mass calcd for $\text{C}_{39}\text{H}_{60}\text{O}_4\text{Si}_2$: 648.4030, found: 648.4044.

Phenol **7**:

To a stirred solution of ether **6a** (4.03 g, 6.2 mmol) in anhydrous tetrahydrofuran (60 mL) was added triethylamine trihydrofluoride (2.02 mL, 12.4 mmol). After 45 min., reaction mixture was partitioned between saturated NaHCO₃ and diethyl ether. The aqueous layer was further extracted with ether and combined organic fractions were dried (MgSO₄), then filtered through a Celite plug, and solvent was removed by rotary evaporation to yield a yellow syrup (4.1 g) which crystallized upon further standing. Recrystallization, first from hexanes, then 1:3 ether:hexanes yielded phenol **7** as a white solid (2.40 g, 85%). ¹H NMR (300 MHz, CDCl₃) δ 7.15 (s, 1 H), 6.73 (dd, *J* = 8.1, 1.2 Hz, 1 H), 6.64 (d, *J* = 8.3 Hz, 1 H), 6.51 (s, 2 H), 5.70 (s, 1 H), 4.68 (br. s, 1 H), 3.32 (app. s, 4 H), 2.20 (s, 6 H), 1.25 (heptet, *J* = 7.3 Hz, 3 H), 1.15 (app. t, *J* = 6.8 Hz, 6 H), 1.08 (d, *J* = 7.2 Hz, 18 H); ¹³C NMR (100 MHz, CDCl₃) δ 154.29, 151.82, 139.70, 137.95, 133.61, 129.06, 124.18, 123.89, 117.33, 115.58, 80.06, 56.19, 26.72, 22.75, 20.73, 18.07, 13.04. HRMS exact mass calcd for C₂₈H₄₄O₃Si: 456.3060, found: 456.3058.

Methyl ester **9**:

To a stirred solution of phenol **7** (2.78 g, 6.08 mmol) in anhydrous dimethylformamide (10 mL), was added methyl bromoacetate (864 μL, 9.13 mmol) and potassium carbonate (1.69 g, 12.2 mmol). Reaction was quenched after 6 h by slow addition of dilute HCl (1 M, 30 mL). Mixture was diluted with 150 mL water and extracted with diethyl ether. Combined organic fractions were washed twice with brine, then dried (MgSO₄), filtered through a Celite plug and solvent removed by rotary evaporation to yield methyl ester **9** as a pale yellow oil (3.7 g, 100%). ¹H NMR (300 MHz, CDCl₃) δ 7.15 (d, *J* = 0.9 Hz, 1 H), 6.71 (dd, *J* = 8.3, 1.6 Hz, 1 H), 6.63 (d, *J* = 8.4 Hz, 1 H), 6.57 (s, 2 H), 5.70 (s, 1 H),

4.63 (s, 2 H), 3.82 (s, 3 H), 3.32 (app. s, 4 H), 2.22 (s, 6 H), 1.26 (heptet, $J = 7.3$ Hz, 3 H), 1.15 (app. t, $J = 6.5$ Hz, 6 H), 1.09 (d, $J = 7.2$ Hz, 18 H); ^{13}C NMR (100 MHz, CDCl_3) δ 169.58, 156.44, 151.80, 139.60, 137.91, 133.57, 130.43, 124.09, 123.82, 117.31, 114.74, 79.95, 65.10, 56.29, 52.21, 26.75, 22.76, 20.92, 18.07, 13.04. HRMS exact mass calcd for $\text{C}_{31}\text{H}_{48}\text{O}_5\text{Si}$: 528.3271, found: 528.3261.

Alkene **9a**:

To a stirred, solution of methyl ether **9** (2.0 g, 3.8mmol), allyltrimethylsilane (15 mL, 95mmol) in anhydrous methylene chloride (50 mL) cooled to -45°C (dry ice/acetonitrile slush), was added trifluoroacetic acid (2.9 mL, 38 mmol). After stirring 15 min. at -45°C , reaction was quenched with 50 mL of saturated NaHCO_3 . The aqueous layer was extracted with diethyl ether and combined organic fractions were dried (MgSO_4), filtered through a Celite plug and solvent removed by rotary evaporation to yield a cloudy tan syrup (1.92 g). Column chromatography (silica, 1.5" x 5", 10% EtOAc/hexanes yielded alkene **9a** (1.68 g, 80%). ^1H NMR (400 MHz, CDCl_3) δ 7.01 (d, $J = 1.7$ Hz, 1 H), 6.71 (dd, $J = 8.3, 1.7$ Hz, 1 H), 6.63 (d, $J = 8.4$ Hz, 1 H), 6.53 (s, 2 H), 5.77-5.67 (m, 1 H), 5.07 (dd, $J = 17.0, 1.3$ Hz, 1 H), 4.92 (d, $J = 10.2$ Hz, 1 H), 4.60 (s, 2 H), 4.49 (app. t, $J = 8.0$ Hz, 1 H), 3.81 (s, 3 H), 3.34 (heptet, $J = 6.9$ Hz, 1 H), 3.06-2.99 (m, 1 H), 2.76-2.68 (m, 1 H), 2.12 (br. s, 6 H), 1.28 (heptet, $J = 7.5$ Hz, 3 H), 1.16 (d, $J = 6.9$ Hz, 3 H), 1.12 (d, $J = 7.0$ Hz, 3 H), 1.09 (d, $J = 7.3$ Hz, 18 H); ^{13}C NMR (100 MHz, CDCl_3) δ .169.70, 155.37, 150.74, 138.53, 137.75, 1375.55, 135.87, 135.08, 124.97, 124.55, 117.51, 115.55, 65.17, 52.15, 42.57, 36.25, 30.89, 26.65, 22.83, 18.08, 17.68, 13.04. HRMS exact mass calcd for $\text{C}_{33}\text{H}_{50}\text{O}_4\text{Si}$: 538.3478, found: 497.3079 ($\text{M} - \text{C}_3\text{H}_5$) $^+$.

Alcohol **9b**:

To a stirred solution of alkene **9a** (1.13 g, 2.1 mmol) in anhydrous tetrahydrofuran, cooled on an ice bath, was added 16 mL of 9-BBN (0.5 M in tetrahydrofuran, 8.25 mmol) via syringe. After 25 min. of stirring, another 6 mL (3 mmol) of 9-BBN was added and stirred for an additional 20 min., when tlc analysis indicated almost all the starting material was consumed. Sodium hydroxide (0.5 M, 5 mL) was added, followed by hydrogen peroxide (3 mL, 30%). The reaction was quenched with the addition of 15 mL of 10% (w/v) sodium metabisulfite pentahydrate and extracted with 3 x 60 mL diethyl ether. Combined organic layers were washed with 15 mL saturated ammonium chloride and 15 mL brine, then dried (MgSO_4), filtered and solvent evaporated to yield 2.19 g of crude product. Flash chromatography (silica 20% EtOAc/hexanes + 0% \rightarrow 5% MeOH) gave 1.02 g (90%) of alcohol **9b**. ^1H NMR (600 MHz, CDCl_3) δ 7.00 (s, 1 H), 6.70 (d, $J = 8.4$ Hz, 1 H), 6.63 (d, $J = 8.1$ Hz, 1 H), 6.53 (br. s, 2 H), 4.60 (s, 2 H), 4.40 (t, $J = 7.7$ Hz, 1 H), 3.81 (s, 3 H), 3.66 (heptet, $J = 6.4$ Hz, 1 H), 3.33 (t, $J = 6.8$ Hz, 2 H), 2.12 (br. s, 6 H), 2.37-2.32 (m, 1 H), 2.06-1.99 (m, 1 H), 1.65-1.58 (m, 1 H), 1.45-1.38 (m, 1 H), 1.28 (heptet, $J = 7.5$ Hz, 3 H), 1.15 (d, $J = 6.9$ Hz, 3 H), 1.12 (d, $J = 7.0$ Hz, 3 H), 1.09 (d, $J = 7.3$ Hz, 18 H); ^{13}C NMR (100 MHz, CDCl_3) δ 169.68, 155.32, 150.69, 138.57, 137.71, 136.07, 135.16, 124.92, 124.43, 117.47, 65.14, 63.19, 52.14, 42.35, 31.43, 30.85, 27.88, 26.64, 22.82, 18.05, 13.01. HRMS exact mass calcd for $\text{C}_{33}\text{H}_{52}\text{O}_5\text{Si}$: 556.3584, found: 556.3586.

Aldehyde **18**:

To a stirred suspension of alcohol **9b** (945 mg, 1.70 mmol) in 25 mL methylene chloride was added pyridinium dichromate (958 mg, 2.55 mmol). Reaction was stirred overnight, then diluted with diethyl ether and filtered through a pad of celite. Evaporation of solvent left 876 mg of crude product, which was chromatographed (silica, 7.5% → 15% EtOAc/Hexanes) to yield 544 mg (65%) of aldehyde **18**. ¹H NMR (600 MHz, CDCl₃) δ 9.71 (s, 1 H), 6.99 (s, 1 H), 6.71 (d, *J* = 6.2 Hz, 1 H), 6.64 (d, *J* = 7.1 Hz, 1 H), 6.55 (s, 2 H), 4.60 (s, 2 H), 4.42-4.40 (m, 1 H), 3.82 (s, 3 H), 3.33 (heptet, *J* = 7.0 Hz, 1 H), 2.64-2.58 (m, 1 H), 2.47-2.41 (m, 1 H), 2.35-2.29 (m, 2 H), 2.13 (br. s, 6 H), 1.28 (heptet, *J* = 7.4 Hz, 3 H), 1.16 (d, *J* = 7.0 Hz, 3 H), 1.12 (d, *J* = 7.0 Hz, 3 H), 1.09 (d, *J* = 7.3 Hz, 18 H); ¹³C NMR (100 MHz, CDCl₃) δ 202.21, 169.57, 155.60, 150.89, 138.75, 137.91, 135.30, 133.83, 124.83, 124.33, 117.57, 65.09, 52.14, 42.36, 41.65, 26.64, 23.73, 22.79, 18.04, 13.01. HRMS exact mass calcd for C₃₃H₅₀O₅Si: 554.3428, found: 554.3433.

8-bromo-N-butyl-N-methyloctanamide (**17**):

To a stirred suspension of 8-bromooctanoic acid (**16**) (1.27 g, 5.69 mmol) and HBTU (2.16 g, 5.69 mmol) in anhydrous methylene chloride (20 mL) was added N-methylbutylamine (673 μL, 5.69 mmol) and triethylamine (1590 μL, 11.4 mmol). After 4 h, brine was added and the aqueous phase extracted with diethyl ether. The combined organic fractions were washed with 1 M HCl (3 x 20 mL), saturated NaHCO₃ (2 x 20 mL) and brine, then dried (MgSO₄), filtered through Celite and solvent removed by rotary evaporation. Column chromatography (silica gel, 1.5" x 5", 20% → 30% EtOAc/Hexanes) yielded compound **17** as a colourless oil (1.219 g, 76%). ¹H NMR (600 MHz, CDCl₃) δ 3.40 (t, *J* = 7.0 Hz, 2 H), 3.36 (t, *J* = 7.3 Hz, 1 H), 3.25 (t, *J* = 7.3 Hz, 1

H), 2.97 (s, 1.5 H), 2.91 (s, 1.5 H), 2.29 (app. q, $J = 7.4$ Hz, 2 H), 1.86 (quintet, $J = 7.1$ Hz, 2 H), 1.66-1.62 (m, 2 H), 1.54 (quintet, $J = 7.4$ Hz, 1 H), 1.49 (quintet, $J = 7.5$ Hz, 1 H), 1.46-1.42 (m, 2 H), 1.36-1.28 (m, 6 H), 0.96 (t, $J = 7.3$ Hz, 1.5 H), 0.92 (t, $J = 7.3$ Hz, 1.5 H)

Alkene 19:

To undiluted bromooctamide **17** (175 mg, 0.60 mmol) was added triphenylphosphine (157 mg, 0.60 mmol). Mixture was stirred at 140-160 °C for 2-1/2hr., then cooled and dissolved in anhydrous tetrahydrofuran (8 mL). The solution was cooled in an ice/ethanol bath and 6 mL of lithium bis(trimethylsilyl)amide (1.0 M in THF, 0.60 mmol) was added over several min. via syringe. After a few min. stirring, aldehyde **18** (166 mg, 0.30 mmol), dissolved in 4 mL anhydrous tetrahydrofuran, was added via syringe. After a few min. of stirring, the reaction was quenched with 60% saturated NH_4Cl and extracted with 2 x 20 mL and 3 x 10 mL CHCl_3 . Combined organic fractions were washed with 10 mL each of saturated NH_4Cl , saturated NaHCO_3 and brine, then dried (MgSO_4), filtered through a Celite pad and solvent removed by rotary evaporation to give 437 mg of crude product. Flash chromatography (silica gel, 25% EtOAc/Hexanes \rightarrow 35% EtOAc/2% MeOH/Hexanes) yielded 130 mg (57%) of alkene **19**. ^1H NMR (400 MHz, CDCl_3) δ 7.01 (d, $J = 1.8$ Hz, 1 H), 6.70 (dd, $J = 8.4, 1.8$ Hz, 1 H), 6.63 (d, $J = 8.4$ Hz, 1 H), 6.54 (s, 2 H), 5.43-5.32 (m, 2 H), 4.60 (s, 2 H), 4.39 (t, $J = 7.1$ Hz, 1 H), 3.80 (s, 3 H), 3.37-3.30 (m, 2 H), 3.24 (t, $J = 7.7$ Hz, 1 H), 2.95 (s, 1.5 H), 2.90 (s, 1.5 H), 2.34-2.25 (m, 4 H), 2.24-1.87 (br. s, m, 10 H), 1.66-1.58 (m, 2 H), 1.35-1.23 (m, 11 H), 1.16 (d, $J = 7.0$ Hz, 3 H), 1.13 (d, $J = 7.0$ Hz, 3 H), 1.09 (d, $J = 7.3$ Hz, 18 H), 1.06-0.94 (m, 3 H); ^{13}C

NMR (100 MHz, CDCl₃) δ 172.82, 172.70, 169.60, 155.26, 150.59, 138.53, 137.59, 136.02, 135.37, 130.28, 129.60, 125.01, 124.48, 117.43, 65.14, 52.05, 49.66, 47.31, 42.27, 35.20, 33.54, 33.23, 32.88, 32.04, 30.58, 29.49, 29.35, 29.01, 27.07, 26.58, 25.87, 25.37, 25.00, 22.79, 19.99, 19.88, 18.01, 13.79, 12.98. HRMS exact mass calcd for C₄₆H₇₅NO₅Si: 749.5415, found: 749.5400.

Methyl ester **19a**:

To an argon-sparged solution of alkene **19** (197 mg, 0.263 mmol) in absolute ethanol, in a Parr flask, was added palladium on carbon (110 mg). Flask was shaken for 12 h under 20 psi hydrogen gas, then filtered through a Celite pad, rinsing with EtOAc. Evaporation of solvent gave 208 mg of methyl ester **19a**, which was used without further purification.

¹H NMR (600 MHz, CDCl₃) δ 6.98 (s, 1 H), 6.70 (d, *J* = 8.4 Hz, 1 H), 6.62 (d, *J* = 8.4 Hz, 1 H), 6.53 (br. s, 2 H), 4.60 (s, 2 H), 4.37-4.34 (m, 1 H), 3.81 (s, 3 H), 3.37-3.30 (m, 2 H), 3.25 (t, *J* = 7.5 Hz, 1 H), 2.96 (s, 1.5 H), 2.90 (s, 1.5 H), 2.30-2.26 (m, 2 H), 2.25-2.21 (m, 1 H), 2.04 (br. s, 6 H), 1.95-1.89 (m, 1 H), 1.64-1.60 (m, 2 H), 1.57-1.52 (m, 1 H), 1.51-1.46 (m, 1 H), 1.35-1.24 (m, 19 H), 1.15 (d, *J* = 7.0 Hz, 3 H), 1.12 (d, *J* = 7.0 Hz, 3 H), 1.09 (d, *J* = 7.3 Hz, 18 H), 0.96-0.91 (m, 3 H); ¹³C NMR (100 MHz, CDCl₃) δ 172.77, 172.65, 169.52, 155.09, 150.43, 138.33, 137.43, 136.34, 135.67, 124.87, 124.43, 117.27, 65.00, 51.92, 49.58, 47.21, 42.57, 35.12, 33.47, 33.13, 32.82, 31.85, 30.50, 30.04, 29.48, 29.42, 29.39, 29.32, 29.29, 29.27, 28.22, 26.52, 25.33, 24.96, 22.70, 19.91, 19.79, 17.94, 13.71, 13.68, 12.90. HRMS exact mass calcd for C₄₆H₇₇NO₅Si: 751.5571, found: 751.5563.

Phenol **19b**:

To a stirred solution of ester **19a** (200 mg, 0.27 mmol) in anhydrous tetrahydrofuran (5 mL) was added, via syringe, triethylamine trihydrofluoride (4.35 mL, 26.6 mmol). After 21 h of stirring at RT, reaction was heated to ~40°C for 1 h, then quenched with potassium carbonate (5.5 g) and water (15 mL) and extracted with 3 x 30 mL ethyl acetate. Combined organic fractions were washed with 2 x 7 mL saturated NH₄Cl, 8 mL brine, then dried (MgSO₄), filtered through Celite and solvent removed by rotary evaporation. Column chromatography (silica gel, 10% EtOAc/Hexanes → 30% EtOAc/5% MeOH/Hexanes) yielded phenol **19b** (120 mg, 76%). ¹H NMR (400 MHz, CDCl₃) δ 6.97 (d, *J* = 1.8 Hz, 1 H), 6.76 (dd, *J* = 8.2, 1.7 Hz, 1 H), 6.63 (d, *J* = 8.4 Hz, 1 H), 6.53 (s, 2 H), 5.03 (br. s, 1 H), 4.60 (s, 2 H), 4.34 (t, *J* = 7.7 Hz, 1 H), 3.81 (s, 3 H), 3.36 (t, *J* = 7.5 Hz, 1 H), 3.25 (t, *J* = 7.7 Hz, 1 H), 3.16 (heptet, *J* = 6.9 Hz, 1 H), 2.96 (s, 1.5 H), 2.91 (s, 1.5 H), 2.33-2.25 (m, 3 H), 2.24-1.97 (m, br. s, 6 H), 1.96-1.88 (m, 2 H), 1.65-1.58 (m, 2 H), 1.56-1.46 (m, 2 H), 1.37-1.28 (m, 8 H), 1.27-1.23 (m, 6 H), 1.21 (d, *J* = 6.6 Hz, 3 H), 1.18 (d, *J* = 7.0 Hz, 3 H), 0.95 (t, *J* = 7.3 Hz, 1.5 H), 0.92 (t, *J* = 7.3 Hz, 1.5 H); ¹³C NMR (100 MHz, CDCl₃) δ 173.39, 173.28, 169.73, 155.05, 151.25, 138.39, 135.73, 135.46, 133.86, 125.08, 124.66, 114.81, 65.06, 52.06, 49.79, 47.49, 42.63, 35.34, 33.58, 33.42, 32.91, 31.98, 30.49, 30.03, 29.48, 29.44, 29.40, 29.34, 29.28, 29.24, 28.26, 26.97, 25.342, 25.04, 22.52, 19.91, 19.81, 13.73, 13.71. HRMS exact mass calcd for C₃₇H₅₇NO₅: 595.4237, found: 595.4236.

Oxyacetic acid **21**:

To a stirred solution of methyl ester **19b** (115 mg, 0.19 mmol) in methanol (6 mL) was added lithium hydroxide monohydrate (18 mg, 0.42 mmol) and water (19 μ L, 1.06 mmol). After 17 h, saturated NH_4Cl (2 mL) was added and the volume was reduced with rotary evaporation. HCl (1 M, 1 mL) was added and the solution was extracted with 3 x 13 mL CHCl_3 . The combined organic fractions were dried (MgSO_4), filtered through Celite and solvent removed by rotary evaporation to yield 128 mg of crude product. Flash chromatography (silica, 7.5% EtOAc, 3% AcOH, CHCl_3) gave compound **21** (100 mg, 90%). ^1H NMR (600 MHz, CDCl_3) δ 7.00 (s, 1 H), 6.75 (d, $J = 7.3$ Hz, 1 H), 6.61 (d, $J = 8.1$ Hz, 1 H), 6.56 (br. s, 2 H), 4.62 (s, 2 H), 4.38-4.35 (m, 1 H), 3.37 (t, $J = 7.5$ Hz, 1 H), 3.26 (t, $J = 7.5$ Hz, 1 H), 3.16 (heptet, $J = 7.1$ Hz, 1 H), 2.98 (s, 1.5 H), 2.93 (s, 1.5 H), 2.36-2.22 (m, 2 H), 2.21-2.15 (m, 1 H), 2.10 (br. s, 6 H), 2.05-1.96 (m, 1 H), 1.63-1.57 (m, 2 H), 1.56-1.52 (m, 1 H), 1.52-1.47 (m, 1 H), 1.37-1.29 (m, 4 H), 1.28-1.23 (m, 4 H), 1.21 (app. d, $J = 7.0$ Hz, 6 H), 1.18 (app. d, $J = 7.0$ Hz, 4 H), 1.15-1.11 (m, 4 H), 0.95 (t, $J = 7.5$ Hz, 1.5 H), 0.92 (t, $J = 7.3$ Hz, 1.5 H); ^{13}C NMR (100 MHz, CDCl_3) δ 174.25, 174.20, 171.20, 155.14, 150.50, 138.57, 136.71, 135.23, 133.70, 125.34, 124.89, 114.92, 64.95, 50.07, 47.76, 42.50, 35.58, 33.69, 33.56, 32.88, 31.61, 30.57, 29.31, 29.25, 29.14, 28.80, 28.68, 27.36, 27.25, 25.72, 25.29, 22.60, 20.00, 19.93, 13.84, 13.80. HRMS exact mass calcd for $\text{C}_{36}\text{H}_{55}\text{NO}_5$: 581.4080, found: 581.4082.

3.6. References

- [1] Braverman, L.E., Utiger, R.D., Werner, S.C. & Ingbar, S.H. (1991). "Werner and Ingbar's the thyroid : a fundamental and clinical text." 6th ed. Lippincott, Philadelphia.

- [2] Zhang, J. & Lazar, M.A. (2000). The mechanism of action of thyroid hormones. *Annual Review of Physiology* 62, 439-66.
- [3] Mangelsdorf, D.J., Thummel, C., Beato, M., Herrlich, P., Schütz, G., Umesono, K., Blumberg, B., Kastner, P., Mark, M. & Chambon, P. (1995). The nuclear receptor superfamily: the second decade. *Cell* 83, 835-9.
- [4] Singh, B.N. & Vaughan Williams, E.M. (1970). The effect of amiodarone, a new anti-anginal drug, on cardiac muscle. *British Journal of Pharmacology* 39, 657-67.
- [5] Burger, A., Dinichert, D., Nicod, P., Jenny, M., Lemarchand-Béraud, T. & Vallotton, M.B. (1976). Effect of amiodarone on serum triiodothyronine, reverse triiodothyronine, thyroxin, and thyrotropin. A drug influencing peripheral metabolism of thyroid hormones. *Journal of Clinical Investigation* 58, 255-9.
- [6] Vanbeeren, H.C., Bakker, O. & Wiersinga, W.M. (1995). Desethylamiodarone Is a Competitive Inhibitor of the Binding of Thyroid Hormone to the Thyroid Hormone Alpha-1-Receptor Protein. *Molecular and Cellular Endocrinology* 112, 15-19.
- [7] Latham, K.R., Sellitti, D.F. & Goldstein, R.E. (1987). Interaction of amiodarone and desethylamiodarone with solubilized nuclear thyroid hormone receptors. *Journal of the American College of Cardiology* 9, 872-6.
- [8] Bakker, O., Vanbeeren, H.C. & Wiersinga, W.M. (1994). Desethylamiodarone Is a Noncompetitive Inhibitor of the Binding of Thyroid Hormone to the Thyroid Hormone Beta(1)-Receptor Protein. *Endocrinology* 134, 1665-1670.

- [9] van Beeren, H.C., Bakker, O. & Wiersinga, W.M. (2000). Desethylamiodarone interferes with the binding of co-activator GRIP-1 to the beta(1)-thyroid hormone receptor. *Febs Letters* 481, 213-216.
- [10] Chiellini, G., Apriletti, J.W., Yoshihara, H.A.I., Baxter, J.D., Ribeiro, R.C.J. & Scanlan, T.S. (1998). A high-affinity subtype-selective agonist ligand for the thyroid hormone receptor. *Chemistry & Biology* 5, 299-306.
- [11] Yoshihara, H.A.I., Chiellini, G., Mitchison, T.J. & Scanlan, T.S. (1998). An efficient substitution reaction for the preparation of thyroid hormone analogues. *Bioorganic & Medicinal Chemistry* 6, 1179-1183.
- [12] Chiellini, G., Nguyen, N.H., Yoshihara, H.A.I. & Scanlan, T.S. (2000). Improved synthesis of the iodine-free thyromimetic GC-1. *Bioorganic & Medicinal Chemistry Letters* 10, 2607-2611.
- [13] Gillard, J.W., Fortin, R., Morton, H.E., Yoakim, C., Quesnelle, C.A., Daignault, S. & Guindon, Y. (1988). Symmetrical Alkoxysilyl Ethers. A New Class of Alcohol-Protecting Group. Preparation of tert-Butoxydiphenylsilyl Ethers. *Journal of Organic Chemistry* 53, 2602-2608.
- [14] Guindon, Y., Fortin, R., Yoakim, C. & Gillard, J.W. (1984). tert-Butylmethoxyphenylsilyl Ether - A New Selective, Stable Alcohol Protecting Group with Remarkable Lability to Fluoride. *Tetrahedron Letters* 25, 4717-4720.
- [15] Imamoto, T., Kusumoto, T., Tawarayama, Y., Sugiura, Y., Mita, T., Hatanaka, Y. & Yokoyama, M. (1984). Carbon-Carbon Bond-Forming Reactions Using Cerium Metal or Organocerium(III) Reagents. *Journal of Organic Chemistry* 49, 3904-3912.

- [16] Imamoto, T., Sugiura, Y. & Takiyama, N. (1984). Organocerium Reagents. Nucleophilic Addition to Easily Enolizable Ketones. *Tetrahedron Letters* 25, 4233-4236.
- [17] Brzozowski, A.M., Pike, A.C.W., Dauter, Z., Hubbard, R.E., Bonn, T., Engstrom, O., Ohman, L., Greene, G.L., Gustafsson, J.-Å. & Carlquist, M. (1997). Molecular basis of agonism and antagonism in the oestrogen receptor. *Nature (London)* 389, 753-758.
- [18] Wagner, R.L., Apriletti, J.W., McGrath, M.E., West, B.L., Baxter, J.D. & Fletterick, R.J. (1995). A structural role for hormone in the thyroid hormone receptor. *Nature (London)* 378, 690-697.
- [19] Wakeling, A.E. & Bowler, J. (1987). Steroidal pure antioestrogens. *Journal of Endocrinology* 112, R7-10.
- [20] Bowler, J., Lilley, T.J., Pittam, J.D. & Wakeling, A.E. (1989). Novel steroidal pure antiestrogens. *Steroids* 54, 71-99.
- [21] Germain, P., Iyer, J., Zechel, C. & Gronemeyer, H. (2002). Co-regulator recruitment and the mechanism of retinoic acid receptor synergy. *Nature* 415, 187-92.
- [22] Zechel, C. (2002). Synthetic retinoids dissociate coactivator binding from corepressor release. *J Recept Signal Transduct Res* 22, 31-61.
- [23] Pike, A.C.W., Brzozowski, A.M., Walton, J., Hubbard, R.E., Thorsell, A.G., Li, Y.L., Gustafsson, J.A. & Carlquist, M. (2001). Structural insights into the mode of action of a pure antiestrogen. *Structure* 9, 145-153.

- [24] Shiau, A.K., Barstad, D., Loria, P.M., Cheng, L., Kushner, P.J., Agard, D.A. & Greene, G.L. (1998). The structural basis of estrogen receptor/coactivator recognition and the antagonism of this interaction by tamoxifen. *Cell* 95, 927-37.
- [25] Wagner, R.L., Huber, B.R., Shiau, A.K., Kelly, A., Cunha Lima, S.T., Scanlan, T.S., Apriletti, J.W., Baxter, J.D., West, B.L. & Fletterick, R.J. (2001). Hormone selectivity in thyroid hormone receptors. *Molecular Endocrinology* 15, 398-410.
- [26] Weatherman, R.V., Fletterick, R.J. & Scanlan, T.S. (1999). Nuclear-receptor ligands and ligand-binding domains. *Annual Review of Biochemistry* 68, 559-81.

Chapter 4: Structural Determinants of Selective Thyromimetics

4.1. Introduction

Thyroid hormone is a classical endocrine hormone that plays important roles in development and regulation of homeostasis [1]. Thyroxine (T_4 , 2, Figure 4.1) is the major secreted form which is enzymatically deiodinated in peripheral tissues to the more active form, 3,5,3'-triiodo-L-thyronine (T_3 , 1, Figure 4.1). Most of thyroid hormone's actions are believed to be mediated through nuclear thyroid hormone receptors (TRs) that regulate transcription of target genes either positively or negatively in response to hormone binding [2]. The two genes for TR, $TR\alpha$ and $TR\beta$ are expressed in most tissues each in two alternatively spliced variants, $TR\alpha_1$, $TR\alpha_2$, $TR\beta_1$ and $TR\beta_2$ [3]. All these forms of the receptor except $TR\alpha_2$ are activated by T_3 , which binds the ligand binding domain (LBD) of the receptor with high affinity. While $TR\alpha$ and $TR\beta$ are widely expressed, they have distinct patterns of expression [3]. Mice deficient in either $TR\alpha$ or $TR\beta$ show different phenotypes [4-8], suggesting that each receptor isoform has significantly different regulatory roles.

T_3 binds both $TR\alpha_1$ and $TR\beta_1$ with near equal affinity [9]. Synthetic ligands that bind preferentially to only one isoform could be powerful tools for studying each isoform's physiological roles. T_3 is a potent serum cholesterol lowering agent [10-12]; however, its therapeutic use in treating hypercholesterolemia is prevented by various side effects. Tachycardia, increased cardiac output and the increased risk of cardiac arrhythmia [13; 14] are the most serious side effects that arise from an excess of T_3 . Mice deficient in $TR\alpha_1$ have a 20% lower heart rate than wild-type mice, and this does not increase to

wild-type levels with T₃ treatment [15]. TRβ is the predominant isoform expressed in the liver [16], and upon T₃ treatment, mice deficient in TRβ do not upregulate CYP7A, the rate-limiting enzyme for the conversion of cholesterol to bile acids [17]. These results suggest that TRβ-selective thyromimetics with the expected tissue-selective action could function as useful therapeutic agents.

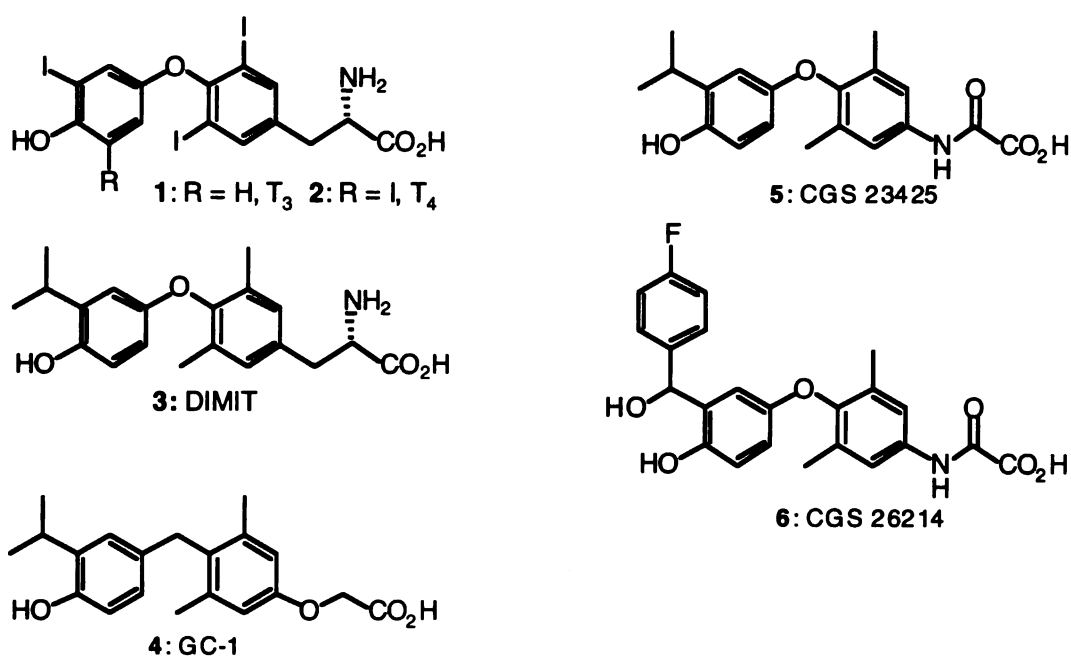


Figure 4.1. Structures of thyroid hormones and thyromimetics

A number of thyromimetics have been reported in recent years to have tissue-selective action. Among these compounds are CGS 23425 [18] (5, Figure 4.1), CGS 26214 [19] (6, Figure 4.1) and GC-1 [9; 20] (4, Figure 4.1). CGS 23425 has a structure resembling the non-selective thyromimetic 3,5-dimethyl-3'-isopropyl-L-thyronine [21] (DIMIT, 3, Figure 4.1) but with an oxamic acid polar side chain replacing DIMIT's alanine side chain. In hypercholesterolemic rats, CGS 23425 lowers low-density lipoprotein

cholesterol by 44% without inducing cardiotoxic effects [18], demonstrating that the compound is a liver-selective, cardiac-sparing thyromimetic. The selective action of CGS 23425 has been attributed to the preferential activation of TR β over TR α . In assays of TR-mediated transcription activation from a rat apoAI promoter in HuH-7 cells, CGS 23425 has EC₅₀ values of 0.002 nM for hTR β ₁ and 0.1 nM for hTR α ₁, a 50-fold preference for activation of TR β over TR α in this system [18]. It has not been reported whether this difference in potency for the TR isoforms reflects differences in affinity.

CGS 26214 resembles CGS 23425 structurally but has a 4-fluorophenyl-hydroxymethyl substituent at the 5' position. When tested in rats and dogs, CGS 26214 is a potent serum cholesterol lowering agent free of cardiovascular effects. In nuclear binding assays using intact neonatal rat cardiac myocytes, CGS 26214 has an apparent 100-fold lower affinity than T₃, while the affinities of the ligands are comparable when the assay is performed using cultured liver (HepG2) cells [19]. These results suggest that the tissue selective thyromimetic effects of CGS 26214 may be due to preferential TR binding in the liver.

The thyromimetic GC-1 was developed in our laboratory and binds hTR β ₁ with an affinity comparable to T₃, but binds hTR α ₁ with a 10-fold lower affinity [9]. This 10-fold selectivity and ability to preferentially activate TR β is reflected in several *in vivo* studies where it exhibits a distinct subset of physiological responses to T₃ in such TR-mediated processes as tadpole metamorphosis [22], lipid metabolism [23], cerebellar development [24] and adaptive thermogenesis [25]. The structural features of GC-1 that confer its

TR β -selectivity are not well defined. GC-1 was designed as a synthetically accessible thyromimetic that would serve as a platform for the development of TR antagonists. Its design was based on DIMIT, which binds TR with approximately 100-fold lower affinity than T₃ [9; 26]. For ease of synthesis, GC-1 was designed with a methylene group joining the two aromatic rings, instead of the ether oxygen of DIMIT and T₃. The α -amino group of T₃ is not required for high affinity binding to TR [26], and the oxyacetic acid polar side chain was intended as a readily synthesized isostere of propionic acid. Comparing the structures and activities of GC-1 and DIMIT, one concludes that the structural changes introduced by the methylene bridge or oxyacetic acid side chain are responsible for the GC-1's higher affinity and selectivity.

Crystallographic studies have shown that only one amino acid residue (Ser277 in hTR α ₁, Asn331 in hTR β ₁) is different in the ligand binding cavity of the two receptors [4; 27]. This residue does not directly contact the ligand, but the comparison of the co-crystal structures of TR β -LBD with GC-1 bound and with T₃ bound shows that Asn331 participates in a hydrogen bonding network with neighboring arginine residues that is arranged differently depending on the ligand present [28]. The role of Asn331/Ser277 in GC-1's TR β selectivity has been confirmed with mutagenesis experiments showing that TR β Asn331Ser has reduced affinity for GC-1 while TR α Ser277Asn has increased affinity [28].

Comparing the structures of T₃, DIMIT, GC-1, CGS 23425 and CGS 26214, a correlation emerges between selective action and the identity of the polar side chain. DIMIT and T₃ have an alanine polar side chain and are not selective, while the TR ligands with oxyacetic or oxamic acid side chains have selective action *in vivo*. For GC-1 this selective action correlates with its preferential binding to TR β .

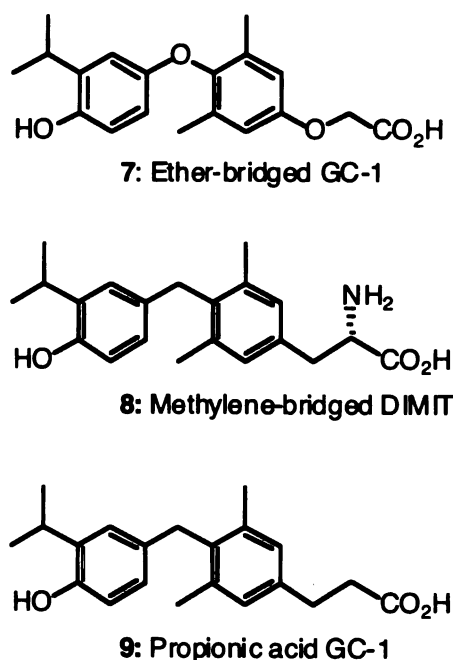


Figure 4.2. Structures of target compounds to study effects of GC-1's methylene bridge and oxyacetic acid side chain on TR selectivity

Seeking to understand better the specific roles of GC-1's methylene bridge and oxyacetic acid side chain in its TR β selectivity, we synthesized analogues of GC-1 and DIMIT bearing only one of the two different structural features. By comparing the binding

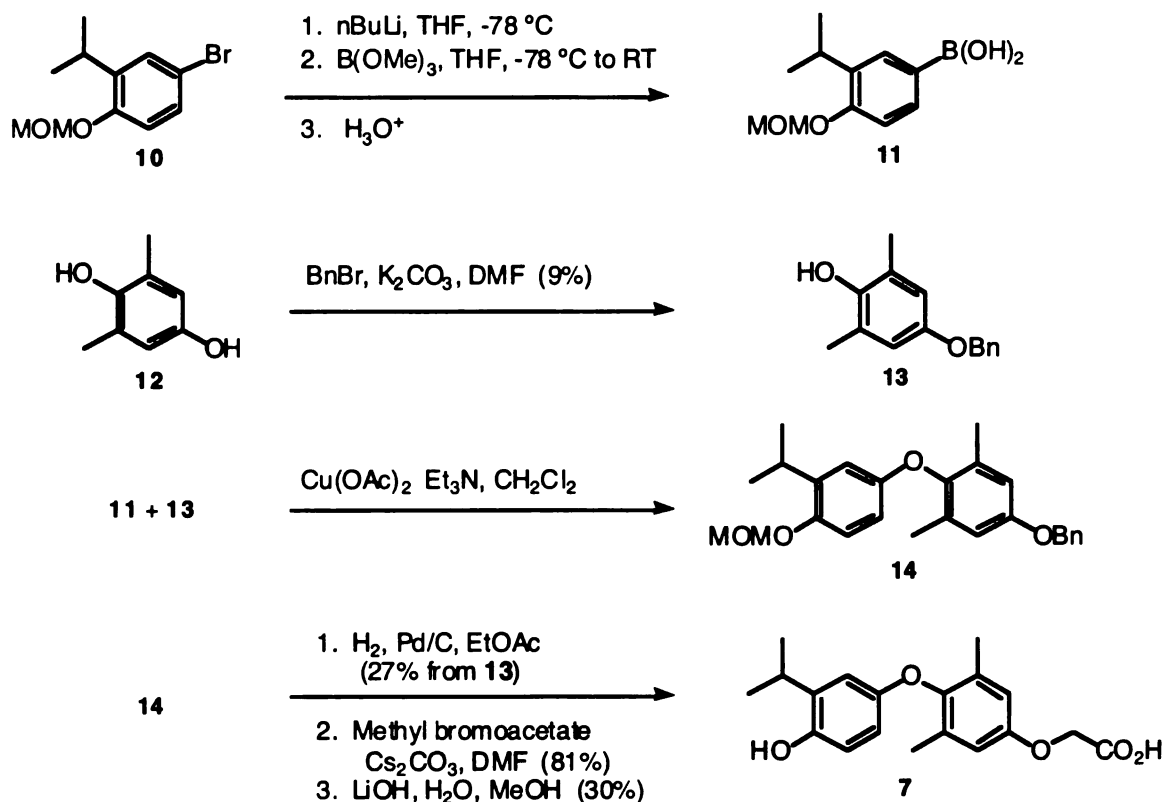


affinities and selectivities of methylene-bridged DIMIT (**8**, Figure 4.2) and GC-1 ether (**7**, Figure 4.2) to those of DIMIT and GC-1 the effects of the ether to methylene and the alanine to oxyacetic acid substitutions can be evaluated individually. The methylene-bridged analogue of T₃ has a 2.5-fold higher affinity for TR than T₃ [26]; however, this result was from a binding assay based on a nuclear extract, making it difficult to evaluate isoform-selective binding. Additionally, the propionic acid side chain analogue of GC-1 (**9**, Figure 4.2) was prepared, in order to assess the effect of the ether oxygen in the polar side chain of GC-1. To ensure the most valid comparisons between thyromimetic ligands, i.e. those with small perturbations, the study was limited to GC-1, DIMIT and their related analogues.

4.2. Results

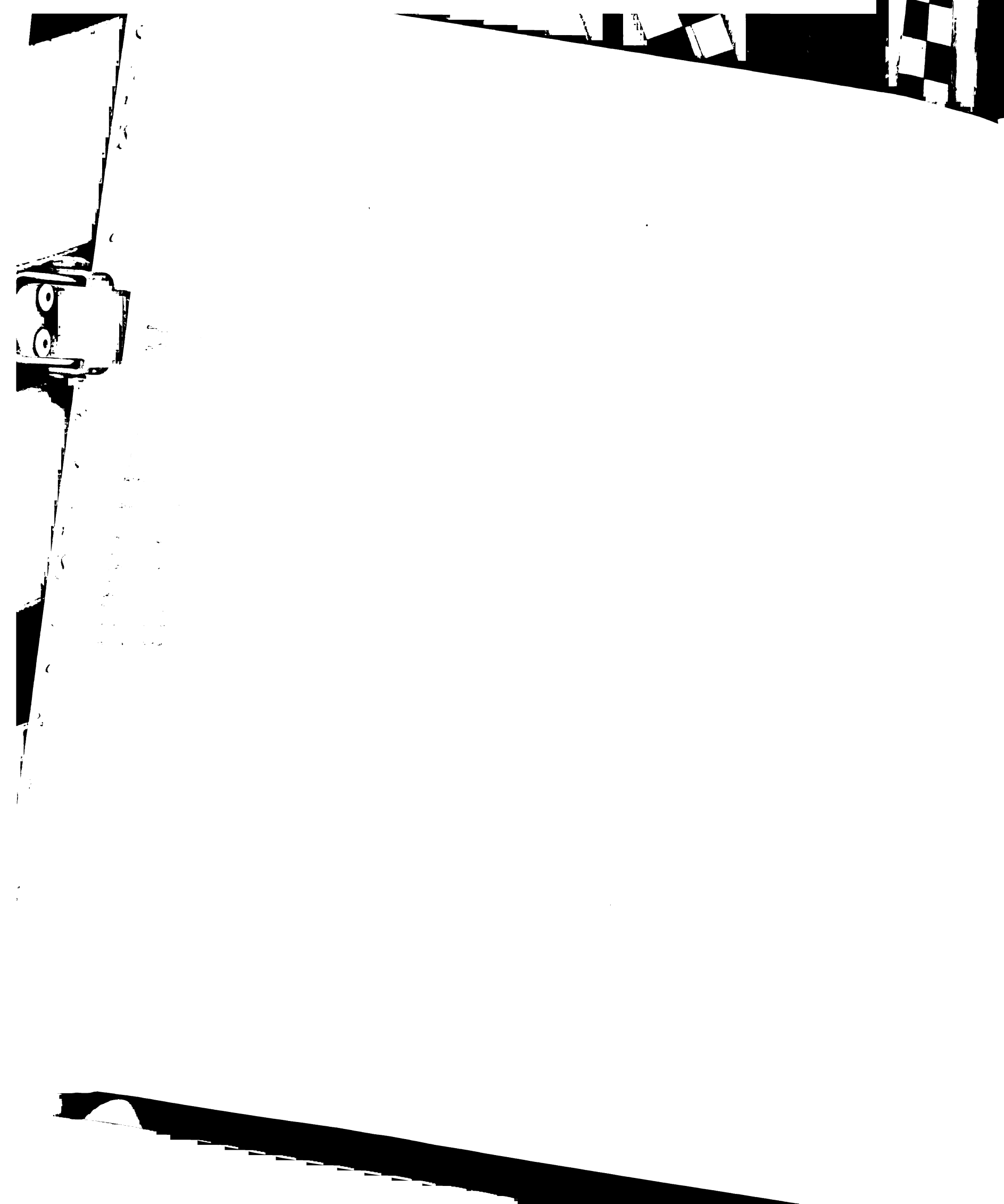
4.2.1. Synthesis of GC-1 Ether

The synthesis of the biaryl ether analogue of GC-1 was achieved in seven linear steps starting from 2-isopropylphenol and 2,6-dimethylhydroquinone. The key step of joining the two aromatic rings in a biaryl ether linkage from arylboronic acid and phenolic intermediates was achieved using the copper(II) catalysed coupling reaction developed by Evans [29] (Scheme 4.1). 4-benzyloxy-2,6-dimethylphenol (**13**) was prepared in low yield from the alkylation of 2,6-dimethylhydroquinone by a Williamson ether synthesis. The site of alkylation was assigned on the basis of ¹H NMR chemical shift perturbations of the 3,5-protons and the 2,6-methyl protons compared to the corresponding chemical shifts in the starting material and the other alkylated products.



Scheme 4.1. Preparation of the ether bridged analogue of GC-1

The arylboronic acid intermediate **11** for the coupling reaction was prepared from the *para*-bromination of 2-isopropylphenol, followed by the protection of the phenol as a methoxymethyl (MOM) ether. The aryl bromide **10** [20] was converted to the arylboronic acid with the sequential addition of *n*-butyllithium and trimethylborate, followed by hydrolysis with aqueous HCl. The coupling of **11** and **13** was effected with copper(II) acetate and triethylamine as the base. The oxyacetic acid polar side chain was installed by deprotection of the 1-hydroxyl of **14** with catalytic hydrogenation, alkylation with methyl bromoacetate and hydrolysis of the ester with lithium hydroxide. The MOM



group protecting the 4'-hydroxyl was unexpectedly cleaved under the saponification conditions, providing **7**, the biaryl ether analogue of GC-1. The L-alanine side chain was synthesized from a propionic acid side chain containing intermediate, using Evans's chiral auxiliary.

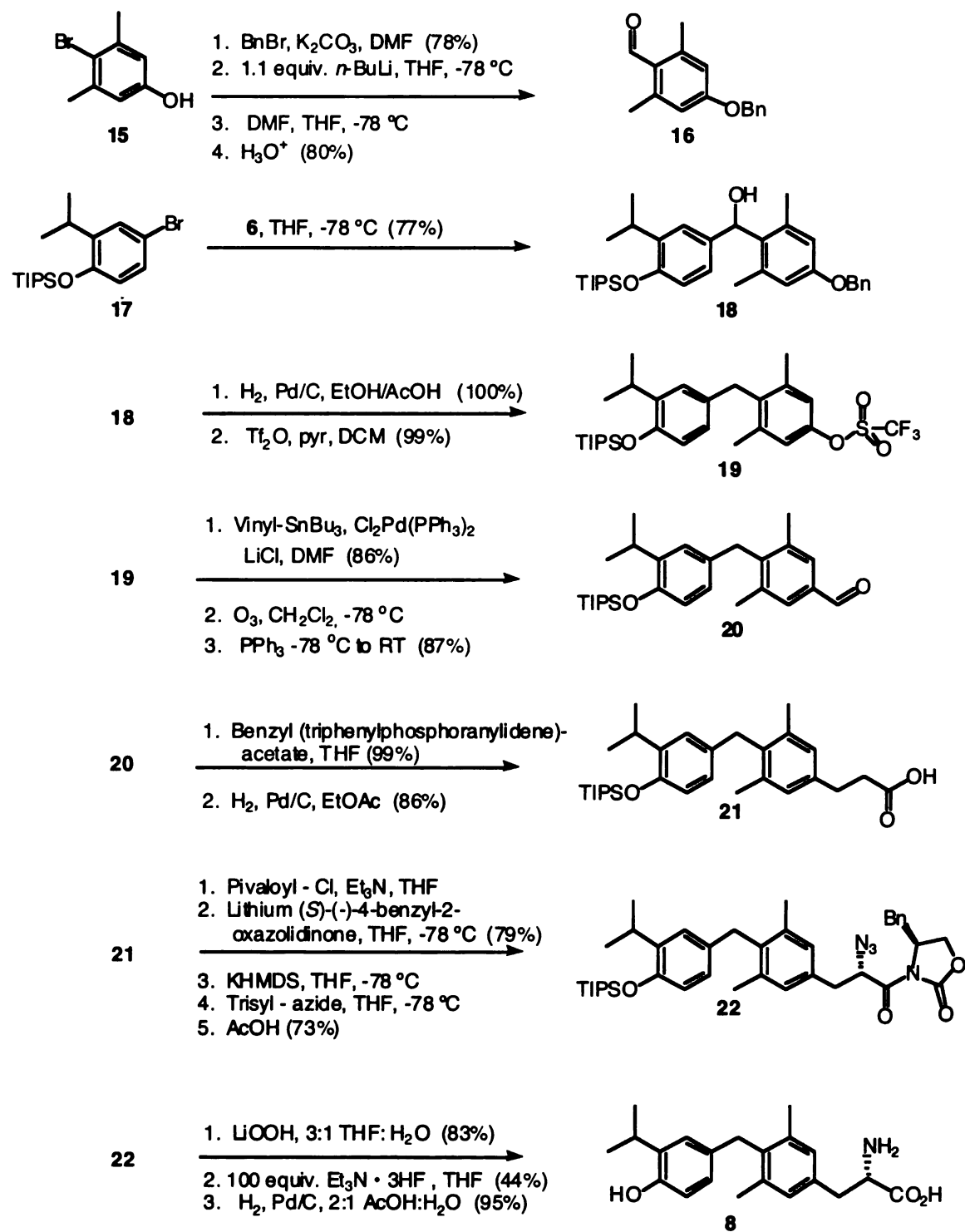
4.2.2. Synthesis of methylene-bridged L-DIMIT

The synthesis of the methylene-bridged analogue of L-DIMIT was achieved in fourteen linear steps starting from 4-bromo-2-isopropylphenol and 4-bromo-3,5-dimethylphenol (Scheme 4.2). The synthesis of the biphenylmethane scaffold employed the same strategy used to make GC-1 [9; 20], with the coupling of the aromatic rings effected by the 1,2-addition of an aryllithium intermediate to a benzaldehyde intermediate. The hydroxyl of 4-bromo-3,5-dimethylphenol was protected as a benzyl ether, which was removed during the catalytic hydrogenolysis of the hydroxyl on the bridging carbon of **18**.

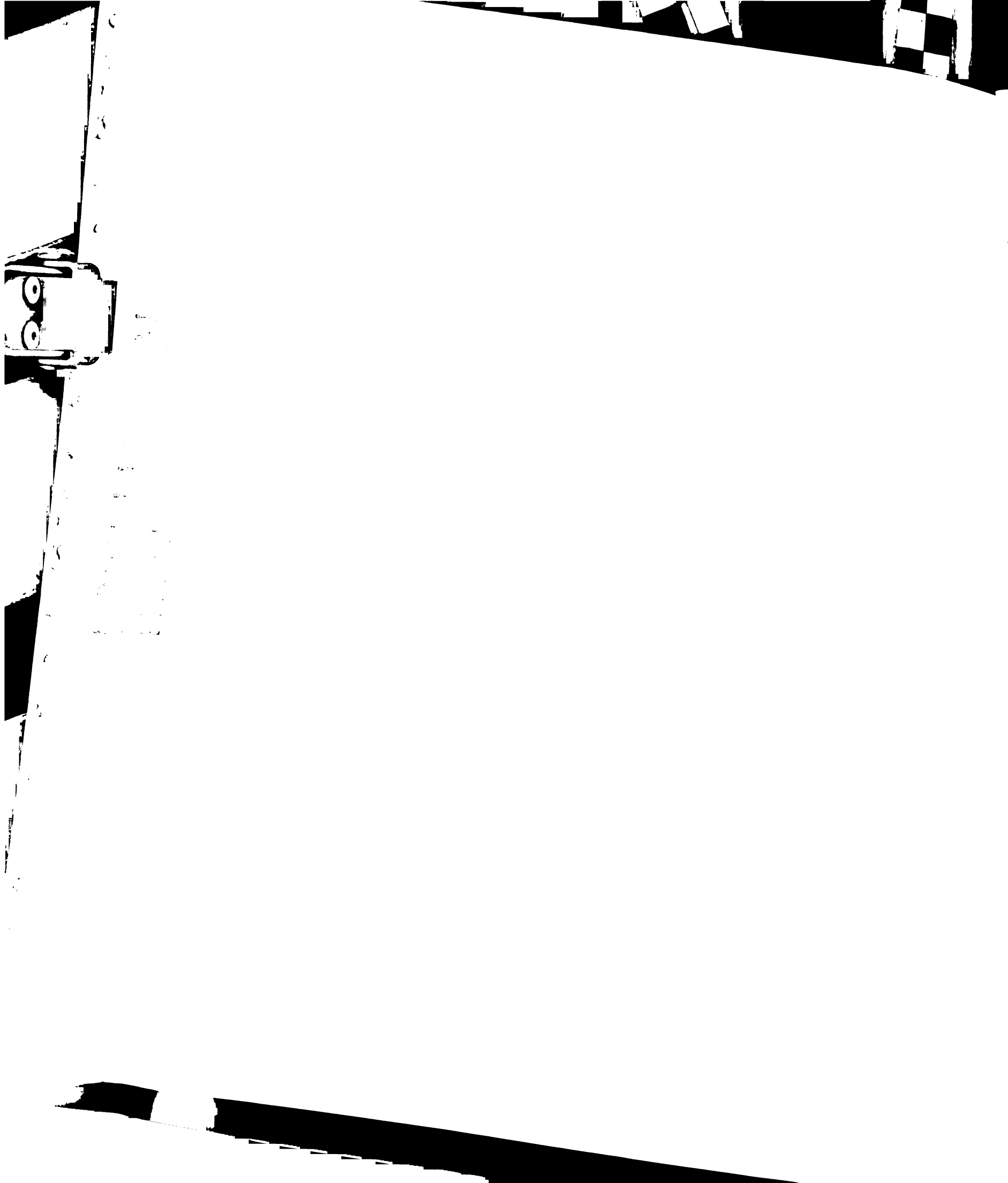
4-benzyloxy-2,6-dimethylbromobenzene was prepared by reaction of 4-bromo-3,5-dimethylphenol (**15**) with benzyl bromide and potassium carbonate in DMF. The benzaldehyde **16** was prepared in the usual fashion by treatment first with *n*-butyllithium, then DMF as a formylating reagent, followed by an aqueous acid workup. Catalytic hydrogenation of **18** yielded a phenolic biarylmethane intermediate, which was reacted with trifluoromethanesulfonic anhydride to produce the aryltrifluoromethanesulfonate (aryltriflate) **19** in high yield. Using a Stille coupling with vinyltributylstannane, aryltriflate, **19** was converted to a styrene intermediate, which was cleaved to the



benzaldehyde **20** via ozonolysis and reduction using triphenylphosphine.



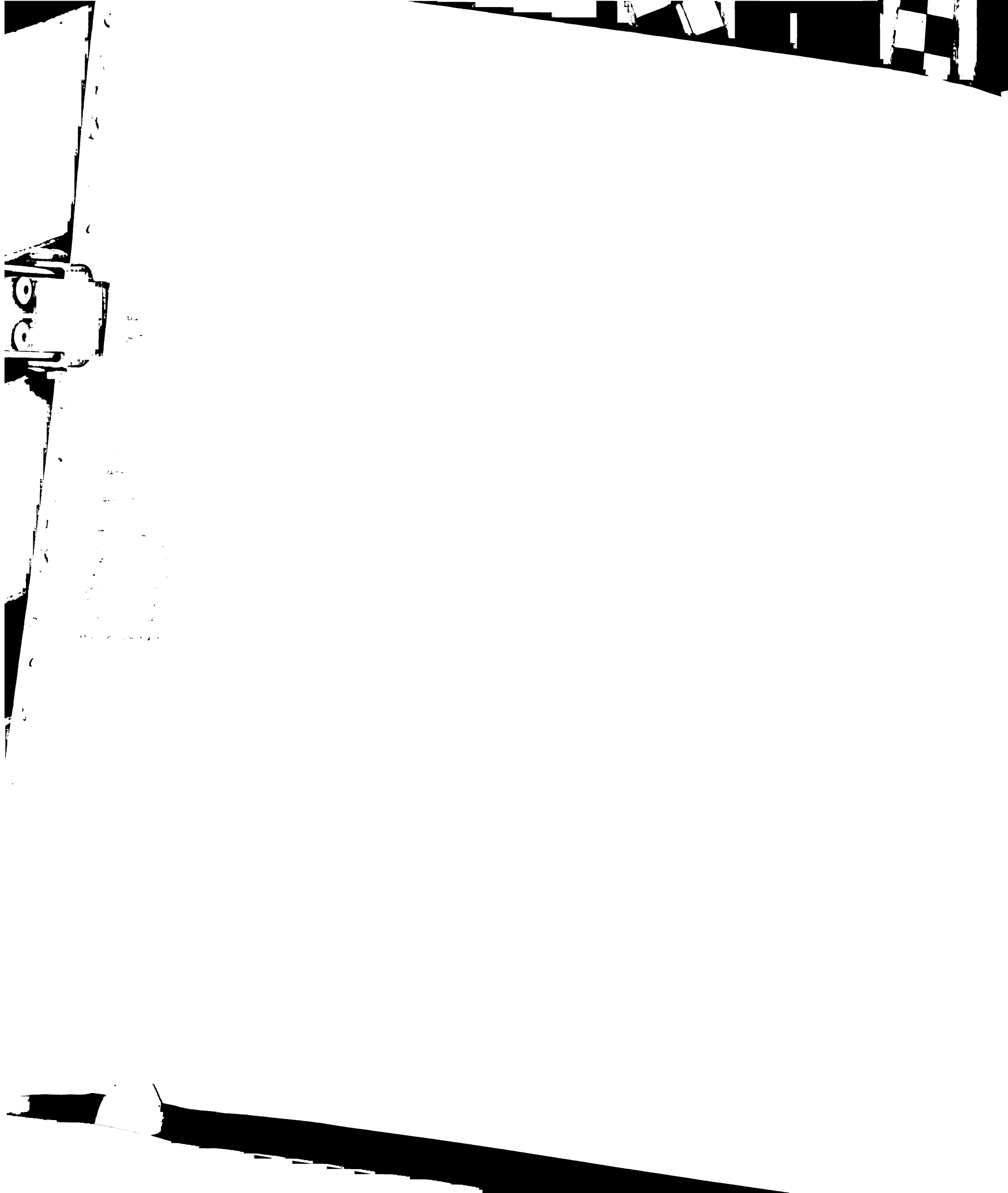
Scheme 4.2. Preparation of the methylene bridged analogue of DIMIT

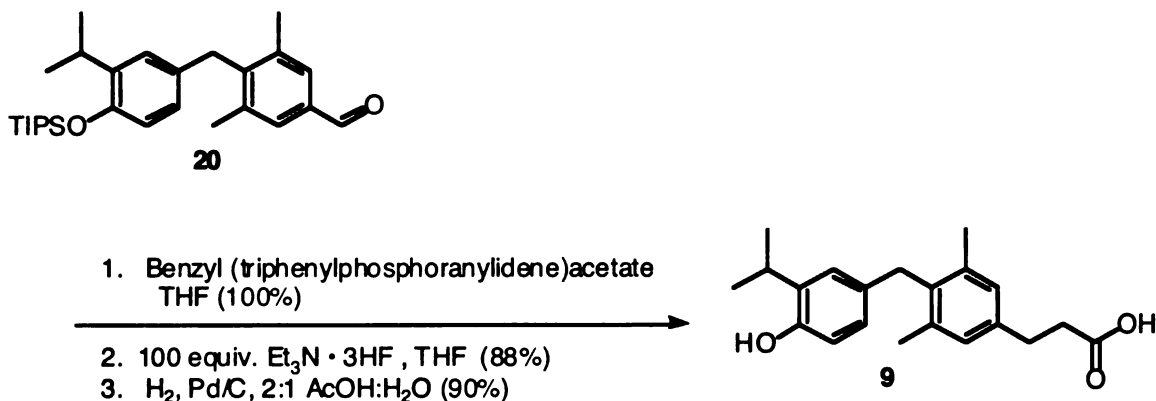


The propionic acid side chain was built from the benzaldehyde by a Wittig olefination with benzyl (triphenylphosphoranylidene)acetate, followed by catalytic hydrogenation to reduce the acrylate ester to propionate and hydrogenolyse the benzyl ester. To install the chiral auxiliary, (S)-4-benzyl-2-oxazolidinone, a mixed anhydride was generated from the propionic acid intermediate **21** and pivaloyl chloride, which was reacted with the lithium salt of (S)-4-benzyl-2-oxazolidinone. The chiral N-acyl oxazolidinone was deprotonated with potassium bis(trimethylsilyl)amide and quickly reacted with 2,4,6-triisopropylbenzenesulfonyl azide, followed rapidly by an acetic acid quench to give the single diastereomer (by ¹H and ¹³C NMR) of the N-(α -azidoacyl) oxazolidinone **22**. The chiral auxiliary was removed with lithium peroxide followed by deprotection of the TIPS ether with triethylamine trihydrofluoride. Finally, the α -azide was reduced to the α -amine with catalytic hydrogenation to yield the methylene-bridged analogue of L-DIMIT (**8**).

4.2.3. Synthesis of propionic acid side chain analogue of GC-1

The GC-1 analogue with a propionic acid polar side chain (**9**, Scheme 4.3) was prepared from the benzaldehyde intermediate (**20**, Scheme 4.2) of the synthesis of methylene-bridged DIMIT. The TIPS protecting group was removed using the standard procedure and the product was hydrogenated to generate the propionic acid side chain.



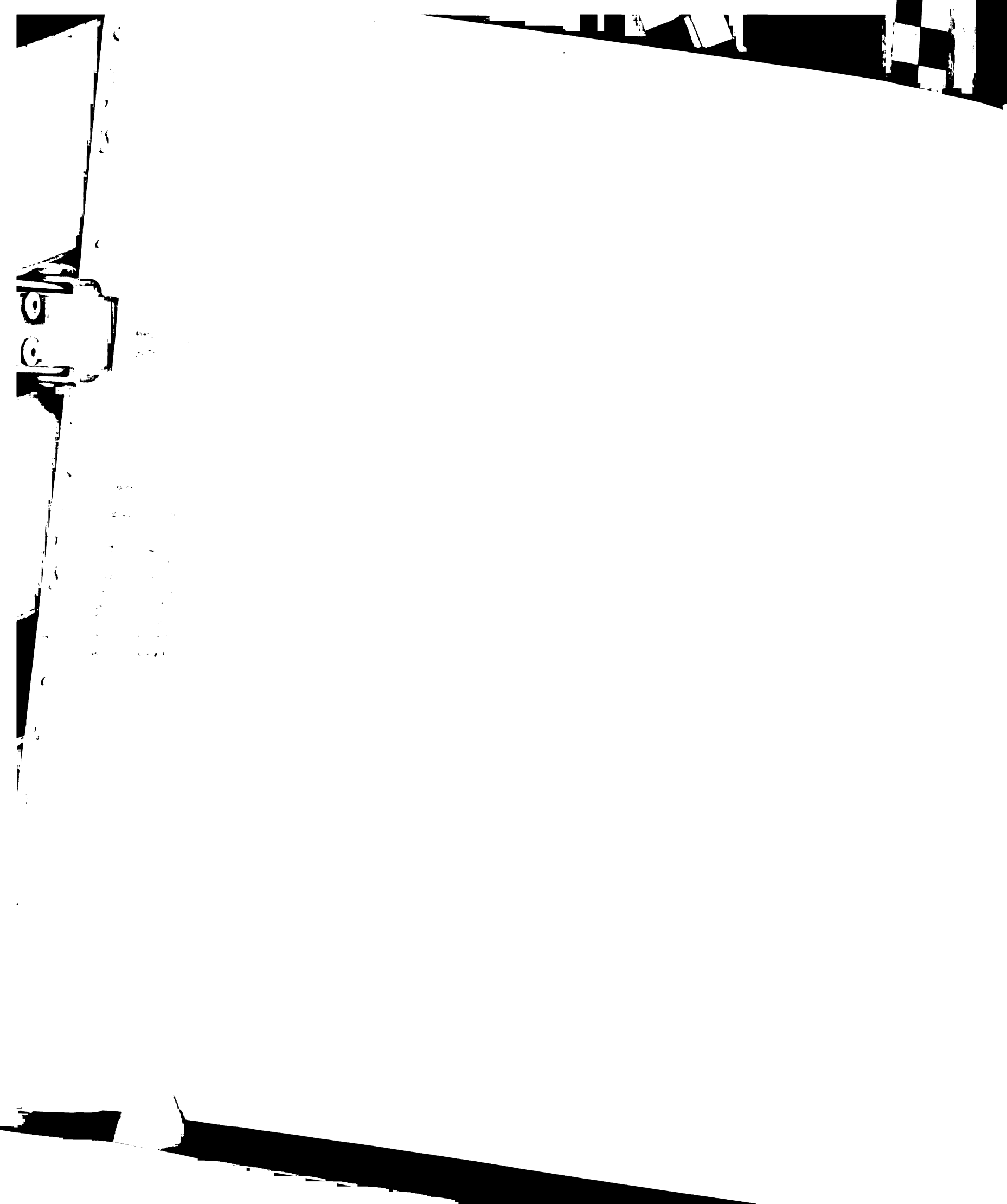


Scheme 4.3. Preparation of the propionic acid side chain analogue of GC-1

4.2.4. TR Binding

The affinities and selectivities of T₃, DIMIT, GC-1, methylene-bridged DIMIT and GC-1 ether for TR α_1 and TR β_1 are summarized in Table 4.1. To ensure a valid comparison of the affinities of different ligands, all the compounds were assayed simultaneously using the same preparation of purified TR. The selectivity was determined by the ratio of K_d hTR α_1 to K_d hTR β_1 and normalized to the ratio of K_d hTR α_1 to K_d hTR β_1 for T₃.

While none of the synthetic thyromimetics, except for GC-1, bind to hTR β_1 as tightly as T₃, the thyromimetics containing the methylene bridge – GC-1, methylene-bridged DIMIT and propionic acid GC-1 – bind with greater affinities than those containing the ether bridge. The ether to methylene substitution thus results in increased affinity for TR with thyromimetics of 3,5-dimethyl-3'-isopropyl substitution pattern as it does with the 3,5,3'-triiodo substitution pattern of T₃. Comparing the affinities and selectivities of



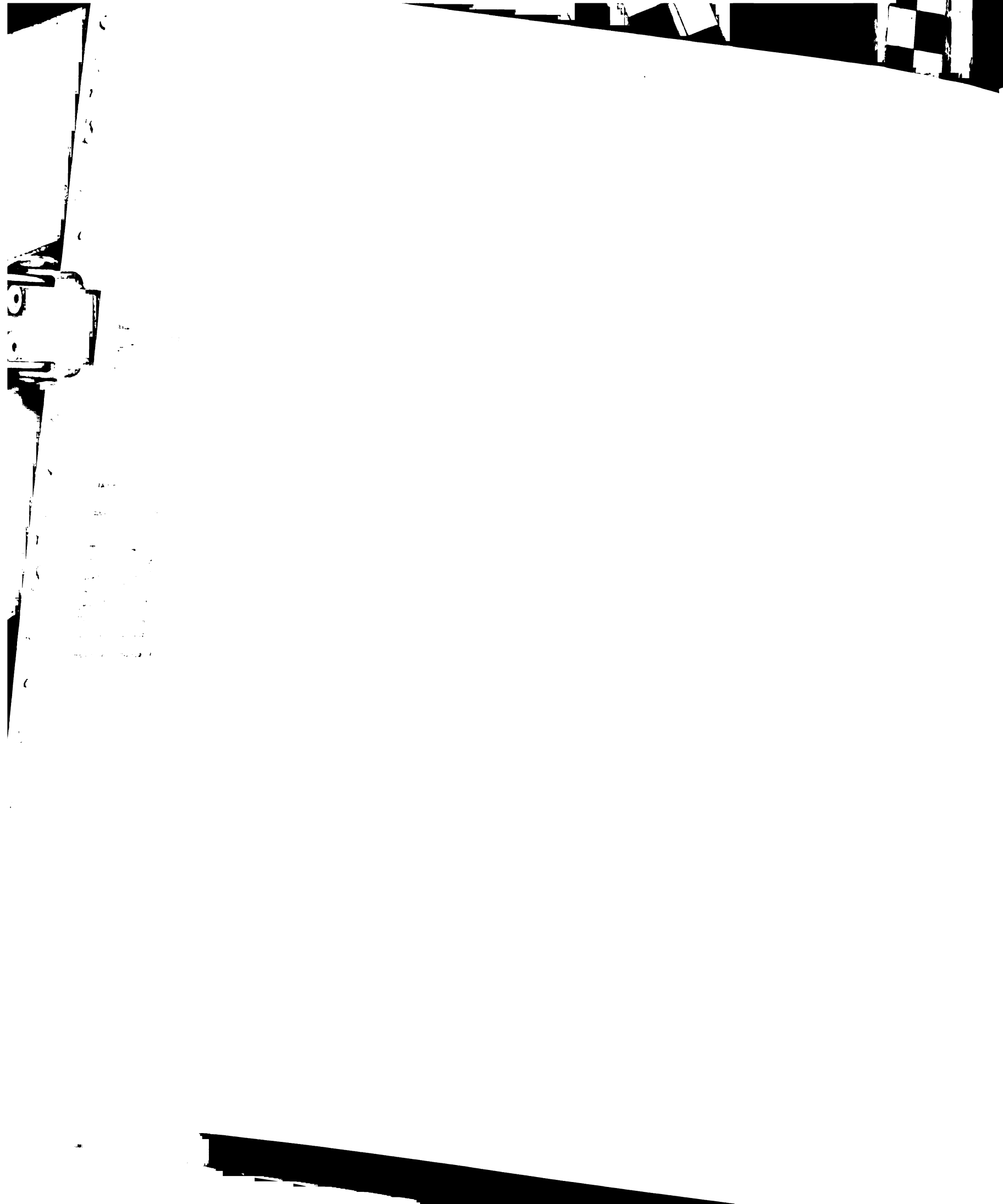
DIMIT and T₃ shows that 3,5-dimethyl-3'-isopropyl substitution results in an approximate loss of affinity of 140-fold for hTR α and 70-fold for hTR β , resulting in a 2-fold gain in TR β selectivity.

Table 4.1. Binding affinities of thyromimetics for TR

Compound	K_d hTR α_1 (nM)	K_d hTR β_1 (nM)	Selectivity
T ₃ (1)	0.060 \pm 0.004	0.087 \pm 0.006	1.0 \pm 0.2
GC-1 (4)	0.66 \pm 0.05	0.10 \pm 0.01	10 \pm 2
Ether-bridged GC-1 (7, HY-6) ^a	2.4 \pm 0.4	0.36 \pm 0.01	10 \pm 2
Propionic acid GC-1 (9, HY-8) ^a	0.69 \pm 0.05	0.22 \pm 0.01	4.5 \pm 0.6
Methylene-bridged DIMIT (8, HY-10) ^a	2.02 \pm 0.09	1.26 \pm 0.03	2.3 \pm 0.3
DIMIT (3)	8.5 \pm 0.8	6.2 \pm 0.2	2.0 \pm 0.3

a. Compound purity >97% by HPLC

To analyse the role of the bridging moiety and polar side chain in influencing TR α /TR β selectivity, pair wise comparisons were made between GC-1, DIMIT, methylene-bridged DIMIT and ether-bridged GC-1. Shown in Figure 4.3, the ether to methylene substitution results in the same change in affinity for TR α and TR β . Methylene-bridged DIMIT shows (4.2 \pm 0.5- and (4.9 \pm 0.2)-fold increases in affinity for TR α and TR β , respectively, compared to DIMIT, while GC-1 correspondingly has (3.6 \pm 0.6)-fold and



(3.8 ± 0.4)-fold greater affinities than ether-bridge GC-1. Thus the ether to methylene substitution has little effect on selectivity.

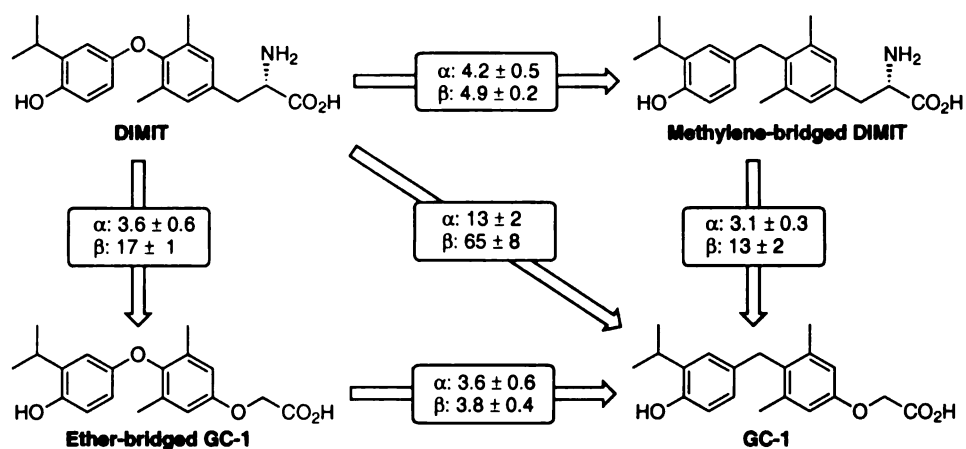
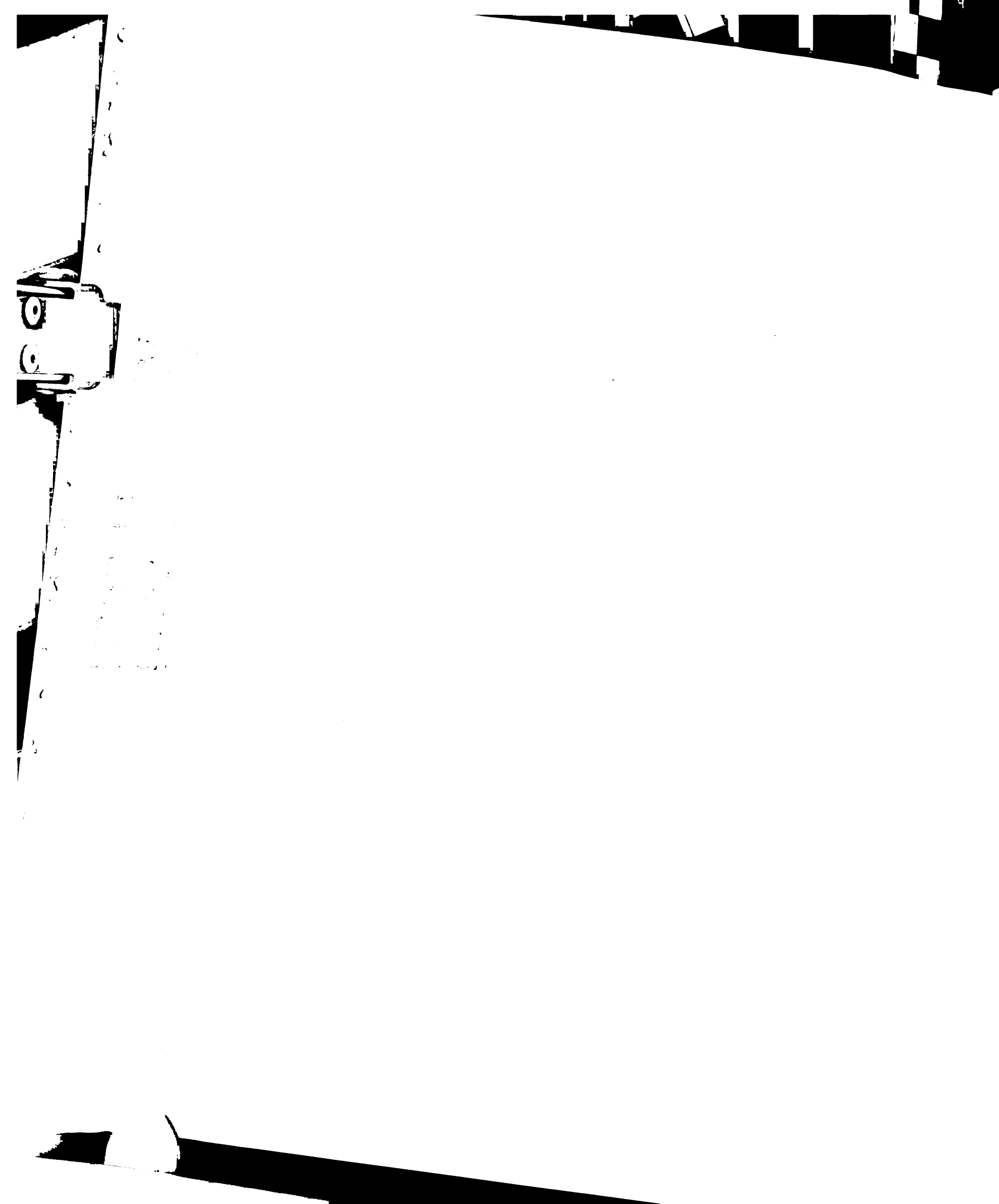


Figure 4.3. The ether oxygen to methylene and alanine to oxyacetic acid side chain substitutions have distinct independent effects on TR affinity and selectivity. Values indicate fold gain in affinity for TR α and TR β .

The gains in affinity for ether-bridged GC-1 compared to DIMIT ((3.6 ± 0.6)-fold for TR α and (17 ± 1)-fold for TR β) and correspondingly of GC-1 compared to methylene-bridged DIMIT ((3.1 ± 0.3)-fold for TR α and (13 ± 2)-fold for TR β) show a strong differential gain in affinity for TR β associated with the alanine to oxyacetic acid polar side chain substitution. In comparison with the results of the ether to methylene substitution, these data clearly demonstrate the key role of the oxyacetic acid side chain in GC-1's preferential binding to TR β .



The change of alanine side chain to oxyacetic acid can be thought of occurring in two steps: first the replacement of the α -amine with hydrogen and then the ether replacing the side chain methylene. To determine the role of these specific structural changes in influencing affinity and selectivity, the preceding analysis was repeated with methylene-bridged DIMIT, GC-1 and propionic acid GC-1. The comparison, shown in Figure 4.4, demonstrates that both changes differentially increase affinity for TR β . The loss of the amino group increases affinity (2.9 ± 0.3)-fold and (5.6 ± 0.4)-fold, respectively, for TR α and TR β , while a corresponding (2.3 ± 0.3)-fold gain in affinity for TR β is observed in the side chain methylene to ether substitution.

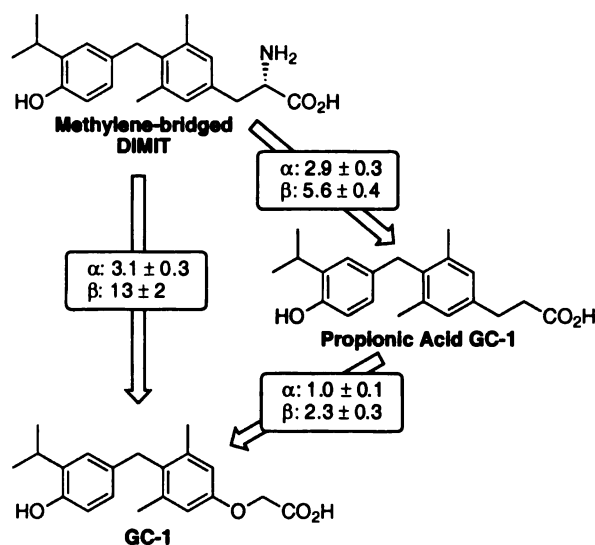


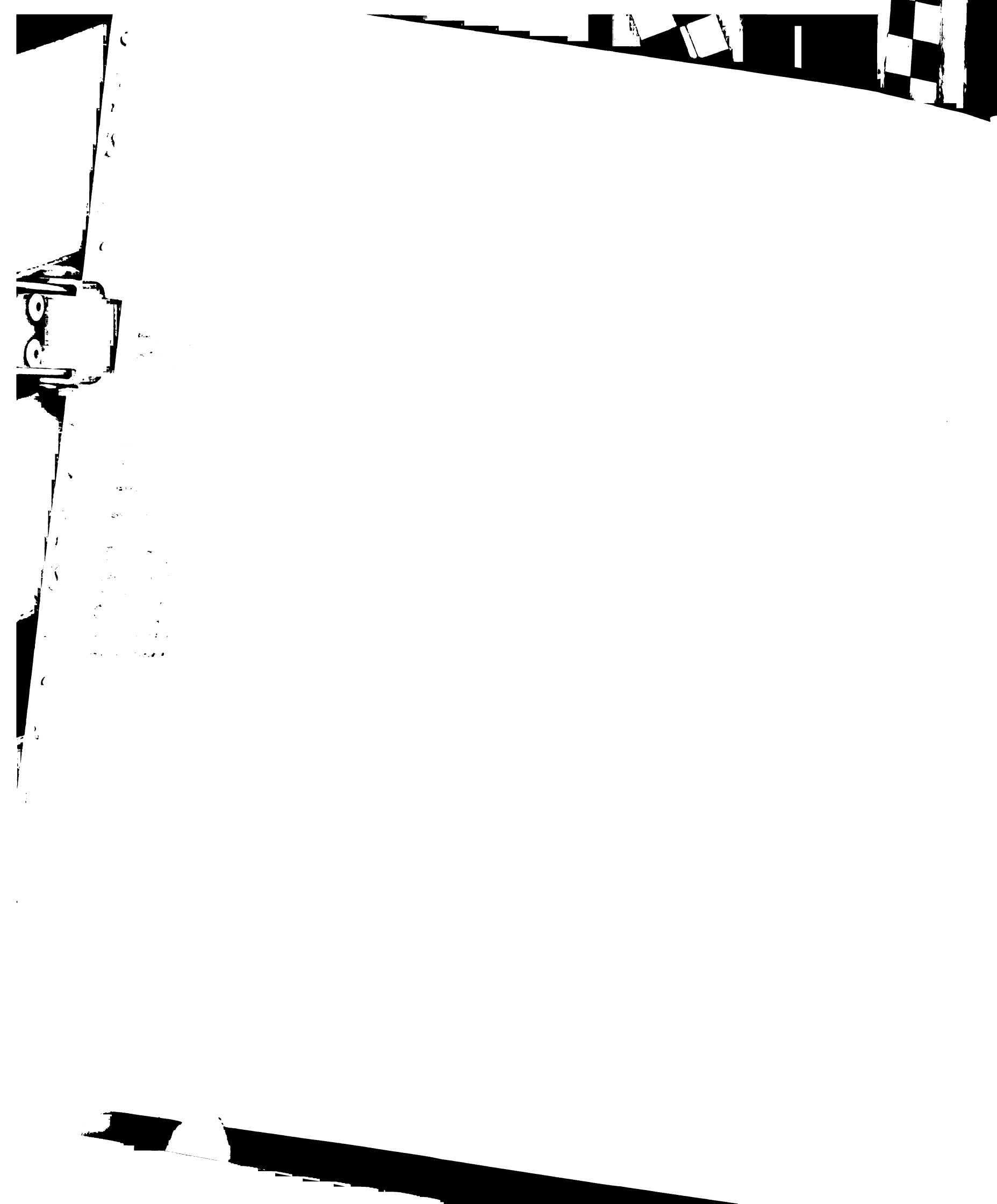
Figure 4.4. The loss of the α -amino group and the side chain ether for methylene substitution both contribute towards TR β -selectivity. Values indicate fold gain in affinity for TR α and TR β .

The free energies of binding associated with the binding affinities of the compounds (calculated with units of moles/liter) are listed in Table 4.2. The changes in selectivity associated with the various structural alterations of the thyromimetics are expressed in Figure 4.5 as the differential gain in free energy of binding, or $\Delta\Delta\Delta G_{\text{bind}}$. Inspection of the ratios of affinities in Figure 4.3 shows the independent effects of the structural changes on affinity. The ether bridge to methylene substitution has practically the same effect on binding affinity regardless of the identity of the polar side chain. Similarly, the side chain substitutions have almost the same effect on affinity and selectivity within the context of either bridging moiety.

Table 4.2. Binding energies of thyromimetics for TR

Compound	$\Delta G_{\text{bind}} \text{ hTR}\alpha_1$ (kcal/mol)	$\Delta G_{\text{bind}} \text{ hTR}\beta_1$ (kcal/mol)
T ₃ (1)	-12.96 ± 0.04	-12.76 ± 0.04
GC-1 (4)	-11.64 ± 0.05	-12.71 ± 0.06
Ether-bridged GC-1 (7, HY-6) ^a	-10.94 ± 0.08	-11.98 ± 0.02
Propionic acid GC-1 (9, HY-8) ^a	-11.61 ± 0.04	-12.24 ± 0.04
Methylene-bridged DIMIT (8, HY-10) ^a	-11.03 ± 0.03	-11.29 ± 0.01
DIMIT (3)	-10.24 ± 0.05	-10.41 ± 0.02

a. Compound purity >97% by HPLC



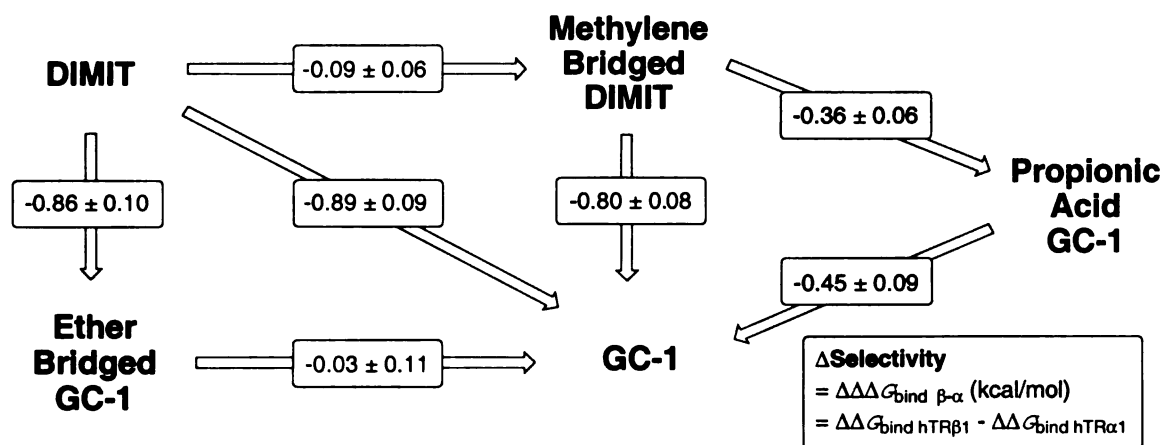


Figure 4.5. The oxyacetic acid polar side chain is the key determinant of TR β -selectivity. Values indicate gain in TR β -selectivity (kcal/mol).

4.2.5. TR Transactivation

The ability of ether-bridged GC-1, methylene-bridged DIMIT and propionic acid GC-1 to activate TR-mediated transcription was also examined using the same assay used in Chapter 3. To ensure the most valid comparison, all the compounds were tested and compared within the same transfection experiment. As shown in Figure 4.6, all the compounds are full agonists, as expected. The greater variability of the transactivation assay does not allow the fine level of detail and analysis possible with the more reproducible binding assay. Even with this level of resolution, a difference between the compounds is apparent. The effects of the bridging moiety are not resolved, however. Instead the thyromimetics cluster into two groups: those with and without the oxyacetic acid side chain. GC-1 and ether-bridged GC-1 behave almost identically with regard to

their preferential activation of TR β , underscoring the importance of the oxyacetic acid side chain in determining TR β -selectivity both in terms of binding and in activation.

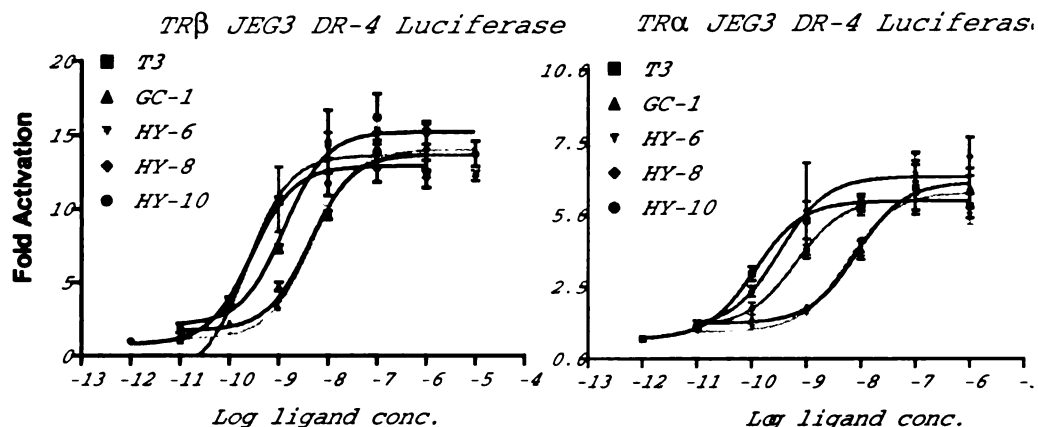


Figure 4.6. GC-1 and ether-bridged GC-1 behave identically in TR transactivation assays. HY-6 is ether-bridged GC-1; HY-8 is propionic acid GC-1; HY-10 is methylene-bridged DIMIT.

4.3. Discussion

The preceding results clearly demonstrate that the TR β -selectivity of GC-1 is determined predominantly by its oxyacetic acid side chain. In comparing the GC-1 analogues with alanine and propionic acid side chains it is also apparent that both the loss of the α -amine and the methylene to ether substitution make significant contributions to differentially increase the affinity for TR β .

That the polar side chain substitution has the same effect on binding and selectivity in the context of either bridging moiety strongly implies that the side side chain and the adjacent aromatic ring (A-ring) interact with the receptors in the same fashion regardless of bridging moiety. Accordingly, the small shift in the relative positions of the A-ring and B-ring caused by the longer carbon-carbon bonds of the methylene bridge (1.54 Å versus 1.39 Å for C-O) would be borne out by the B-ring with the A-ring remaining in the same position relative to the receptor.

Because the improvement in affinity observed with the introduction of the methylene bridge is nearly equal for both receptors in the context of either side chain, it is possible that a factor external to the interaction of ligand with receptor is mostly responsible for the increased affinity. One such factor could be the increased hydrophobicity of the ligands containing the methylene bridge. Increased hydrophobicity of a ligand increases the free energy in the unbound state by increasing the energetic cost of solvation and results in a greater free energy of binding and higher affinity. This effect may not be functioning in this case as diphenylmethane has a reported logP value of 4.14 while the corresponding value for diphenylether is 4.21 [30], suggesting that a significant increase in hydrophobicity does not occur with the methylene for oxygen substitution. Alternatively, the methylene bridge may cause the B-ring to interact with the receptor in a more energetically favorable fashion to cause the observed 3-5 fold increase in affinity. Interestingly, the B-ring of GC-1 shows a slightly shifted position, while the B-rings of triac, DIMIT and T₃ all closely overlap in structural alignments of the crystal structures of liganded TR-LBDs [27; 28; 31].

While the effects of these substitutions are independent of each other for TR α , they do appear to affect each other slightly for TR β . As shown in Figure 4.3, there are small but significant differences in the values of changes in affinity for TR β for the bridge substitutions depending on the side chain present. Thus for TR β , the ether to methylene bridge substitution results in a 20% higher gain in affinity in the presence of the alanine side chain and the gain in affinity of the alanine to oxycetic acid substitution is correspondingly 20% greater with the ether bridge. While this effect is small, it does represent a slight deviation from the model where the substitutions of the bridge and of the side chain have completely independent effects.

While we have shown the importance of the character of the polar side chain in determining selectivity toward binding TR β , we do know that other features of the ligand can influence selectivity. Our laboratory has prepared over 20 analogues of GC-1 in studies of TR antagonism [32-34]. Their structures are summarized in Figure 4.6. Most of these analogues bear substituted phenyl or phenylethynyl substituents at the 5'-position (24-38), while a racemic series with alkyl, allyl and aryl substituents at the bridging carbon (39-42) has also been prepared. All show reduced affinity for TR on the order of 200- to 7000-fold lower than GC-1. TR β selectivity is observed with most of these GC-1 analogues; however, the degree of TR β selectivity varies considerably between 0.33- and 20- fold, in a manner that is not easily explained by the character of the extra substituent. The analogues with 5' substituents all bind better to TR β than TR α ,

though the degree of selectivity varies between 0.33- and 20-fold [33; 34]. Analogues with hydroxyalkyl, aryl and alkylamide substituents at the bridging carbon (**40–42**) show 3.6- to 1.5-fold TR α selectivity, while the allyl substituted analogue (**39**) is 7-fold TR β selective [32]. Substitution at the bridging carbon can, but does not necessarily, confer slight TR α selectivity. The binding characteristics of these analogues indicate that their perturbations of the ligand binding cavity are not equally tolerated by TR α and TR β , presumably from structural differences in the ligand binding domains.

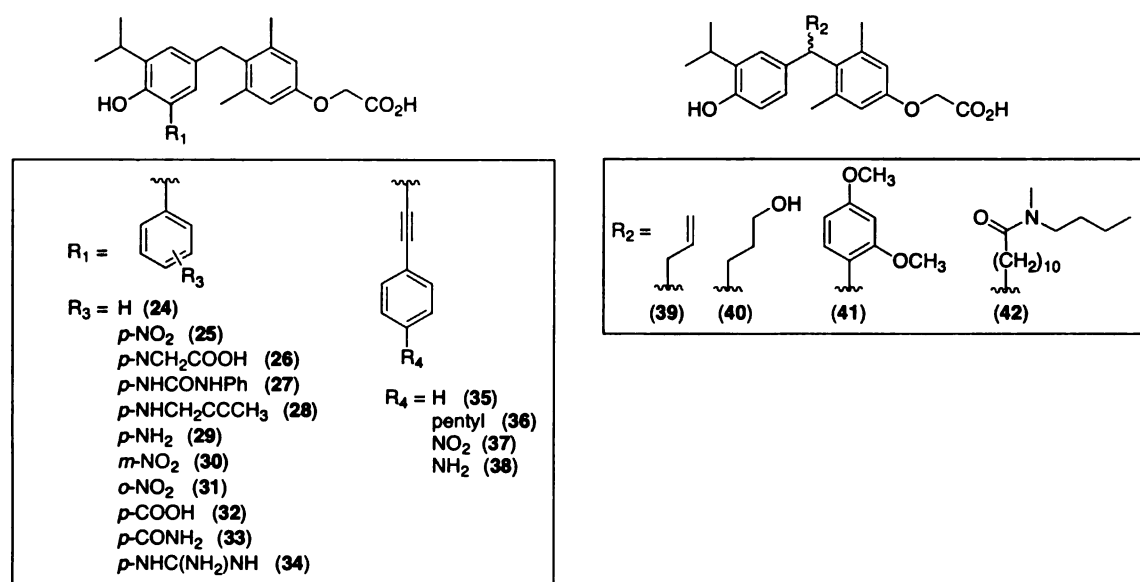


Figure 4.7. Structures of previously reported GC-1 analogues with substituents at the 5'-position and at the bridging carbon.

This study demonstrates that subtle changes to the structures of the polar side chains of high-affinity thyromimetics can have significant effects on selectivity. Our understanding of selectivity from these results, along with the earlier structural and

mutagenesis studies [28], emphasizes the importance of polar interactions between ligand and receptor in the vicinity of the one varying amino acid residue in the ligand binding cavity. While the precise ligand-receptor interactions that govern selectivity remain elusive, structural features of both the receptor and ligand that influence selectivity have been identified.

4.4. Experimental

4.4.1. Thyroid hormone receptor binding assays

hTR α_1 and hTR β_1 were expressed in *Escherichia coli* and purified as described previously [35]. Competition ligand binding affinities were determined using 0.1 nM [¹²⁵I]-T₃ in gel filtration binding assays performed in duplicate as described [35]. The K_d and standard error (SE) values were calculated by fitting the competition data using the GraphPad Prism computer program (GraphPad Software, Inc.)

4.4.2. General Methods

Unless otherwise indicated, solvents and reagents were purchased from the Aldrich Chemical Company and used without further purification. Tetrahydrofuran was distilled from sodium benzophenone ketyl prior to use. Other anhydrous solvents were from Aldrich SureSeal bottles. Water-sensitive reactions were performed using oven- or flame-dried glassware. Unless indicated, reactions were performed under argon inert

atmosphere. NMR spectra were obtained using a Varian Inova 400 MHz spectrometer. Target compounds **7**, **8** and **9** were purified by reverse-phase preparative HPLC.

4-Benzyloxy-2,6-dimethylphenol (**13**):

To a stirred suspension of 2,6-dimethylhydroquinone (Rütgers Organics) (3.00 g, 21.7 mmol) and potassium carbonate (6.30 g, 45.6 mmol) in DMF (anhydrous, 10 mL) was added benzyl bromide (2.6 mL, 22 mmol). The reaction was cooled in a cold water bath and was stirred overnight at rt. After 21 h, the reaction was quenched by the cautious addition of 1 M HCl (50 mL), followed by extraction with ethyl acetate (4 x 50 mL). The combined organic fractions were washed with sat. aq. NH₄Cl (2 x 20 mL) and brine (2 x 20 mL), then dried (MgSO₄), filtered through a Celite pad and concentrated under reduced pressure. The residue was purified by flash chromatography (silica, 5 → 10% Ethyl acetate in hexanes) to give product (440 mg, 9% yield) as a white solid. ¹H NMR (400 MHz, CDCl₃) δ 7.30–7.43 (m, 5 H), 6.63 (s, 2 H), 4.97 (s, 2 H), 4.25 (s, 1 H), 2.21 (s, 6 H); ¹³C NMR (100 MHz, CDCl₃) δ 152.23, 146.32, 137.48, 128.49, 127.77, 127.43, 124.09, 114.90, 70.56, 16.24. HRMS exact mass calcd for C₁₂H₁₆O₂: 228.1150, found: 228.1148

3-Isopropyl-4-methoxymethoxyphenylboronic acid (**11**):

A stirred solution of 3-isopropyl-4-methoxymethoxy-bromobenzene (2.5 g, 9.6 mmol) in THF (25 mL) was chilled to $-78\text{ }^{\circ}\text{C}$ and *n*-butyllithium (2.5 M in hexanes, 4.0 mL, 10 mmol) was added via syringe over several minutes. After 15 min stirring, trimethyl borate (1.2 mL, 11 mmol) was added via syringe. The mixture was stirred overnight, slowly warming to rt, then 1 M HCl (25 mL) was added and stirring was continued for another hour. The aqueous and organic layers were separated and the aqueous layer extracted with methylene chloride (2 x 40 mL). Combined organic fractions were dried (MgSO_4), filtered through a Celite pad and concentrated under reduced pressure to yield product (2.0 g) as a thick clear syrup that solidified over a few days. Product was used directly in the next reaction without further purification.

α -[4-(3-Isopropyl-4-methoxymethoxyphenoxy)-3,5-dimethylphenoxy]-toluene (**14**):

To a stirred solution of 3-Isopropyl-4-methoxymethoxyphenylboronic acid (**11**) (approx. 290 mg, 1.3 mmol) and 4-Benzyloxy-2,6-dimethylphenol (**13**) in methylene chloride (anhydrous, 10 mL) was added copper(II) acetate (80 mg, 0.44 mmol), triethylamine (305 μL , 2.19 mmol) and powdered 4 Å molecular sieves (spatula tip). A drying tube was attached and the mixture was stirred under ambient atmosphere. After 25 h, the mixture was filtered through a pad of Celite, which was rinsed with ethyl acetate. Rotary evaporation yielded a brown/green semi-solid which was purified by flash chromatography to yield enriched product (149 mg) which was used directly in the next reaction.

4-(3-Isopropyl-4-methoxymethoxyphenoxy)-3,5-dimethylphenol (14a):

A solution of α -[4-(3-isopropyl-4-methoxymethoxyphenoxy)-3,5-dimethylphenoxy]-toluene (**14**) (approx. 0.25 mmol), in ethyl acetate was sparged with Ar and a spatula tip of palladium on carbon (10%) was added. The flask was purged with H₂ and the mixture was stirred overnight under H₂ atmosphere maintained with balloon pressure, then filtered through a Celite pad which was rinsed with ethyl acetate. After rotary evaporation, the crude product was purified by flash chromatography (silica, 5 \rightarrow 20% ethyl acetate in hexanes) to yield product (36 mg, 27% yield from **13**). ¹H NMR (400 MHz, CDCl₃) δ 6.89 (d, *J*=9.3 Hz, 1 H), 6.74 (d, *J*=2.9 Hz, 1 H), 6.54 (s, 2 H), 6.36 (dd, *J*=8.8, 2.9 Hz, 1 H), 5.12 (s, 2 H), 4.93 (s, 1 H), 3.49 (s, 3 H), 3.29 (heptet, *J*=6.8, Hz, 1 H), 2.06 (s, 6 H), 1.18 (d, *J*=6.8 Hz, 6 H); ¹³C NMR (100 MHz, CDCl₃) δ 153.19, 152.06, 148.81, 145.10, 139.47, 132.70, 115.41, 115.17, 112.91, 111.14, 95.38, 55.97, 27.05, 22.76, 22.63, 16.47. HRMS exact mass calcd for C₁₉H₂₄O₃: 316.1675, found: 316.1665.

[4-(3-Isopropyl-4-methoxymethoxyphenoxy)-3,5-dimethylphenoxy]acetic acid methyl ester (14b):

To a stirred suspension of **14a** (30 mg, 0.095 mmol) and cesium carbonate (46 mg, 0.14 mmol) in DMF (anhydrous, 200 μ L) was added methyl bromoacetate (13 μ L, 0.14 mmol) via syringe. The mixture was stirred overnight at rt, then quenched with half-sat. NH₄Cl (8 mL) and extracted with diethyl ether (2 x 10 mL). The combined organic fractions were washed with brine (2 x 2 mL) and dried (MgSO₄), filtered through a Celite pad and concentrated under reduced pressure to yield product (30 mg, 81% yield). ¹H NMR (400

MHz, CDCl₃) δ) 6.88 (d, *J*=9.3 Hz, 1 H), 6.73 (d, *J*=2.9 Hz, 1 H), 6.63 (s, 2 H), 6.34 (dd, *J*=9.0, 3.2 Hz, 1 H), 5.11 (s, 2 H), 4.62 (s, 2 H), 3.82 (s, 3 H), 3.48 (s, 3 H), 3.29 (heptet, *J*=6.8, Hz, 1 H), 2.09 (s, 6 H), 1.18 (d, *J*=7.3 Hz, 6 H) ; ¹³C NMR (100 MHz, CDCl₃) δ 169.55, 154.30, 153.02, 148.90, 146.00, 139.44, 132.68, 115.34, 114.63, 112.94, 111.12, 95.35, 65.64, 55.94, 52.21, 27.05, 22.73, 16.66. HRMS exact mass calcd for C₂₂H₂₈O₆: 388.1886, found: 388.1895.

[4-(4-Hydroxy-3-isopropylphenoxy)-3,5-dimethylphenoxy]acetic acid (7):

To a stirred suspension of methyl ester **14b** (30 mg, 0.077 mmol) and lithium hydroxide monohydrate (7.0 mg, 0.17 mmol) in methanol (2 mL) was added water (7.6 μL, 0.42 mmol). The mixture was stirred at rt for 4 h, then solvent was removed under reduced pressure. The residue was resuspended in a 1:1 mixture of sat. NH₄Cl:1 M HCl (6 mL) and extracted with ethyl acetate (3 x 6 mL). The combined organic fractions were dried (MgSO₄), filtered through a Celite pad and concentrated under reduced pressure. The crude product was purified by flash chromatography (silica, 7.5% ethyl acetate, 3% acetic acid in chloroform) and prep. TLC (silica, 20 cm x 20 cm, 15% ethyl acetate, 3% acetic acid in chloroform, eluted with 10% methanol in chloroform) to give a white solid (7 mg, 30% yield). ¹H NMR (400 MHz, CD₃OD) δ 6.70-6.65 (m, 2 H), 6.67 (s, 2 H), 6.25 (dd, *J*=8.8, 2.9 Hz, 1 H), 4.61 (s, 2 H), 3.21 (heptet, *J*=6.8 Hz, 1 H), 2.05 (s, 6 H), 1.13 (d, *J*=7.3 Hz, 6 H); ¹³C NMR (100 MHz, CDCl₃) δ 172.94, 155.94, 152.78, 149.66, 147.25, 137.52, 133.64, 116.52, 115.65, 113.28, 112.33, 66.22, 28.11, 22.95, 16.75. HRMS exact mass calcd for C₁₉H₂₂O₅: 330.1467, found: 330.1471.

4-Benzyloxy-2,6-dimethylbromobenzene (**15a**):

A suspension 4-bromo-3,5-dimethylphenol (20.0 g, 99.5 mmol), benzyl bromide (17 g, 99 mmol) and potassium carbonate (20.6 g, 149 mmol) in DMF (anhydrous, 20 mL) was stirred overnight at rt. The reaction was diluted with diethyl ether (150 mL) and quenched with the cautious addition of 1 M HCl (250 mL). The aqueous and organic phases were separated and the aqueous phase was extracted with diethyl ether (2 x 180 mL). The combined organic phases were washed with sat. NH_4Cl (2 x 50 mL) and brine (2 x 50 mL), then dried (MgSO_4), filtered through a Celite pad and concentrated under reduced pressure. The crude product was purified with two rounds of KugelRohr distillation, giving an off-white solid (22.3 g, 78% yield). ^1H NMR (400 MHz, CDCl_3) δ 7.43-7.32 (m, 5 H), 6.73 (s, 2 H), 5.01 (s, 2 H), d ppm 2.38 (s, 6 H); ^{13}C NMR (100 MHz, CDCl_3) δ 157.25, 139.12, 136.84, 128.57, 127.97, 127.40, 118.49, 114.72, 70.04, 24.06. HRMS exact mass calcd for $\text{C}_{15}\text{H}_{15}\text{BrO}$: 290.0306, found: 290.0320.

4-Benzyloxy-2,6-dimethylbenzaldehyde (**16**):

A stirred solution of bromobenzene **15a** (21.0 g, 72.1 mmol) in THF (200 mL) was cooled to $-78\text{ }^\circ\text{C}$; then *n*-butyllithium (2.5 M in hexanes, 32 mL, 79 mmol) was added via syringe over several minutes. A thick precipitate formed and stirring was maintained manually. After 10 min, DMF (anhydrous, 8.4 mL, 110 mmol) was added via syringe over a period of 10 min with frequent shaking of the flask as the precipitate dissolved. Stirring at $-78\text{ }^\circ\text{C}$ was maintained for 20 min, then the reaction was quenched by the

addition of 1 M HCl (150 mL). The aqueous and organic layers were separated and the aqueous phase was extracted with diethyl ether (3 x 100 mL). The combined organic fractions were washed with sat. NaHCO₃ (100 mL), brine (100 mL) and then dried (MgSO₄), filtered through a Celite pad and concentrated under reduced pressure. Purification by short-path vacuum distillation, followed by Kugelrohr distillation (c. 1 torr, 160 °C) gave product (14.0 g, 80% yield) as an off-white solid. ¹H NMR (400 MHz, CDCl₃) δ 10.47 (s, 1 H), 7.42-7.32 (m, 5 H), 6.67 (s, 2 H), 5.09 (s, 2 H), 2.60 (s, 6 H); ¹³C NMR (100 MHz, CDCl₃) δ 191.56, 161.85, 144.44, 136.17, 128.64, 128.18, 127.42, 126.13, 115.61, 69.84, 21.06. HRMS exact mass calcd for C₁₆H₁₆O₂: 240.1150, found: 240.1151

3-isopropyl-4-triisopropylsilyloxybromobenzene (**17**):

To a stirred solution of triisopropylsilyl chloride (12 mL, 56 mmol) in anhydrous 1,2-dichloroethane (70 mL) was added 4-bromo-2-isopropylphenol (9.6 g, 46 mmol) and imidazole (7.8 g, 114 mmol). Reaction was refluxed for 30 min, then allowed to stir overnight at room temperature. Reaction was refluxed 1 hour further, then 150 mL of 0.6 M HCl was added, layers separated and the aqueous phase extracted with diethyl ether. Combined organic fractions were washed with saturated NaHCO₃, dried (MgSO₄), filtered through a Celite plug and solvent was removed by rotary evaporation to yield an oil (18.3 g). Purification by fractional distillation (bp 137 °C, 0.3 mm) yielded bromobenzene **17** as a white solid (12.3 g, 72%). ¹H NMR (600 MHz, CDCl₃) δ 7.27 (d, *J* = 2.6 Hz, 1 H), 7.11 (dd, *J* = 8.4, 2.6 Hz, 1 H), 6.64 (d, *J* = 8.8 Hz, 1 H), 3.33 (heptet, *J*

= 6.8 Hz, 1 H), 1.30 (heptet, $J = 7.5$ Hz, 3 H), 1.19 (d, $J = 6.6$ Hz, 6 H), 1.10 (d, $J = 7.7$ Hz, 18 H); ^{13}C NMR (100 MHz, CDCl_3) δ 152.29, 140.98, 129.27, 128.93, 119.36, 113.14, 26.85, 22.61, 18.04, 13.05. HRMS exact mass calcd for $\text{C}_{18}\text{H}_{31}\text{BrOSi}$: 370.1328, found: 370.1336.

4-Benzyloxy-2,6-dimethylphenyl-[3-isopropyl-4-(triisopropylsilyloxy)-phenyl]-methanol (18):

A stirred solution of **17** (13.9 g, 37.5 mmol) in THF (250 mL) was cooled to -78 °C and *n*-butyllithium (2.5 M in hexanes, 16 mL, 40 mmol) was added via syringe over 10 min. After 10 min stirring at -78 °C, **16** (9.00 g, 37.5 mmol), dissolved in THF (10 mL), was added dropwise via cannula over 20 min, followed by rinses with THF (2 x 5 mL). After stirring 30 min at -78 °C, the reaction was quenched with 1 M HCl (45 mL). The aqueous and organic layers were separated and the aqueous phase as extracted with diethyl ether (4 x 40 mL). The combined organic fractions were washed with sat. NaHCO_3 (30 mL) and brine (30 mL) then dried (MgSO_4), filtered through a Celite pad and concentrated under reduced pressure. Flash chromatography of the residue (2 \rightarrow 7% ethyl acetate in hexanes) gave purified product (15.5 g, 77% yield). ^1H NMR (400 MHz, CDCl_3) δ 7.45-7.32 (m, 4 H), 7.23 (d, $J=1.5$ Hz, 1 H), 6.75 (dd, $J=8.2, 1.5$ Hz, 1 H), 6.67-6.65 (m, 3 H), 6.24 (d, $J=4.3$ Hz, 1 H), 5.04 (s, 2 H), 3.36 (heptet, $J=7.0$, Hz, 1 H), 2.24 (s, 6 H), 1.29 (heptet, $J=7.6$ Hz, 3 H), 1.17 (dd, $J=8.2, 7.0$ Hz, 6 H), 1.10 (d, $J=7.3$ Hz, 18 H); ^{13}C NMR (100 MHz, CDCl_3) δ 157.62, 151.72, 138.72, 138.13, 137.16, 135.07, 132.49, 128.53, 127.87, 127.48, 123.50, 123.39, 117.46, 115.20, 70.95, 69.74, 26.74,

22.83, 20.99, 18.09, 13.07. HRMS exact mass calcd for C₃₄H₄₈O₃Si: 532.3373, found: 532.3379.

4-[3-Isopropyl-4-(triisopropylsilyloxy)-benzyl]-3,5-dimethylphenol (**18a**):

A solution of **18** (9.35 g, 17.8 mmol) in 1:1 ethyl acetate:ethanol (30 mL) in a glass Parr hydrogenator flask was sparged with Ar. Palladium on carbon (10%, 1.3 g) was added and the flask was attached to a Parr hydrogenator and shaken for 24 h under H₂ at 35 psi. The mixture was then filtered through a pad of Celite, which was then rinsed with ethyl acetate and the filtrate was concentrated to yield product (7.77 g, 100% yield) as a white solid. ¹H NMR (400 MHz, CDCl₃) δ 6.92 (s, 1 H), 6.61 (d, *J*=8.3 Hz, 1 H), 6.54-6.51 (m, 3 H), 4.96 (s, 1 H), 3.87 (s, 2 H), 3.33 (heptet, *J*=6.9 Hz, 1 H), 2.18 (s, 6 H), 1.27 (heptet, *J*=7.3 Hz, 3 H), 1.16 (d, *J*=6.9 Hz, 6 H), 1.09 (d, *J*=7.6 Hz, 18 H); ¹³C NMR (100 MHz, CDCl₃) δ 153.20, 150.96, 138.65, 138.10, 131.96, 130.02, 125.82, 124.83, 117.60, 114.72, 33.74, 26.62, 22.83, 20.32, 18.09, 13.05. HRMS exact mass calcd for C₂₇H₄₂O₂Si: 426.2954, found: 426.2950.

4-[3-isopropyl-4-(triisopropylsilyloxy)-benzyl]-3,5-dimethylphenyltrifluoromethanesulfonate (**19**):

A stirred solution of **18a** (10.0 g, 23.4 mmol) and pyridine (anhydrous, 20 mL, 250 mmol) in methylene chloride (anhydrous, 150 mL) was cooled in an ice bath. Triflic anhydride (4.3 mL, 26 mmol) was added via syringe over 5 min, with vigorous stirring

1

2
3
4
5
6
7
8
9
10
11
12
13
14
15
16
17
18
19
20
21
22
23
24
25
26
27
28
29
30
31
32
33
34
35
36
37
38
39
40
41
42
43
44
45
46
47
48
49
50
51
52
53
54
55
56
57
58
59
60
61
62
63
64
65
66
67
68
69
70
71
72
73
74
75
76
77
78
79
80
81
82
83
84
85
86
87
88
89
90
91
92
93
94
95
96
97
98
99
100

maintained. The mixture was stirred 4 h, slowly warming to room temperature, then a 1:1 mixture of sat. NH_4Cl and 1 M HCl (100 mL) was added. The aqueous and organic layers were separated and the aqueous phase was extracted with diethyl ether (3 x 100 mL). The combined organic fractions were dried (MgSO_4), filtered through a Celite pad and concentrated under reduced pressure. Flash chromatography (silica, 9% diethyl ether in hexanes) gave product (9.2 g, 99% yield with recovered starting material) and unreacted phenol (2.9 g). ^1H NMR (400 MHz, CDCl_3) δ 6.96 (s, 2 H), 6.88 (d, $J=2.0$ Hz, 1 H), 6.62 (d, $J=8.3$ Hz, 1 H), 6.46 (dd, $J=8.3, 2.4$ Hz, 1 H), 3.94 (s, 2 H), 3.32 (heptet, $J=6.8$ Hz, 1 H), 2.27 (s, 6 H), 1.27 (heptet, $J=7.8$ Hz, 3 H), 1.15 (d, $J=6.8$ Hz, 6 H), 1.09 (d, $J=7.3$ Hz, 18 H); ^{13}C NMR (100 MHz, CDCl_3) δ 151.37, 147.41, 139.74, 138.50, 138.25, 130.23, 125.82, 124.76, 120.20, 118.77 (qt, $J=320.7$ Hz), 117.78, 34.10, 26.64, 22.78, 20.42, 18.09, 13.07. HRMS exact mass calcd for $\text{C}_{28}\text{H}_{41}\text{F}_3\text{O}_4\text{SSi}$: 558.2457, found: 558.2447.

[4-(2,6-Dimethyl-4-vinylbenzyl)-2-isopropylphenoxy]-triisopropylsilane (19a):

To a stirred suspension of triflate **19** (5.00 g, 8.95 mmol), lithium chloride (1.14 g, 26.8 mmol) and dichlorobis(triphenylphosphine)palladium(II) (314 mg, 0.447 mmol) in DMF (anhydrous, degassed, 25 mL) was added vinyltributyltin (2.8 mL, 9.8 mmol). The reaction flask was fitted with a heating mantle and thermocouple needle attached to a temperature controller. The reaction was stirred for 2 h at 60 °C, then most of the solvent was removed under reduced pressure. The residue was resuspended in 1:1 diethyl ether:hexanes (50 mL) and aqueous saturated potassium fluoride (10 mL), stirred 2 h,

1

2

then filtered through a pad of Celite, which was rinsed with diethyl ether (200 mL). Hexanes (200 mL) were added to the filtrate and the aqueous and organic phases were separated. The organic layer was washed with sat. NaHCO₃ (25 mL) and half-sat. brine (4 x 25 mL), then dried (MgSO₄), filtered through a Celite pad and concentrated under reduced pressure. Flash chromatography (silica, hexanes), followed by Kugelrohr vacuum distillation to remove the organotin residue, gave a cloudy syrup that contained ~13 mole percent organotin residue (¹H NMR) (3.80 g, 85% yield). A small sample was re-purified for characterization. ¹H NMR (400 MHz, CDCl₃) δ 7.10 (s, 2 H), 6.94 (d, *J*=2.0 Hz, 1 H), 6.66 (dd, *J*=17.6, 10.7 Hz, 1 H), 6.59 (d, *J*=8.3 Hz, 1 H), 6.50 (dd, *J*=8.3, 2.0 Hz, 1 H), 5.71 (d, *J*=17.6 Hz, 1 H), 5.18 (d, *J*=11.7 Hz, 1 H), 3.94 (s, 2 H), 3.32 (heptet, *J*=6.8 Hz, 1 H), 2.24 (s, 6 H), 1.27 (heptet, *J*=7.3 Hz, 3 H), 1.16 (d, *J*=6.8 Hz, 6 H), 1.08 (d, *J*=7.3 Hz, 18 H); ¹³C NMR (100 MHz, CDCl₃) δ 151.06, 138.17, 137.54, 137.24, 136.88, 135.20, 131.44, 125.99, 125.94, 124.90, 117.65, 112.65, 34.43, 26.66, 22.84, 20.29, 18.11, 13.07. HRMS exact mass calcd for C₂₉H₄₄OSi: 436.3161, found: 436.3163.

4-[3-Isopropyl-4-(triisopropylsilyloxy)-benzyl]-3,5-dimethylbenzaldehyde (**20**):

A stirred solution of styrene **19a** (2.15 g, 4.9 mmol) in methylene chloride (anhydrous, 200 mL) was cooled to -78 °C and sparged with an oxygen-ozone mixture until the solution took on a light violet colour. The solution was then sparged with Ar for 15 min and then triphenylphosphine (7.5 g, 29 mmol) dissolved in methylene chloride was added via cannula. After stirring 50 min, the solvent was removed under reduced

1
2
3
4
5
6
7
8
9
10
11
12
13
14
15
16
17
18
19
20
21
22
23
24
25
26
27
28
29
30
31
32
33
34
35
36
37
38
39
40
41
42
43
44
45
46
47
48
49
50
51
52
53
54
55
56
57
58
59
60
61
62
63
64
65
66
67
68
69
70
71
72
73
74
75
76
77
78
79
80
81
82
83
84
85
86
87
88
89
90
91
92
93
94
95
96
97
98
99
100

pressure. The residue was purified by flash chromatography (silica, 0.5 → 1% diethyl ether in hexanes) to give **20** (1.79 g, 86% yield) as a white solid. ¹H NMR (400 MHz, CDCl₃) δ 9.94 (s, 1 H), 7.56 (s, 2 H), 6.90 (d, *J*=2.0 Hz, 1 H), 6.61 (d, *J*=8.3 Hz, 1 H), 6.48 (dd, *J*=8.3, 2.44 Hz, 1 H), 4.02 (s, 2 H), 3.32 (heptet, *J*=6.8, Hz, 1 H), 2.33 (s, 6 H), 1.26 (heptet, *J*=7.3, Hz, 3 H), 1.15 (d, *J*=7.3 Hz, 6 H), 1.09 (d, *J*=7.3 Hz, 18 H); ¹³C NMR (100 MHz, CDCl₃) δ 192.51, 151.35, 145.30, 138.50, 138.18, 134.44, 130.07, 129.38, 125.93, 124.84, 117.78, 34.92, 26.63, 22.79, 20.23, 18.08, 13.05. HRMS exact mass calcd for C₂₈H₄₂O₂Si: 438.2954, found: 438.2959.

(E)-3-{4-[3-Isopropyl-4-(triisopropylsilyloxy)-benzyl]-3,5-dimethylphenyl}-acrylic acid benzyl ester (**20a**):

A solution of benzaldehyde **20** (500 mg, 1.13 mmol) and benzyl (triphenylphosphoranylidene)acetate (834 mg, 2.03 mmol) in THF (25 mL) was stirred at reflux overnight. Solvent was removed under reduced pressure and the residue was purified by flash chromatography (silica, 2 → 4% ethyl acetate in hexanes) to give **20a** (646 mg, 100% yield) as a syrup. ¹H NMR (400 MHz, CDCl₃) δ 7.68 (d, *J*=16.1 Hz, 1 H), 7.42-7.31 (m, 5 H), 7.21 (s, 2 H), 6.92 (d, *J*=1.5 Hz, 1 H), 6.60 (d, *J*=8.3 Hz, 1 H), 6.50-6.44 (m, 2 H), 5.25 (s, 2 H), 3.96 (s, 2 H), 3.32 (heptet, *J*=6.8 Hz, 1 H), 2.25 (s, 6 H), 1.27 (heptet, *J*=7.3 Hz, 3 H), 1.15 (d, *J*=6.8 Hz, 6 H), 1.08 (d, *J*=7.3 Hz, 18 H); ¹³C NMR (100 MHz, CDCl₃) δ 167.03, 151.18, 145.46, 140.71, 138.32, 137.76, 136.19, 132.01, 130.76, 128.53, 128.17, 128.13, 127.86, 125.94, 124.82, 117.69, 116.63, 66.17,

34.59, 26.63, 22.80, 20.25, 18.08, 13.03. HRMS exact mass calcd for $C_{37}H_{50}O_3Si$: 570.3529, found: 570.3524.

3-[4-(4-Hydroxy-3-isopropylbenzyl)-3,5-dimethylphenyl]-acrylic acid benzyl ester (**20b**):

A solution of aryl silyl ether **20a** (60 mg, 0.11 mmol) and triethylamine trihydrofluoride (1.7 mL, 11 mmol) in THF (3 mL) was stirred overnight and then cooled in an ice bath and quenched with the cautious addition of potassium carbonate (2.0 g, 15 mmol) dissolved in water (5 mL). After adding sat. $NaHCO_3$ (5 mL), the mix was extracted with diethyl ether (3 x 15 mL), then dried ($MgSO_4$), filtered through a Celite pad and concentrated under reduced pressure. Purification of the residue with flash chromatography (silica, 10 \rightarrow 20% ethyl acetate in hexanes) gave **20b** (40 mg, 88% yield). 1H NMR (400 MHz, $CDCl_3$) δ 7.68 (d, $J=16.1$ Hz, 1 H), 7.42-7.32 (m, 5 H), 7.20 (s, 2 H), 6.59 (d, $J=8.3$ Hz, 1 H), 6.53 (d, $J=8.3$ Hz, 1 H), 6.46 (d, $J=16.1$ Hz, 1 H), 5.25 (s, 2 H), 3.96 (s, 2 H), 3.17 (heptet, $J=6.8$ Hz, 1 H), 2.24 (s, 6 H), 1.20 (d, $J=6.8$ Hz, 6 H); ^{13}C NMR (100 MHz, $CDCl_3$) δ 167.26, 151.07, 145.62, 140.50, 137.72, 136.05, 134.45, 132.00, 130.89, 128.53, 128.46, 128.17, 127.90, 126.16, 125.27, 116.57, 115.22, 66.30, 34.46, 27.07, 22.52, 20.18. HRMS exact mass calcd for (M – benzyl) $C_{21}H_{23}O_3$: 323.1647, found: 323.1632.

3-{4-[3-Isopropyl-4-(triisopropylsilyloxy)-benzyl]-3,5-dimethylphenyl}propionic acid (**21**):

1
2
3
4
5
6
7
8
9
10
11
12
13
14
15
16
17
18
19
20
21
22
23
24
25
26
27
28
29
30
31
32
33
34
35
36
37
38
39
40
41
42
43
44
45
46
47
48
49
50
51
52
53
54
55
56
57
58
59
60
61
62
63
64
65
66
67
68
69
70
71
72
73
74
75
76
77
78
79
80
81
82
83
84
85
86
87
88
89
90
91
92
93
94
95
96
97
98
99
100

A solution of benzyl ester **20a** (490 mg, 0.86 mmol) in ethyl acetate (30 mL) and acetic acid (2 mL) was put in a Parr hydrogenator flask and sparged with Ar. Palladium on carbon (10%, 90 mg) was added and the mixture was shaken 20 h under H₂ atmosphere at 33 psi. The mixture was then filtered through a Celite pad, which was rinsed with ethyl acetate and ethanol. The filtrate was concentrated under reduced pressure, with toluene azeotroping to remove residual acetic acid. Flash chromatography (silica, 10% ethyl acetate, 1% acetic acid in hexanes) gave **21** (355 mg, 86% yield) as a crystalline solid. ¹H NMR (400 MHz, CDCl₃) δ 6.94 (s, 1 H), 6.89 (s, 2 H), 6.59 (d, *J*=7.8 Hz, 1 H), 6.49 (d, *J*=8.3 Hz, 1 H), 3.92 (s, 2 H), 3.32 (heptet, *J*=6.8 Hz, 1 H), 2.90 (t, *J*=7.8 Hz, 2 H), 2.69 (t, *J*=8.3 Hz, 2 H), 2.22 (s, 6 H), 1.27 (heptet, *J*=7.8 Hz, 3 H), 1.16 (d, *J*=6.8 Hz, 6 H), 1.08 (d, *J*=7.3 Hz, 18 H); ¹³C NMR (100 MHz, CDCl₃) δ 178.73, 151.01, 138.12, 137.65, 137.31, 135.69, 131.57, 127.87, 126.00, 124.82, 117.61, 35.62, 34.23, 30.18, 26.63, 22.83, 20.25, 18.11, 13.06. HRMS exact mass calcd for C₃₀H₄₆O₃Si: 482.3216, found: 482.3217.

3-[4-(4-Hydroxy-3-isopropylbenzyl)-3,5-dimethylphenyl]propionic acid (**9**):

A solution of benzyl ester **20b** (21 mg, 0.051 mmol) in ethyl acetate (2 mL) was sparged with Ar and then palladium on carbon (10%, small spatula tip) was added. After stirring overnight under H₂ atmosphere maintained with balloon pressure, the mixture was filtered through a Celite pad, which was rinsed with ethyl acetate and ethanol. The filtrate was concentrated under reduced pressure, and the residue was purified by preparative TLC (silica, 20 cm x 20 cm x 1000 μm, 4% methanol, 1% acetic acid in

chloroform) to give **9** (15 mg, 90% yield). ¹H NMR (400 MHz, CD₃OD) δ 6.88 (s, 2 H), 6.81 (s, 1 H), 6.56 (d, *J*=8.3 Hz, 1 H), 6.49 (dd, *J*=8.3, 2.0 Hz, 1 H), 3.89 (s, 2 H), 3.19 (heptet, *J*=7.3 Hz, 1 H), 2.82 (t, *J*=7.6 Hz, 2 H), 2.57 (t, *J*=7.8 Hz, 2 H), 2.18 (s, 6 H), 1.12 (d, *J*=6.8 Hz, 6 H); ¹³C NMR (100 MHz, CD₃OD) δ 176.98, 153.39, 139.61, 138.08, 136.65, 135.82, 131.78, 128.94, 126.70, 126.33, 115.82, 36.92, 34.85, 31.67, 28.01, 23.05, 20.30. HRMS exact mass calcd for C₂₁H₂₆O₃: 326.1882, found: 326.1888.

(S)-(4)-Benzyl-3-(3-{4-[3-isopropyl-4-(triisopropylsilyloxy)-benzyl]-3,5-dimethylphenyl}-propionyl)-oxazolidin-2-one (**21a**):

A stirred solution of carboxylic acid **21** (304 mg, 0.63 mmol) in THF (15 mL) was chilled to -78 °C, and triethylamine (114 μL, 0.82 mmol) and pivaloyl chloride (85 μL, 0.69 mmol) were added via syringe. The mixture was stirred 15 min at -78 °C, then 30 min on an ice bath and then at -78 °C again. To a separate stirred solution of (S)-4-benzyl-2-oxazolidinone (200 mg, 1.13 mmol) in THF (9 mL) cooled to -78 °C was added *n*-butyllithium (2.5 M in hexane, 450 μL, 1.13 mmol). After 10 min stirring, the oxazolidinone lithium salt was added via cannula to the mixed anhydride solution. After stirring 30 min at -78 °C and another 30 min while slowly warming to rt, the reaction was quenched with the addition of 1 M NaHSO₄ (15 mL). After removing most of the THF under reduced pressure, the residue was extracted with ethyl acetate (3 x 20 mL). The combined organic fractions were washed with sat. NaHCO₃ (15 mL) and brine (10 mL), then dried (MgSO₄), filtered through a Celite pad and concentrated under reduced pressure. Purification of the residue by flash chromatography (silica, 5% ethyl acetate in

hexanes) gave **21a** (359 mg, 89% yield) as a colourless syrup. ¹H NMR (400 MHz, CDCl₃) δ 7.31-7.23 (m, 3 H), 7.18 (d, *J*=6.8 Hz, 2 H), 6.96 (d, *J*=2.4 Hz, 1 H), 6.94 (s, 2 H), 6.58 (d, *J*=8.3 Hz, 1 H), 6.48 (dd, *J*=8.3, 2.4 Hz, 1 H), 4.67 (td, *J*=6.4, 3.4 Hz, 1 H), 4.19-4.13 (m, 2 H), 3.92 (s, 2 H), 3.36-3.21 (m, 4 H), 3.02-2.90 (m, 2 H), 2.76 (dd, *J*=13.4, 9.5 Hz, 1 H), 2.22 (s, 6 H), 1.26 (m, *J*=7.8 Hz, 3 H), 1.17 (d, *J*=6.4 Hz, 6 H), 1.08 (d, *J*=7.3 Hz, 18 H); ¹³C NMR (100 MHz, CDCl₃) δ 172.59, 153.38, 150.96, 138.04, 137.86, 137.14, 135.54, 135.19, 131.61, 129.37, 128.89, 128.15, 127.29, 126.02, 124.79, 117.56, 66.11, 55.07, 37.81, 37.22, 34.21, 29.85, 26.62, 22.81, 20.22, 18.08, 13.01. HRMS exact mass calcd for C₄₀H₅₅NO₄Si: 641.3900, found: 641.3905.

3-((S)-2-Azido-3-{4-[3-isopropyl-4-(triisopropylsilyloxy)-benzyl]-3,5-dimethylphenyl}-propionyl)-(S)-(4)-benzyl-oxazolidin-2-one (**22**):

To a stirred solution of N-acyloxazolidinone **21a** (290 mg, 0.45 mmol) in THF (20 mL) cooled to -78 °C was added potassium bis(trimethylsilyl)-amide (0.5 M in toluene, 0.90 mL, 0.45 mmol). After stirring 15 min, a prechilled solution of trisyl azide (Omega, Inc., 175 mg, 0.57 mmol) in THF (15 mL) was added via Teflon cannula over 1 min. After approx. 45 s from the end of the addition, acetic acid (78 μL, 1.4 mmol) was added via syringe, and the reaction was allowed to slowly warm to rt over 2.5 h. Solvent was removed under reduced pressure and the residue was dissolved in methylene chloride (100 mL) and washed with half-sat. NaHCO₃ (20 mL) and brine (20 mL). The solution was dried (MgSO₄), filtered through a Celite pad and concentrated under reduced pressure. The residue was purified by flash chromatography (silica, 5 → 10% ethyl

1
2
3
4
5
6
7
8
9
10
11
12
13
14
15
16
17
18
19
20
21
22
23
24
25
26
27
28
29
30
31
32
33
34
35
36
37
38
39
40
41
42
43
44
45
46
47
48
49
50
51
52
53
54
55
56
57
58
59
60
61
62
63
64
65
66
67
68
69
70
71
72
73
74
75
76
77
78
79
80
81
82
83
84
85
86
87
88
89
90
91
92
93
94
95
96
97
98
99
100

acetate in hexanes) to give **22** (226 mg, 73%) as a thick syrup. ¹H NMR (400 MHz, CDCl₃) δ 7.37-7.27 (m, 3 H), 7.22-7.18 (m, 2 H), 6.98 (s, 2 H), 6.95 (d, *J*=2.0 Hz, 1 H), 6.58 (d, *J*=8.3 Hz, 1 H), 6.47 (dd, *J*=8.1, 2.2 Hz, 1 H), 5.29 (dd, *J*=8.8, 5.9 Hz, 1 H), 4.60-4.55 (m, 1 H), 4.13 (dd, *J*=9.0, 2.7 Hz, 1 H), 3.99 (t, *J*=8.3 Hz, 1 H), 3.92 (dd, *J*=16.1, 5.9 Hz, 2 H), 3.35-3.28 (m, 2 H), 3.14 (dd, *J*=13.7, 5.9 Hz, 1 H), 3.00 (dd, *J*=13.4, 9.0 Hz, 1 H), 2.83 (dd, *J*=13.4, 9.5 Hz, 1 H), 2.23 (s, 6 H), 1.31-1.24 (m, 3 H), 1.16 (dd, *J*=6.8, 2.0 Hz, 6 H), 1.08 (d, *J*=6.8 Hz, 18 H); ¹³C NMR (100 MHz, CDCl₃) δ 170.77, 152.69, 151.04, 138.14, 137.45, 136.79, 134.71, 132.92, 131.31, 129.38, 129.01, 128.85, 127.48, 126.04, 124.78, 117.54, 66.42, 61.17, 55.40, 37.58, 37.34, 34.26, 26.62, 22.79, 20.21, 18.07, 13.02. HRMS exact mass calcd for C₄₀H₅₄N₄O₄Si: 682.3914, found: 682.3932.

(S)-2-Azido-3-{4-[3-isopropyl-4-(triisopropylsilyloxy)-benzyl]-3,5-dimethylphenyl}-propionic acid (**22a**):

To a stirred solution of N-acyloxazolidinone **22** (58 mg, 0.085 mmol) in 3:1 THF:water (4 mL) cooled to 0 °C was added hydrogen peroxide (50 wt% soln, 20 μL, 0.34 mmol) and lithium hydroxide monohydrate (7.1 mg, 0.17 mmol). After 2.5 h of stirring, the reaction was quenched with Na₂S₂O₃ (0.4 M, 935 μL, 0.37 mmol) and half-sat. NaHCO₃ (5 mL). After acidifying to pH 1 with HCl, the mixture was extracted with methylene chloride (4 x 10 mL). The combined organic fractions were washed with 1 M NaHSO₄ (5 mL), then dried (MgSO₄), filtered through a Celite pad and concentrated under reduced pressure. Purification of the residue with flash chromatography (silica, 7.5% ethyl

acetate, 1% acetic acid in hexanes) gave **22a** (37 mg, 83% yield). ¹H NMR (400 MHz, CDCl₃) δ 6.94 (s, 2 H), 6.92 (d, *J*=1.95 Hz, 1 H), 6.60 (d, *J*=8.30 Hz, 1 H), 6.50 (dd, *J*=8.30, 1.95 Hz, 1 H), 4.14 (dd, *J*=9.28, 4.88 Hz, 1 H), 3.94 (s, 2 H), 3.32 (heptet, *J*=6.84 Hz, 1 H), 3.19 (dd, *J*=14.16, 4.88 Hz, 1 H), 2.95 (dd, *J*=13.92, 9.52 Hz, 1 H), 2.24 (s, 6 H), 1.26 (heptet, *J*=7.81 Hz, 3 H), 1.15 (d, *J*=6.84 Hz, 6 H), d ppm 1.09 (d, *J*=7.32 Hz, 18 H); ¹³C NMR (100 MHz, CDCl₃) δ 175.48, 151.06, 138.19, 137.61, 136.85, 133.13, 131.29, 128.74, 125.94, 124.85, 117.63, 63.23, 37.22, 34.28, 26.62, 22.80, 20.26, 18.10, 13.05. HRMS exact mass calcd for C₃₀H₄₅N₃O₃Si: 523.3230, found: 523.3245.

(S)-2-Azido-3-{4-[3-isopropyl-4-hydroxybenzyl]-3,5-dimethylphenyl}-propionic acid (**22b**):

To a stirred solution of silyl ether **22a** (35 mg, 0.067 mmol) in THF (3 mL) was added triethylamine trihydrofluoride (1.1 mL, 6.7 mmol). After stirring overnight, most of the THF was removed under reduced pressure, and the reaction was cooled in an ice bath and quenched with the cautious addition of potassium carbonate (1.3 g, 9.0 mmol) dissolved in water (5 mL). The solution was re-acidified to pH 3 with 6 M HCl and extracted with methylene chloride (3 x 10 mL). The combined organic fractions were dried (MgSO₄), filtered through a Celite pad and concentrated under reduced pressure. The residue was purified by preparative TLC (silica, 20 cm x 20 cm x 1000 μm, 8% methanol, 1% acetic acid in chloroform) to give **22b** (11 mg, 44% yield). ¹H NMR (400 MHz, CD₃OD) δ 6.95 (s, 2 H), 6.80 (d, *J*=2.0 Hz, 1 H), 6.56 (d, *J*=8.3 Hz, 2 H), 6.50 (dd, *J*=8.3, 2.0 Hz, 1 H), 4.13 (br s, 1 H), 3.91 (s, 2 H), 3.19 (heptet, *J*=6.8 Hz, 1 H), 3.11 (dd, *J*=13.9, 4.2 Hz, 1

1-11-1918

1-11-1918

1-11-1918

H), 2.90 (dd, $J=13.4, 8.6$ Hz, 1 H), 2.19 (s, 6 H), 1.11 (d, $J=6.8$ Hz, 6 H); ^{13}C NMR (100 MHz, CD_3OD) δ 153.41, 138.26, 137.60, 135.86, 135.42, 131.57, 129.97, 126.66, 126.36, 115.83, 38.38, 34.87, 28.00, 23.04, 20.29. HRMS exact mass calcd for $\text{C}_{21}\text{H}_{25}\text{N}_3\text{O}_3$: 367.1896, found: 367.1936.

(S)-2-Amino-3-{4-[3-isopropyl-4-hydroxybenzyl]-3,5-dimethylphenyl}-propionic acid (**8**):

A solution of azidocarboxylic acid **22b** (11 mg, 0.11 mmol) in 2:1 acetic acid:water (3 mL) was sparged with Ar, then palladium on carbon (10%, 22 mg) was added, and the mixture was stirred overnight under H_2 atmosphere maintained with balloon pressure. The reaction mixture was filtered through a small plug of cotton, concentrated under reduced pressure and dried *in vacuo* to give **8** (10 mg, 97% yield) as a white solid. ^1H NMR (400 MHz, CD_3OD) δ 6.99 (s, 2 H), 6.87 (s, 1 H), 6.56 (d, $J=8.3$ Hz, 1 H), 6.51 (dd, $J=8.3, 2.0$ Hz, 1 H), 3.90 (d, $J=7.8$ Hz, 2 H), 3.76 (br s, 1 H), 3.27-3.16 (m, 2 H), 2.91 (dd, $J=13.7, 8.8$ Hz, 1 H), 2.22 (s, 6 H), 1.12 (d, $J=7.3$ Hz, 6 H); ^{13}C NMR (100 MHz, CD_3OD) δ 169.33, 153.54, 138.73, 138.12, 135.88, 134.73, 131.47, 130.03, 126.94, 126.36, 115.85, 34.98, 28.13, 23.04, 20.38. HRMS exact mass calcd for $\text{C}_{21}\text{H}_{27}\text{NO}_3$: 341.1991, found: 341.1993.

4.5. Acknowledgements

This work was supported by the National Institutes of Health (DK52798, T.S.S. and DK41842, J.D.B.).

4.6. References

- [1] Braverman, L.E., Utiger, R.D., Werner, S.C. & Ingbar, S.H. (1991). "Werner and Ingbar's the thyroid : a fundamental and clinical text." 6th ed. Lippincott, Philadelphia.
- [2] Yen, P.M. (2001). Physiological and molecular basis of thyroid hormone action. *Physiological Reviews* **81**, 1097-1142.
- [3] Lazar, M.A. (1993). Thyroid hormone receptors: multiple forms, multiple possibilities. *Endocrine Reviews* **14**, 184-93.
- [4] Forrest, D., Hanebuth, E., Smeyne, R.J., Everds, N., Stewart, C.L., Wehner, J.M. & Curran, T. (1996). Recessive resistance to thyroid hormone in mice lacking thyroid hormone receptor beta: evidence for tissue-specific modulation of receptor function. *EMBO Journal* **15**, 3006-15.
- [5] Forrest, D., Erway, L.C., Ng, L., Altschuler, R. & Curran, T. (1996). Thyroid hormone receptor beta is essential for development of auditory function. *Nature Genetics* **13**, 354-7.
- [6] Fraichard, A., Chassande, O., Plateroti, M., Roux, J.P., Trouillas, J., Dehay, C., Legrand, C., Gauthier, K., Kedinger, M., Malaval, L., Rousset, B. & Samarut, J. (1997). The T3R alpha gene encoding a thyroid hormone receptor is essential for

- post-natal development and thyroid hormone production. *EMBO Journal* **16**, 4412-20.
- [7] Gauthier, K., Chassande, O., Plateroti, M., Roux, J.P., Legrand, C., Pain, B., Rousset, B., Weiss, R., Trouillas, J. & Samarut, J. (1999). Different functions for the thyroid hormone receptors TRalpha and TRbeta in the control of thyroid hormone production and post-natal development. *EMBO Journal* **18**, 623-31.
- [8] Ng, L., Hurley, J.B., Dierks, B., Srinivas, M., Salto, C., Vennstrom, B., Reh, T.A. & Forrest, D. (2001). A thyroid hormone receptor that is required for the development of green cone photoreceptors. *Nature Genetics* **27**, 94-8.
- [9] Chiellini, G., Apriletti, J.W., Yoshihara, H.A.I., Baxter, J.D., Ribeiro, R.C.J. & Scanlan, T.S. (1998). A high-affinity subtype-selective agonist ligand for the thyroid hormone receptor. *Chemistry & Biology* **5**, 299-306.
- [10] Boyd, G.S. & Oliver, M.F. (1960). The effect of certain thyroxine analogues on the serum lipids in human subjects. *Journal of Endocrinology* **21**, 33-43.
- [11] Ballantyne, F.C., Epenetos, A.A., Caslake, M., Forsythe, S. & Ballantyne, D. (1979). The composition of low-density lipoprotein and very-low-density lipoprotein subfractions in primary hypothyroidism and the effect of hormone-replacement therapy. *Clinical Science* **57**, 83-8.
- [12] Hansson, P., Valdemarsson, S. & Nilssonehle, P. (1983). Experimental Hyperthyroidism in Man - Effects on Plasma-Lipoproteins, Lipoprotein-Lipase and Hepatic Lipase. *Hormone and Metabolic Research* **15**, 449-452.
- [13] Gomberg-Maitland, M. & Frishman, W.H. (1998). Thyroid hormone and cardiovascular disease. *American Heart Journal* **135**, 187-96.

1
[Illegible text]

- [14] Klein, I. & Ojamaa, K. (2001). Mechanisms of disease: thyroid hormone and the cardiovascular system. *New England Journal of Medicine* **344**, 501-509.
- [15] Wikstrom, L., Johansson, C., Salto, C., Barlow, C., Campos Barros, A., Baas, F., Forrest, D., Thoren, P. & Vennstrom, B. (1998). Abnormal heart rate and body temperature in mice lacking thyroid hormone receptor alpha 1. *EMBO Journal* **17**, 455-61.
- [16] Schwartz, H.L., Strait, K.A., Ling, N.C. & Oppenheimer, J.H. (1992). Quantitation of rat tissue thyroid hormone binding receptor isoforms by immunoprecipitation of nuclear triiodothyronine binding capacity. *Journal of Biological Chemistry* **267**, 11794-9.
- [17] Gullberg, H., Rudling, M., Forrest, D., Angelin, B. & Vennstrom, B. (2000). Thyroid hormone receptor beta-deficient mice show complete loss of the normal cholesterol 7alpha-hydroxylase (CYP7A) response to thyroid hormone but display enhanced resistance to dietary cholesterol. *Molecular Endocrinology* **14**, 1739-49.
- [18] Taylor, A.H., Stephan, Z.F., Steele, R.E. & Wong, N.C.W. (1997). Beneficial effects of a novel thyromimetic on lipoprotein metabolism. *Molecular Pharmacology* **52**, 542-547.
- [19] Stephan, Z.F., Yurachek, E.C., Sharif, R., Wasvary, J.M., Leonards, K.S., Hu, C.W., Hintze, T.H. & Steele, R.E. (1996). Demonstration of Potent Lipid-Lowering Activity by a Thyromimetic Agent Devoid of Cardiovascular and Thermogenic Effects. *Atherosclerosis* **126**, 53-63.

1
2
3
4
5
6
7
8
9
10
11
12
13
14
15
16
17
18
19
20
21
22
23
24
25
26
27
28
29
30
31
32
33
34
35
36
37
38
39
40
41
42
43
44
45
46
47
48
49
50
51
52
53
54
55
56
57
58
59
60
61
62
63
64
65
66
67
68
69
70
71
72
73
74
75
76
77
78
79
80
81
82
83
84
85
86
87
88
89
90
91
92
93
94
95
96
97
98
99
100

- [20] Chiellini, G., Nguyen, N.H., Yoshihara, H.A.I. & Scanlan, T.S. (2000). Improved synthesis of the iodine-free thyromimetic GC-1. *Bioorganic & Medicinal Chemistry Letters* **10**, 2607-2611.
- [21] Jorgensen, E.C., Murray, W.J. & Block, P., Jr. (1974). Thyroxine analogs. 22. Thyromimetic activity of halogen-free derivatives of 3,5-dimethyl-L-thyronine. *Journal of Medicinal Chemistry* **17**, 434-9.
- [22] Baxter, J.D., Dillmann, W.H., West, B.L., Huber, R., Furlow, J.D., Fletterick, R.J., Webb, P., Apriletti, J.W. & Scanlan, T.S. (2001). Selective modulation of thyroid hormone receptor action. *Journal of Steroid Biochemistry and Molecular Biology* **76**, 31-42.
- [23] Trost, S.U., Swanson, E., Gloss, B., Wang-Iverson, D.B., Zhang, H.J., Volodarsky, T., Grover, G.J., Baxter, J.D., Chiellini, G., Scanlan, T.S. & Dillmann, W.H. (2000). The thyroid hormone receptor-beta-selective agonist GC-1 differentially affects plasma lipids and cardiac activity. *Endocrinology* **141**, 3057-3064.
- [24] Morte, B., Manzano, J., Scanlan, T., Vennstrom, B. & Bernal, J. (2002). Deletion of the thyroid hormone receptor alpha 1 prevents the structural alterations of the cerebellum induced by hypothyroidism. *Proceedings of the National Academy of Sciences of the United States of America* **99**, 3985-3989.
- [25] Ribeiro, M.O., Carvalho, S.D., Schultz, J.J., Chiellini, G., Scanlan, T.S., Bianco, A.C. & Brent, G.A. (2001). Thyroid hormone-sympathetic interaction and adaptive thermogenesis are thyroid hormone receptor isoform-specific. *Journal of Clinical Investigation* **108**, 97-105.

- [26] Koerner, D., Schwartz, H.L., Surks, M.I. & Oppenheimer, J.H. (1975). Binding of selected iodothyronine analogues to receptor sites of isolated rat hepatic nuclei. High correlation between structural requirements for nuclear binding and biological activity. *Journal of Biological Chemistry* **250**, 6417-23.
- [27] Wagner, R.L., Apriletti, J.W., McGrath, M.E., West, B.L., Baxter, J.D. & Fletterick, R.J. (1995). A structural role for hormone in the thyroid hormone receptor. *Nature* **378**, 690-7.
- [28] Wagner, R.L., Huber, B.R., Shiau, A.K., Kelly, A., Lima, S.T.C., Scanlan, T.S., Apriletti, J.W., Baxter, J.D., West, B.L. & Fletterick, R.J. (2001). Hormone selectivity in thyroid hormone receptors. *Molecular Endocrinology* **15**, 398-410.
- [29] Evans, D.A., Katz, J.L. & West, T.R. (1998). Synthesis of diaryl ethers through the copper-promoted arylation of phenols with arylboronic acids. An expedient synthesis of thyroxine. *Tetrahedron Letters* **39**, 2937-2940.
- [30] Hansch, C., Leo, A. & Hoekman, D. (1995). "Exploring QSAR: Hydrophobic, Electronic, and Steric Constants." 2. 2 vols. American Chemical Society, Washington, D.C.
- [31] Darimont, B.D., Wagner, R.L., Apriletti, J.W., Stallcup, M.R., Kushner, P.J., Baxter, J.D., Fletterick, R.J. & Yamamoto, K.R. (1998). Structure and specificity of nuclear receptor-coactivator interactions. *Genes and Development* **12**, 3343-56.
- [32] Yoshihara, H.A.I., Apriletti, J.W., Baxter, J.D. & Scanlan, T.S. (2001). A designed antagonist of the thyroid hormone receptor. *Bioorganic & Medicinal Chemistry Letters* **11**, 2821-2825.



- [33] Chiellini, G., Nguyen, N.H., Apriletti, J.W., Baxter, J.D. & Scanlan, T.S. (2002). Synthesis and biological activity of novel thyroid hormone analogues: 5'-aryl substituted GC-1 derivatives. *Bioorganic & Medicinal Chemistry* **10**, 333-346.
- [34] Nguyen, N.H., Apriletti, J.W., Cunha Lima, S.T., Webb, P., Baxter, J.D. & Scanlan, T.S. (2002). Rational design and synthesis of a novel thyroid hormone antagonist that blocks coactivator recruitment. *Journal of Medicinal Chemistry* **45**, 3310-20.
- [35] Apriletti, J.W., Baxter, J.D., Lau, K.H. & West, B.L. (1995). Expression of the rat alpha 1 thyroid hormone receptor ligand binding domain in *Escherichia coli* and the use of a ligand-induced conformation change as a method for its purification to homogeneity. *Protein Expression and Purification* **6**, 363-70.

Conclusions

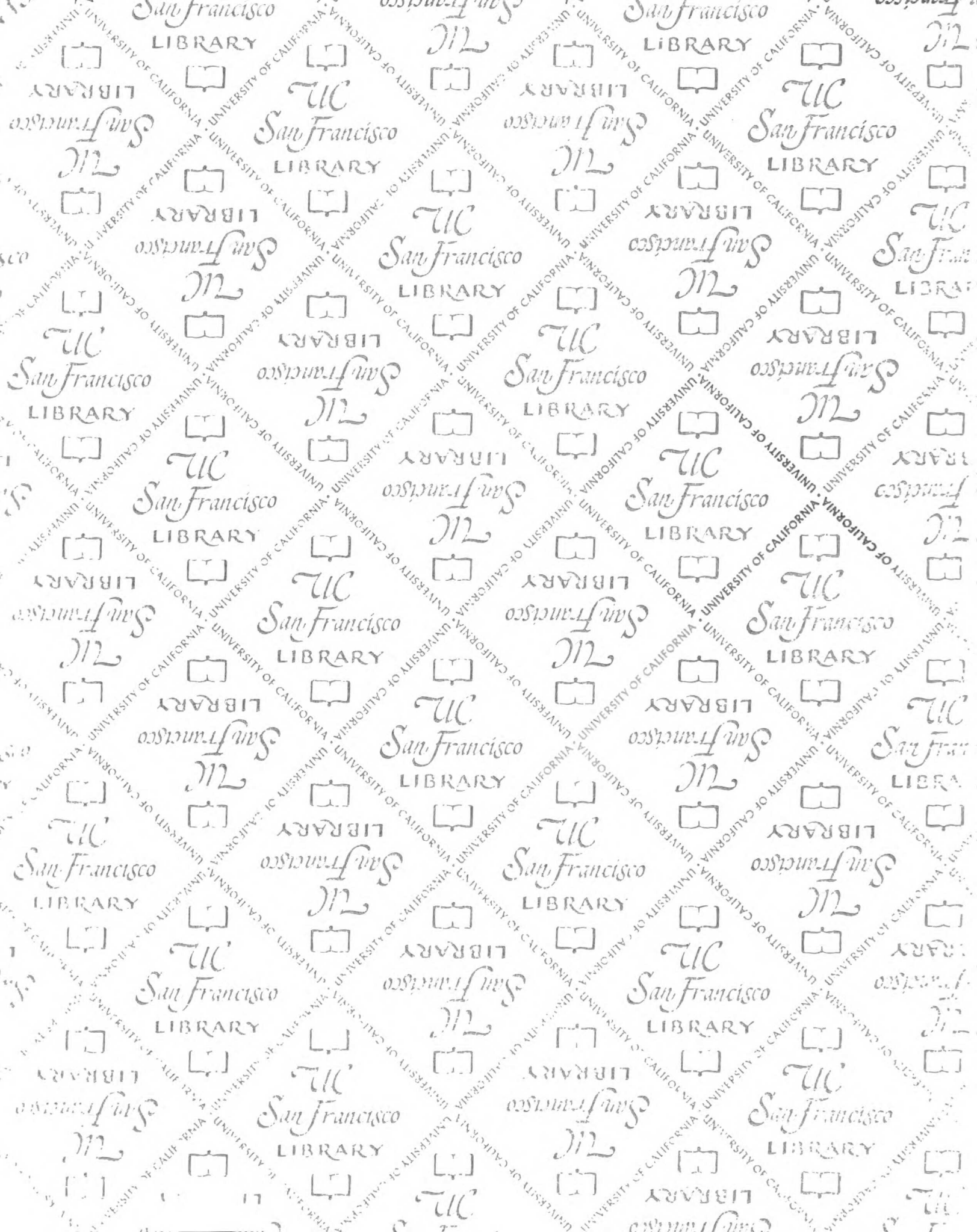
The results of the experiments in the preceding chapters of this thesis may serve as starting points in the design of new TR modulators. HY-4, the antagonist described in chapter 3 serves as the proof of concept for the design of TR antagonists. Whether compounds of the class of bridge-substituted GC-1 analogues can be optimized into potent TR ligands with *in vivo* activity remains an open question. The substantial drop in affinity associated with substitution at the bridge suggests that such a task will not be trivial. That, and the effectiveness of 5'-substituted GC-1 analogues as TR antagonists with *in vivo* activity, suggests that bridge-substituted antagonists may not be the best approach to pursue. The effect of HY-4 on TR – co-repressor interactions remains unresolved, but given the very low levels of activation of TR by HY-4, it is possible that it may not disrupt TR – co-repressor interactions. Since it is already established that the TR antagonist NH-3, a 5'-substituted GC-1 analogue, allows co-repressor dissociation, this could be an interesting avenue of investigation.

The studies of Chapter 4 demonstrate the importance to activity of small changes in ligand structure. The TR β -selectivity of GC-1 can be mostly attributed to the substitution of two atoms. The study was designed to elucidate the structural features of GC-1 responsible for its selectivity, and the results do not show clearly how to make TR ligands with increased or inverted selectivity. Given the importance of the nature of the polar side chain in determining selectivity and the proximity of the side chain to the most varying region of the ligand binding pocket, the side chain is the most obvious feature to target in attempting to make other selective compounds. However, there may be an upper

1
2
3
4
5
6
7
8
9
10
11
12
13
14
15
16
17
18
19
20
21
22
23
24
25
26
27
28
29
30
31
32
33
34
35
36
37
38
39
40
41
42
43
44
45
46
47
48
49
50
51
52
53
54
55
56
57
58
59
60
61
62
63
64
65
66
67
68
69
70
71
72
73
74
75
76
77
78
79
80
81
82
83
84
85
86
87
88
89
90
91
92
93
94
95
96
97
98
99
100

limit to the selectivity that can be achieved by this approach. The data are not complete, but it appears that various thyromimetics with alternative polar side chains have about the same 10-fold TR β -selectivity. Greater TR β -selectivity has been achieved by the combination of alternative side chains with bulky substituents at the 3'-position, and it seems likely that compounds with greater selectivity will need to interact with other parts of the ligands binding pocket where structural perturbations are tolerated differentially by TR β and TR α .

It remains possible that other sites of substitution may be tolerated better by TR α than TR β , or that other polar moieties at the 1-position may have more favorable interactions with TR α . The best indication for TR α -selectivity is HY-4, which while bearing an oxyacetic acid chain, showed either equal binding to TRs or a slight preference for TR α . But a large substituent at the bridging position is required for this effect, resulting in a substantial loss of affinity, and the binding mode of the ligand may be different from that of GC-1. However, because of the interest in developing a TR α -selective antagonist, if both the TR α -selectivity and the overall affinity of HY-4 could be drastically improved, the resulting compound would be a very useful TR ligand.



For reference

Not to be taken
from the room.

7230348



3 1378 00723 0348

